AN ABSTRACT OF THE THESIS OF

Hang Tuah for the degree of Doctor of Philosophy

in Civil Engineering presented on August 30, 1982

Title: CABLE DYNAMICS IN AN OCEAN ENVIRONMENT

Redacted for Privacy

Abstract approved: Dr. John W. Leonard

The nonlinear dynamic analysis of cable and cable-large body systems subject to both deterministic and non-deterministic loading is presented in this study. Nonlinearities occur due to large displacements, material non-linearity, lack of stiffness in compression, and the non-conservative fluid loading.

A finite element model is used to model the cable and rigid motions of the large body. The linearized incremental equations of motion for both linear elastic and viscoelastic materials are derived. Solution procedures for both static and dynamic analyses are presented. A wake-oscillator model is used to model cable strumming effects: transverse motions of the cable are assumed to be small compared to the in-line displacements and the transverse frequency is much higher than the in-line frequency. The computational

procedure for the prediction of cable strumming using a mode-superposition technique is given.

The stochastic response of the cable system is analyzed in the frequency domain. Cable vibrations were assumed to be small displacement about the static configuration. The nonlinear fluid drag force is linearized by a least square method. The linearized equation of motions are decoupled by a method proposed by Foss (1958).

Numerical examples are presented to demonstrate the validity and the capability of the finite element models and the proposed numerical techniques.

CABLE DYNAMICS IN AN OCEAN ENVIRONMENT

by

Hang Tuah

A THESIS

submitted to

Oregon State University

in partial fulfillment of
the requirements for the
degree of

Doctor of Philosophy

Commencement June 1983

APPROVED:

Redacted for Privacy

Professor of Civil Engineering in charge of major

Redacted for Privacy

Head of Department of Civil Engineering

Redacted for Privacy

Dean of Graduate School

Date thesis is presented August 30, 1982

Typed by Phyllis Petersen for Hang Tuah

ACKNOWLEDGEMENTS

The author greatly appreciated the support and guidance provided by Professor Dr. John W. Leonard in the preparation and development of the investigation. The advice of Dr. R. T. Hudspeth in the wave force modeling is also gratefully acknowledged.

The research was funded through MUCIA-AID-INDONESIAN HIGHER EDUCATION. A portion of the computer time was provided by the Oregon State University Computer Center. The finances provided by these organizations were accepted in gratitude.

Last but not least, the author thanks Phyllis Petersen for her friendly cooperation in the typing of the dissertation.

TABLE OF CONTENTS

TABLE OF CONTENTS
(Continued)

LIST OF FIGURES

LIST OF FIGURES
(Continued)

LIST OF TABLES

CABLE DYNAMIC IN AN OCEAN ENVIRONMENT

1.0 INTRODUCTION

Cable-supported structures become increasingly important to offshore designers as an increasing number of structures are constructed in deep ocean waters and in areas which are subjected to hazardous environmental conditions. A common condition is one in which the structures are sited near or in a storm-generating area. In this case, the structures are subjected to irregular and often nonlinear waves.

Cables are highly nonlinear. The nonlinearities are due to inherent properties of cable response, such as large displacement, lack of stiffness in compression, and constitutive relations. Other nonlinearities may be introduced because of position-dependent loads and boundary conditions. The analysis of the nonlinear behavior of cable-supported structures under both deterministic and nondeterministic dynamic loadings is the subject of the present study. Finite element models will be employed to simulate the structural responses.

1.1 Review of Previous Studies

Numerous scientific investigations on cable dynamic behavior have been undertaken since Brook Taylor (see Rayleigh, 1945) first introduced the equation of motion of an uniform taut string. There have been hundreds of papers on this subject with various kinds of solution techniques adopted. Those techniques may be categorized into four general classes: 1) analytical methods; 2) semi-analytical methods; 3) lumped parameter methods; and 4) finite element methods.

Analytical methods. Analytical methods refer to those methods which can be used to obtain a closed-form solution. In early studies of cable vibration, Daniel Bernoulli (see Rayleigh, 1945) presented a general solution in the form of infinite series for the vibration of an uniform inextensible string supported at both ends. Later, Lagrange (see Rayleigh, 1945) introduced a discrete model of a continuous string. A set of linear-differential equations in terms of generalized coordinates describing the lateral displacements of lumped masses were derived by a minimum energy principle. Solutions for these equations were obtained by assuming the motion is harmonic in time. Irvine and Caughey (1979) gave an exact solution for both in-plane and out-of-plane vibrations of a uniform suspended cable with finite sag ratio. Unlike Bernoulli and Lagrange,

they include the stretching effect of the cable in the equation of motion by the linear stress-strain relationship.

General equations governing the three-dimensional motion of the cable were presented by Cannon and Genin (1970). Basically the cable is considered to be flexible and to have its mass continuously distributed along its length. The equations are highly nonlinear. The closed form solution is restricted to prediction of small motions about the equilibrium configuration (Irvine and Caughey, 1974).

Analytical methods may be the most desirable techniques to use since they give an explicit expression for a cable motion. Unfortunately, the available mathematical tools are limited to relatively simple problems.

Semi-analytical methods. The term semi-analytical is used to describe those solution methods which start with the governing partial differential equations and use a numerical procedure to obtain solutions. One of the popular techniques in this class is the method of characteristic (Reid, 1968; Nath, 1969): the nonlinear partial differential equations of cable motions are transformed to a set of ordinary differential equations which can be integrated numerically.

An interesting approach to the solution of the statical equations of underwater cables using a Newton-Raphson method is reported by Leonard (1978). The non-linear governing differential equations are solved by successive solutions of equations linearized about previous iterates.

Lumped parameter methods (LPM). In the usual mathematical development of a lumped parameter model, the continuum is discretized into straight-line elements. The continuous mass, material properties, force distributions, and structural constitutive models are summed over the regions between the midpoints of the elements between the nodes. A set of nonlinear ordinary differential equations are derived for each node and are integrated numerically in time. An application of this method to underwater cable dynamics may be found in references (Nath and Tresher, 1975) and (Patel, 1974).

A somewhat different application of a lumped mass parameter approach to the static problem is a technique called the method of imaginary reactions (Skop and O'Hara, 1970). The technique is similar to the cut structure approach used in redundant frame analysis. Direct iteration on selected cable forces or reactions are used to eliminate errors in corresponding displacement continuity equations. This method was utilized by Dominguez and Smith (1972) to

first determine the stable equilibrium configuration of cable systems and then to evaluate the flexibility matrix of these systems by applying a unit force at nodal points. Nodal displacements from the equilibrium configuration were expressed as the product of the flexibility matrix and the external forces. The inertial and damping forces in the dynamic systems were treated as external forces.

Sergev and Iwan (1979) developed an algorithm to determine the natural frequencies and mode shapes of cables with attached masses. The equations of motion were derived for each element between two nodes, and continuity of displacements and balance of forces at nodes was imposed to evaluate the unknown coefficients and frequencies. This technique is equivalent to the shooting technique used for initial value problems.

Finite element methods (FEM). The basic concept of the finite element method is that the physical behavior within and around a typical element is characterized by the behaviors of its end points, called nodes. The locations of the nodes are then traced as functions of time similar to the LPM. A set of nonlinear ordinary differential equations are derived for each node and are integrated numerically in time.

In general, the elements are assumed to be straight lines (Webster, 1974). However, more accurate results with

fewer cable elements were reported by Leonard (1972) when he used curved elements for which continuity of slope across nodal points was enforced. Ma (1976) utilized isoparametric curved elements developed by Coons (1967) in his study on the effects of slackening (zero tension) or plasticity under load on cable responses. Lo and Leonard (1978) extended that work to include hydrodynamic effects.

Based on O'Brien's work (1964, 1967), Peyrot and Goulis (1978, 1979) developed an algorithm to analyze three-dimensional elastic cable substructures which were subjected to gravity, thermal, or wind loads. The algorithm was built around a cable subprogram. From given loads and given positions of the ends of a cable, the subprogram determined the complete geometry of the cable, its end forces and its increment stiffness matrix. The cable elements were assumed to have a two-dimensional catenary shape and were connected together to substructure nodes. The equilibrium configuration of the assembly was approached by successive iterations which decrease the imbalance of forces which may exist at each node at the end of the previous iteration. This technique was extended further by Peyrot (1980) to include hydrodynamic loads and contact with the sea floor effects. Jayaraman and Knudson (1981) improved the method so as to handle concentrated loads and

to utilize the more efficient Newton-Raphson method for solving the cable equation of motions.

A computer program called SEADYN (Webster, 1974) has been developed for analyzing underwater cable structures. The program utilizes finite element techniques which can incorporate both linear and nonlinear materials. SEADYN is currently used as a standard program for investigating cable motion in an ocean environment. Unfortunately, SEADYN is not equipped to simulate the motion of cables made of inelastic or viscoelastic materials.

Numerical techniques for solving a set of nonlinear ordinary differential equations. Systems of nonlinear discrete, second-order differential equations are often encountered in the dynamic analysis of structures. They are usually solved by an incremental method, an iterative method, or a combination of both methods. For static problems in which the time variable is not involved, the approaches to finding solutions are similar to those used in dynamic problems. An excellent review of static solution methods is presented by Tillerson, Stricklin and Haisler (1974). Webster (1974) outlined a general review of the applications of the incremental and iterative methods to both static and dynamic problems.

The basis of the incremental method for dynamic problems is the subdivision of the total time into many small time steps. In each increment, or time step, the nonlinear differential equations are locally linearized and experessed in terms of incremental displacement (Bathe et al., 1975). These equations may then be solved by step-by-step integration (e.g., by the Newmark Beta method). At the end of each increment the dependent coefficients to be used in the next increment have to be re-evaluated based on the new parameters. This procedure is simple to apply and has been widely used, particularly for elasto-plastic problems (Ma, 1976). However, unless the time steps are very small the computed response may deviate appreciably from the true response, because equilibrium is not satisfied exactly at any step. The accuracy of the computed response can be improved by applying equilibrium correction terms (Webster, 1974).

Two types of iterative procedure are commonly used, namely Newton-Raphson iteration and successive approximations. In Newton-Raphson iteration the structural tangent stiffness matrix is reformed at every iteration, and a disadvantage of this procedure is that a large amount of computational effort may be required to form and decompose the stiffness matrix. In successive approximations the stiffness matrix is kept constant and is formed only once,

usually in an initial configuration. Successive approximations will typically converge more slowly than the Newton-Raphson iteration method, and schemes to accelerate convergence may be desirable. It is sometimes advantageous to use mixed strategies incorporating a combination of Newton-Raphson and successive approximations (Tillerson et al., 1974).

The mixing of the incremental and iterative procedure is often employed to overcome the drifting tendencies of the incremental techniques. In this procedure usually the Newton-Raphson method is used in each increment (Bathe et al., 1975).

1.2 Thesis Objectives

The basic objective of this research is to simulate the nonlinear responses of cables and cable-large body systems in an ocean environment. The finite element method is used to model the motion of the cable continuum and the six degree-of-freedom rigid motion is assumed for modeling the large body motion. The equilibrium equations developed from these models are then solved numerically by either an incremental method or a combination of incremental and iterative methods. The scope of work which will fulfill these objectives is as follows:

(1) development of a mathematical model for hydrodynamic forces which are represented by Morrison's equation for forces acting on the cable line and are derived by a diffraction theory for large bodies connected with the cables;

(2) utilization of the wake-oscillator model developed by Griffin et al. (1975) for the strumming effects on cable lines;

(3) development of an equilibrium equation for cables and cable-large body systems for both elastic and viscoelastic materials;

(4) development of an incremental residual feedback method and mixed incremental/iterative method for application in the solution of the equations of motion developed in (3) subject to nonconservative and nonlinear hydrodynamic forces;

(5) development of a linearized equation of motion of the cable-large body systems subjected to random hydrodynamic loadings;

(6) employment of the mode-superposition technique to solve (5) in the frequency domain with subsequent transformation to the time domain utilizing the Fast Fourier Transform (FFT) algorithm;

(7) development of a computer program based on models and methods developed in (1) through (6);

(8) validation of the computer program by comparison of example problems with existing data from previous analytical or experimental studies.

In Chapter 2, the governing equations of motion for a cable element are derived by the virtual work principle. The constitutive equations for both elastic and viscoelastic materials are incorporated in the equations. The finite element model for the incremental hydrodynamic forces and the assembly procedure for a six degree-of-freedom rigid body connected to cable elements are presented in Chapter 3. Numerical methods for solving the static and dynamic equations are given in Chapter 4. In Chapter 5, techniques for stochastic analysis of a cable-large body system are developed. Example problems are presented in Chapter 6 to validate the models developed in the previous chapters. Chapter 7 contains a summary and conclusions of the present study.

1.3 Significance of Study

The strumming analysis of cables using a wake-oscillator model, in which the interaction of the cable

vibration and the vortex is included, is expected to provide a better means for simulating cable motions. Similar expectations are anticipated for the inclusion of the displacement and tension coupling in the cable-large body system. The finite element model for linear viscoelastic materials will be useful in the study of the motions of cables made of nylon, or other synthetic fibers. The stochastic analysis of the response of the cable-large body system subject to random wave forces will be useful for investigating the effects of fatigue on the cable material and for the statistical prediction of the cable stress and displacement.

2.0 DEVELOPMENT OF THE EQUATION OF MOTIONS

Early nonlinear formulations of the equations of motion for large displacement response of structures were merely extensions of the existing linear formulations (Bathe, 1976). This approach was considered because finite element codes could easily be modified to apply incremental linear analyses with corrections to account for changes in geometry and in the state of material.

In this chapter, a general formulation for the nonlinear incremental equation of motion of cables is presented. Cables are assumed to accept only axial stresses and no assumption is made on the magnitudes of displacement and strain. The principle of virtual displacement is then used to describe the motion between two neighboring configurations of the cables. The treatment presented here closely follows those presented by Cescotto et al. (1979).

With regard to subscripts and superscripts, in general, the following convention is employed: A left superscript with capital Roman letters denotes the configuration in which the quantity occurs. A left subscript denotes the configuration in which the quantity is referred to. When both configurations are identical, the left subscript can be omitted.

A right superscript with Greek symbols denotes nodal quantities. A right subscript denotes the components of a vector or second-order tensor. All notations are defined following their first occurrence.

2.1 Equation of Equilibrium

Basically, two different approaches have been successfully used in incremental nonlinear finite element analyses. In the first approach, static and kinematic variables are referred to the initial undeformed configuration. This procedure is called Total Lagrangian Description (TLD). In the second approach, which is generally called Updated Lagrangian Description (ULD), all static and kinematic variables are referred to an updated configuration in each load step.

Basic equations of both formulations may be derived by means of virtual work or energy principles. The former will be used here since it is more general and directly enables one to consider history-dependent constitutive laws. The incremental forms may be obtained, either by subtracting the equilibrium equations of two neighboring configurations and then linearizing the results, or by expanding the nonlinear equation from the known current configuration to the next incremental equation. The

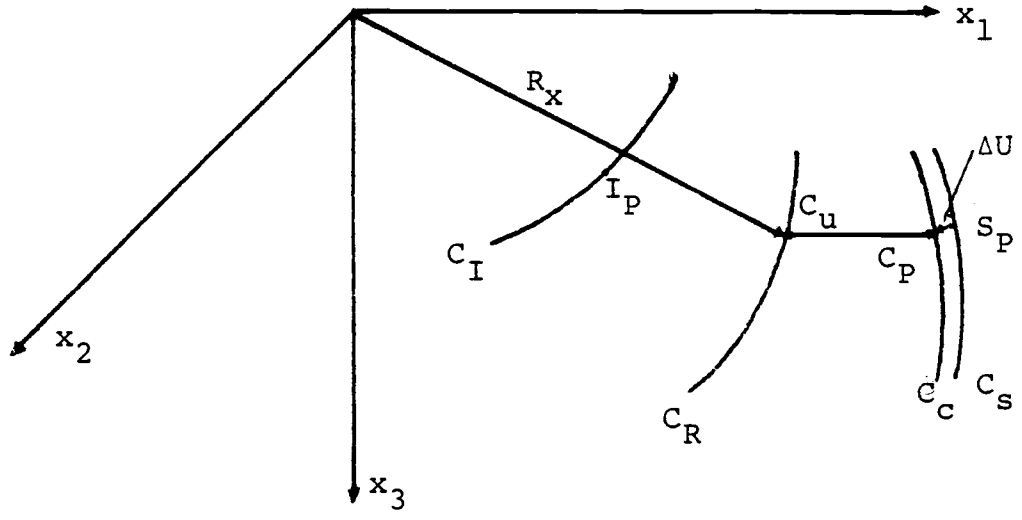

Figure 2.1-1. Successive configurations of the cable.

latter is more straightforward and easier to employ than the former; therefore, it will be used in this study.

In the motion of the body--in this case, the cable--four successive configurations are considered (Figure 2.1-1): the initial (unstrained, undeformed) configuration C_I, the reference configuration C_R, the current updated configuration C_C, and the incremented configuration C_S.

The equilibrium of a body in the incremented configuration C_S may be expressed by means of the stress equations of equilibrium,

$$\frac{\partial}{\partial {}^S\bar{x}_i} ({}^S\sigma_{ij}) + {}^S\rho({}^Sb_j - {}^S\ddot{u}_j) = 0 \qquad (2.1.1)$$

in which ${}^S\sigma_{ij}$ = the Cauchy stress component; ${}^S\rho$ = mass density; ${}^Sb_j$ = body force; ${}^Su_j$ = jth component of the displacement; and ${}^S\bar{x}_i$ = ith component of the position vector.

Let δu_j be the variations in ${}^Su_j$, assumed consistent with kinematical constraints. Multiplying Equation (2.1.1) by δu_j and integrating over the volume ${}^SVol$ of the body gives the virtual work expression (Fung, 1965).

$$\int_{{}^SVol} {}^S\sigma_{ij}\, \delta {}^S\varepsilon_{ij}\, d{}^SV = {}^SR \qquad (2.1.2)$$

in which

$$2\, \delta {}^S\varepsilon_{ij} = \frac{\partial}{\partial {}^S\bar{x}_i} (\delta u_j) + \frac{\partial}{\partial {}^S\bar{x}_j} (\delta u_i) \qquad (2.1.3)$$

and

$$ {}^{S}R = \int_{S_S} {}^{S}T_j \cdot \delta u_j \, d^{S}a + \int^{S}\rho ({}^{S}b_j - {}^{S}\ddot{u}_j) \cdot \delta u_j \, d^{S}V \qquad (2.1.4) $$

in which ${}^{S}T_j$ = surface traction force; ${}^{S}S$ = total surface area; and $d^{S}a$ = differential surface area.

Equations (2.1.2) and (2.1.4) cannot be solved directly because the incremental configuration C_S is unknown. A solution can be obtained by referring all variables to a previous equilibrium configuration. For this purpose, in principle, any one of the already calculated equilibrium configurations could be used (C_R in Figure 2.1.1). However, the choice lies essentially between two different descriptions, that is, the Total Lagrangian Description (TLD) and the Updated Lagrangian Description (ULD). The following section will present the general Lagrangian description in which the reference configuration is the arbitrary equilibrium configuration C_R. The equation becomes TLD when C_R approaches C_I and ULD when C_R approaches C_C.

2.1.a General Lagrangian Description

For cables, it is assumed the cable is stressed only in the direction of the cable axis; the axial stress

is uniform over the cross-sectional area; and the cross-sectional area remains plane during deformation. Thus, the cable geometry and kinematic variables can be described by one parameter, that is, the arc length. Using the arc length ${}^{R}D$ associated with the configuration C_R as the independent variable, Equation (2.1.2) may be transformed into

$$\int_{R_D} {}^{S}_{R}\sigma \; {}^{R}A \; \delta {}^{S}_{R}\varepsilon \; d^{R}s = {}^{S}_{R}\mathcal{R} \tag{2.1.a.1}$$

in which ${}^{R}A$ = the cross-sectional area; $d^{R}s$ = the infinitesimal arc length in C_R ; ${}^{S}_{R}\sigma$ = the axial second Piola-Kirchhoff stress in C_S but measured in C_R; and ${}^{S}_{R}\varepsilon$ = the axial Green-Lagrange strain in C_S but measured in C_R (Fung, 1965):

$${}^{S}_{R}\sigma = S_{\sigma}\left(\frac{d^{R}s}{d^{S}s}\right)^{2} \frac{R_{\rho}}{S_{\rho}} \tag{2.1.a.2}$$

$${}^{S}_{R}\varepsilon = \left\{\frac{1}{2}\left(\frac{d^{S}s}{d^{R}s}\right)^{2} - 1\right\} \tag{2.1.a.3}$$

The curved lengths $d^{S}s$ and $d^{R}s$ may be expressed by the sum of the products, of the cartesian coordinate position; i.e.,

$$d^S s = (d^S x_i \; d^S x_i)^{1/2} = (d^R x_i + {}^S u_i)^{1/2} (d^R x_i + {}^S u_i)^{1/2} \tag{2.1.a.4}$$

$$d^R s = (d^R x_i \; d^R x_i)^{1/2} \tag{2.1.a.5}$$

Substituting Equations (2.1.a.4) and (2.1.a.5) into Equations (2.1.a.2) and (2.1.a.3) gives, for incompressible material:

$$\overset{S}{R}\sigma = {}^S\sigma (1+2 \frac{d^R x_i}{d^R s} \frac{d^S u_i}{d^R s} + \frac{d^S u_i}{d^R s} \frac{d^S u_i}{d^R s}) \tag{2.1.a.6}$$

$$\overset{S}{R}\varepsilon = \frac{d^R x_i}{d^R s} \frac{d^S u_i}{d^R s} + \frac{1}{2} \frac{d^S u_i}{d^R s} \frac{d^S u_i}{d^R s} \tag{2.1.a.7}$$

Further, substituting Equations (2.1.a.6) and (2.1.a.7) into Equation (2.1.a.1) results in

$$\int_{R_D}^{R_A} \overset{S}{R}\sigma (\frac{d^R x_i}{d^R s} + \frac{d^S u_i}{d^R s}) \delta (\frac{d^S u_i}{d^R s}) d^R s = \overset{S}{R}R \tag{2.1.a.8}$$

Since the stress $\overset{S}{R}\sigma$ and displacement ${}^S u_i$ are unknown, the following incremental decompositions are used,

$$\overset{S}{R}\sigma = \overset{C}{R}\sigma + \Delta\sigma + \ldots \tag{2.1.a.9}$$

$$S_{u_i} = C_{u_i} + \Delta u \qquad (2.1.a.10)$$

$$C_{x_i} = R_{x_i} + C_{u_i} \qquad (2.1.a.11)$$

Equation (2.1.a.8) can now be written as

$$\int_{R_D} {}^{R}_{A} \left({}^{C}_{R}\sigma + \Delta\sigma\right) \left(\frac{d^{C}x_i}{d^{R}s} + \frac{d\Delta u_i}{d^{R}s}\right) \delta \left(\frac{d^{S}u_i}{d^{R}s}\right) d^{R}s = {}^{S}_{R}R \qquad (2.1.a.12)$$

The unknown quantities in Equation (2.1.a.12) are the incremental displacement components, Δu_i , and stress, $\Delta\sigma$. The incremental stress is related to Δu_i by a constitutive relationship dependent on the material.

2.1.b Total Lagrangian Description (TLD)

In the Total Lagrangian Description (TLD), all the variables are referred to the undeformed configuration. The configuration C_R now coincides with the configuration C_I and the Equation (2.1.a.12) becomes

$$\int_{I_D} {}^{I}_{A} \left({}^{C}_{I}\sigma + \Delta\sigma\right) \left(\frac{d^{C}x_i}{d^{I}s} + \frac{d\Delta u_i}{d^{I}s}\right) \delta \left(\frac{d^{S}u_i}{d^{I}s}\right) d^{I}s = {}^{S}_{I}R \qquad (2.1.b.1)$$

Now, assume that the coordinate x_i , and the displacement, u_i , can be represented by the approximation function

$$x_i(\xi) = \psi^{\alpha}(\xi)\ X_i^{\alpha} \qquad (2.1.b.2)$$

$$u_i(\xi) = \psi^{\alpha}(\xi)\ U_i^{\alpha} \qquad (2.1.b.3)$$

in which $\psi^{\alpha}(\xi)$ = the interpolation function of the natural coordinate ξ ; X_i^{α} , U_i^{α} = the ith components of position and displacement vectors of the nodal point α , respectively. This type of approximation function in which both the interpolation functions for the position and the displacement are identical is associated with the isoparametric element in the finite element method. The position and the displacement derivative with respect to arc length may be approximated by

$$\frac{dx_i}{ds} = \phi^{\alpha}(\xi)\ X_i^{\alpha} \qquad (2.1.b.4)$$

$$\frac{du_i}{ds} = \phi^{\alpha}(\xi)\ U_i^{\alpha} \qquad (2.1.b.5)$$

with

$$\phi^{\alpha}(\xi) = \frac{d\psi^{\alpha}(\xi)}{d\xi}\ \frac{d\xi}{ds} \qquad (2.1.b.6)$$

Substituting Equations (2.1.b.4-6) into Equation (2.1.b.1) and neglecting products of the incremental quantities, gives a linearized equation in the form

$$\int_{I_D} {}^{I}A\,{}^{C}_{I}\sigma\,\phi^{\alpha}(\xi)\phi^{\beta}(\xi)\Delta U_i^{\alpha}\delta\,{}^{S}U_i^{\beta}\; d^{I}s \;+$$

$$\int_{I_D} {}^{I}A\Delta\sigma\phi^{\alpha}(\xi)\phi^{\beta}(\xi)\; {}^{C}X_i^{\alpha}\;\delta\,{}^{S}U_i^{\beta}\; d^{I}s = \qquad (2.1.b.7)$$

$$ {}^{S}_{I}R - \int_{I_D} {}^{I}A\; {}^{C}_{I}\sigma\phi(\xi)\phi^{\beta}(\xi)\; {}^{C}X_i^{\alpha}\; {}^{S}U_i^{\beta}\; d^{I}s$$

in which

$$ {}^{S}_{I}R = -\int_{I_D} {}^{I}A\,{}^{I}\rho\psi^{\alpha}(\xi)\psi^{\beta}(\xi)\,{}^{S}\ddot{U}_i^{\alpha}\delta\,{}^{S}U_i^{\beta}\; d^{I}s \;+$$

$$\int_{I_D} {}^{S}_{I}F_i\psi^{\beta}(\xi)\delta\,{}^{S}U_i^{\beta}\; d^{I}s \qquad (2.1.b.8)$$

where the traction and the body forces are included in ${}^{S}_{I}F_i$.

Since the virtual displacement $\delta\,{}^{S}U_i^{\beta}$ is arbitrary, Equation (2.1.b.7) may be reduced to

$$\int_{I_D} {}^{I}A\,{}^{C}_{I}\sigma\phi^{\alpha}(\xi)\phi^{\beta}(\xi)\Delta U^{\alpha}_{i}\, d^{I}s \;+$$

$$\int_{I_D} {}^{I}A\Delta\sigma\phi^{\alpha}(\xi)\;\phi^{\beta}(\xi)\,{}^{C}X^{\alpha}_{i}\, d^{I}s = \qquad (2.1.b.9)$$

$${}^{S}_{I}\bar{R} - \int_{I_D} {}^{I}A\,{}^{C}_{I}\sigma\phi^{\alpha}(\xi)\phi^{\beta}(\xi)\,{}^{C}X^{\alpha}_{i}\, d^{I}s$$

in which

$${}^{S}_{I}\bar{R} = -\int_{I_D} {}^{I}A\,{}^{I}\rho\psi^{\alpha}(\xi)\psi^{\beta}(\xi)\;{}^{S}\ddot{U}^{\alpha}_{i}\; d^{I}s$$

$$+ \int_{I_D} {}^{S}_{I}F_{i}\psi^{\beta}(\xi)\, d^{I}s \qquad (2.1.b.10)$$

Equations (2.1.b.9) and (2.1.b.10) represent a linearized equation for the incremental displacement ΔU^{α}_{i} .

2.1.c Updated Lagrangian Description (ULD)

In the Updated Lagrangian Description, all variables in Equation (2.1.a.1) are referred to the current configuration, C_C ; namely, the updated configuration of the cable. The equilibrium configuration C_R in this case approaches the deformed configuration C_C . By doing so,

we may express Equation (2.1.b.1) as

$$\int_{C_D} {}^{C}A\left({}^{C}\sigma+\Delta\sigma\right)\left(\frac{d^{C}x_i}{d^{C}s}+\frac{d\Delta u_i}{d^{C}s}\right)\delta\left(\frac{d^{S}u_i}{d^{C}s}\right)d^{C}s = {}^{S}_{C}R \qquad (2.1.c.1)$$

Following a similar procedure to that used in the derivation for the TLD, Equation (2.1.c.1) may be transformed to

$$\int_{C_D} {}^{C}A\ {}^{C}\sigma\phi^{\alpha}(\xi)\phi^{\beta}(\xi)\ \Delta U_i^{\alpha}\ d^{C}s\ +$$

$$\int_{C_D} {}^{C}A\ \Delta\sigma\phi^{\alpha}(\xi)\phi^{\beta}(\xi)\ {}^{C}X_i^{\alpha}\ d^{C}s\ = \qquad (2.1.c.2)$$

$${}^{S}_{C}\bar{R} - \int_{C_D} {}^{C}A\ {}^{C}\sigma\ \phi^{\alpha}(\xi)\phi^{\beta}(\xi)\ {}^{C}X_i^{\alpha}\ d^{C}s$$

in which

$${}^{S}_{C}\bar{R} = -\int_{C_D} {}^{C}A\ {}^{C}\rho\ \psi^{\alpha}(\xi)\psi^{\beta}(\xi)\ {}^{S}\ddot{U}_i^{\alpha}\ d^{C}s\ +$$

$$\int_{C_D} {}^{S}_{C}F_i\psi^{\beta}(\xi)\ d^{C}s \qquad (2.1.c.3)$$

The interpolation function $\phi^{\alpha}(\xi)$ used in Equation (2.1.c.3) is not the same as the one used in TLD. Later, in the finite element formulation it will be shown how they differ.

Equations (2.1.c.2) and (2.1.c.3) are the nonlinear incremental equations in C_S referenced to the current configuration C_C . The equilibrium equations in TLD and ULD are theoretically equivalent because they use the same balance principle. The choice between the two formulas, therefore, depends on the ease and efficiency of the formulation. The advantage of using the TLD over ULD is that the element properties need not be explicitly transformed to account for updating of the nodal coordinates resulting from changes in geometry. However, this advantage is counteracted by requiring to transform the computed true stress into the pseudo stress used in TLD. In the following section we will show that for the pseudo-Hookean material, both TLD and ULD will give the same stiffness matrix.

2.2 Stress-Strain Relationship

In this study, two types of materials are considered. The first is a pseudo-Hookean material in which the stress is expressed in terms of the tangent modulus and the incremental strain. The second is a linear viscoelastic material in which the stress is dependent on the time history of the strain. The standard linear solid model is chosen in this study because it represents most of the cable materials used in ocean applications (Bitting, 1979).

2.2.a Pseudo-Hookean Material

The constitutive equation of the pseudo-Hookean material is represented by

$$S_{\bar{\sigma}} = {}^{C}_{\bar{\sigma}} + {}^{C}E \left[\frac{d^{S}s - d^{C}s}{d^{I}s}\right] \qquad (2.2.a.1)$$

in which $S_{\bar{\sigma}}$ = traction force in the incremented configuration C_S, per unit area in the unstrained state C_I; $C_{\bar{\sigma}}$ = traction force in the current configuration C_C, per unit area in C_I; and ^{C}E = Young's modulus in the deformed state C_C.

The stress and displacement relationship may be obtained by substituting Equations (2.1.a.4), (2.1.a.5) in which C_R approaches C_C, and Equations (2.1.b.4), (2.1.b.5) into Equation (2.2.a.1); i.e.,

$$S_{\bar{\sigma}} = {}^{C}_{\bar{\sigma}} + {}^{C}E\lambda_C \phi^{\gamma}(\xi)\phi^{\eta}(\xi) \; {}^{C}X_i^{\gamma} \; \Delta U_i^{\eta} \qquad (2.2.a.2)$$

with

$$\lambda_C = \frac{d^{C}s}{d^{I}s} \qquad (2.2.a.3)$$

Before applying this relation in both the TLD and ULD forms of the equations of equilibrium it is necessary to relate the stress in Equation (2.2.a.2) with the second Piola-Kirchhoff stress employed in both TLD and ULD

$$S_{\bar{\sigma}}\, {}^{I}A = S_{\sigma} S_{A} \tag{2.2.a.4}$$

in TLD, for incompressible material (Fung, 1965).

$$S_{\bar{\sigma}} {}^{I}A = \left(\frac{d^{I}s}{d^{S}s}\right)^{2} S_{\sigma} {}^{I}A = \left(\frac{d^{I}s}{d^{S}s}\right)^{2} \frac{S_{\bar{\sigma}}({}^{I}A)^{2}}{S_{A}} \tag{2.2.a.5}$$

with

$$\frac{{}^{I}A}{S_{A}} = \frac{d^{S}s}{d^{I}s} \tag{2.2.a.6}$$

Substituting Equations (2.2.a.2) and (2.2.a.6) into Equation (2.2.a.5) gives

$$S_{\sigma} {}^{I}A = \frac{1}{\lambda_{C}}\, C_{\bar{\sigma}} {}^{I}A \left(\frac{d^{S}s}{d^{C}s}\right) + \frac{C_{E}}{\lambda_{C}^{2}}\, {}^{I}A\phi^{\gamma}(\xi) \cdot \cdot \phi^{\eta}(\xi)\, {}^{C}X_{i}^{\gamma}\, \Delta U_{i}^{\eta} \left(\frac{d^{S}s}{d^{C}c}\right) \tag{2.2.a.7}$$

The factor λ_{C}^{2} in the second term of the right hand side

of the equation appears because of the transformation of the interpolation function $\phi^{\alpha}(\xi)$ in Equation (2.2.a.2) for C_C to the $\phi^{\alpha}(\xi)$ in C_I.

Recalling that ${}^{S}_{I}\sigma = {}^{C}_{I}\sigma + \Delta\sigma$, we may write Equation (2.1.b.9) as

$$\int_{I_D} \frac{I_A}{\lambda_C} C_{\bar{\sigma}} \phi^{\alpha}(\xi)\phi^{\beta}(\xi)\ \Delta U_i^{\alpha}\ d^{I}s + \int_{I_D} \frac{I_A}{\lambda_C^3} [C_{\bar{\sigma}} + C_{E\lambda_C}]\phi^{\alpha}(\xi)\phi^{\beta}(\xi)\phi^{\gamma}(\xi)\phi^{\eta}(\xi) \cdot \cdot C_{X_i^{\alpha}}\ C_{X_j^{\gamma}}\ \Delta U_j^{\eta}\ d^{I}s = {}^{S}_{I}\bar{R} - \int_{I_D} \frac{I_A C_{\bar{\sigma}}}{\lambda_C} \phi^{\alpha}(\xi)\phi^{\beta}(\xi) C_{X_i^{\alpha}}\ d^{I}s \tag{2.2.a.8}$$

with

$${}^{S}_{I}\bar{R} = -\int_{I_D} {}^{I}_{A}I_{\rho\psi}{}^{\alpha}(\xi)\psi^{\beta}(\xi)\, {}^{S}\ddot{U}_i^{\alpha}\ d^{I}s + \int_{I_D} {}^{S}_{I}F_i\psi^{\beta}(\xi)\ d^{I}s \tag{2.2.a.9}$$

By an analogous procedure to the derivation of the constitutive equation in TLD, Equation (2.2.a.7) can be transformed into

$$ {}^{S}_{C}\sigma\,{}^{C}A = \{{}^{C}\bar{\sigma}\,{}^{I}A + {}^{C}E\,{}^{I}A\lambda_C $$

$$ \cdot \phi^{\gamma}(\xi)\phi^{\eta}(\xi)\,{}^{C}X^{\gamma}_{j}\Delta U^{\eta}_{j}\} \frac{d^{S}s}{d^{C}s} \qquad (2.2.a.10) $$

Substituting Equation (2.2.a.10) into Equation (2.1.c.2) and recalling that ${}^{S}_{C}\sigma = {}^{C}\sigma + \Delta\sigma$, one obtained the incremental equation of equilibrium in ULD as

$$ \int_{C_D} {}^{I}A\,{}^{C}\bar{\sigma}\phi^{\alpha}(\xi)\phi^{\beta}(\xi)\Delta U^{\alpha}_{i}\; d^{C}s + $$

$$ \int_{C_D} {}^{I}A[{}^{C}\bar{\sigma} + {}^{C}E\lambda_C]\phi^{\alpha}(\xi)\phi^{\beta}(\xi)\phi^{\gamma}(\xi)\phi^{\eta}(\xi)\,{}^{C}X^{\alpha}_{i}\,{}^{C}X^{\gamma}_{j}\Delta U^{\eta}_{j}\; d^{C}s = $$

$$ {}^{S}_{C}\bar{R} - \int_{C_D} {}^{I}A\,{}^{C}\bar{\sigma}\phi^{\alpha}(\xi)\phi^{\beta}(\xi)\,{}^{C}X^{\alpha}_{i}\; d^{C}s \qquad (2.2.a.11) $$

with

$$ {}^{S}_{C}\bar{R} = -\int_{C_D} \frac{{}^{I}A\,{}^{I}\rho}{\lambda_C}\psi^{\alpha}(\xi)\psi^{\beta}(\xi)\;{}^{S}U''^{\alpha}_{i}\; d^{C}s $$

$$ + \int_{C_D} \frac{{}^{S}_{C}F_i}{\lambda_C}\psi^{\beta}(\xi)\; d^{C}s \qquad (2.2.a.12) $$

Equation (2.2.a.8) and Equation (2.2.a.11) will result in identical forms when

$$\phi^{\alpha}(\xi)(\text{in TLD}) = \lambda_c \, \phi^{\alpha}(\xi)(\text{in ULD}) \qquad (2.2.a.13)$$

which will subsequently be shown to be true later in the finite element model.

2.2.b Linear-Viscoelastic Material

For viscoelastic materials, the constitutive relations involve, generally, stress rates and strain rates. In particular, for linear-viscoelastic materials, it is possible to represent their behavior by a model made up of springs and dashpots. Therefore, the stress-strain relationships for linear viscoelastic materials (Fung, 1965) is

$$a_o \varepsilon(t) + \sum_{n=1}^{N} a_n \frac{d^n}{dt^n} \varepsilon(t) = b_o \sigma(t) + \sum_{n=1}^{N} b_n \frac{d^n}{dt^n} \sigma(t) \qquad (2.2.b.1)$$

in which $\frac{d^n}{dt}$ = the nth derivative with respect to time, t ; $a_o, \ldots, a_n$ and $b_o, \ldots, b_n$ = real-valued constants.

In this study, a three-parameter standard linear solid model which is employed by the NOAA (National Oceanic and Atmospheric Administration) Data Buoy Model (see Bitting, 1979) is utilized to represent viscoelastic materials which are frequently used in the ocean environment. The

stress-strain equation of this model is given by Equation (2.2.b.1) when only the first and lower derivative terms are retained, i.e.,

$$K_o \varepsilon(t) + \tau(K_o+K_1) \frac{d\varepsilon(t)}{dt} = \sigma(t) + \tau \frac{d\sigma(t)}{dt} \quad (2.2.b.2)$$

A mechanical analog of this three-parameter model is shown in Figure (2.2.b-1). The spring constant, K_o, represents quasi-static behavior of the cable. The energy dissipation mechanism is represented by the dashpot, having damping constant N, and the spring, having spring constant K_1. The characteristic time τ appearing in Equation (2.2.b.2) is the ratio of damping N to spring constant K_1.

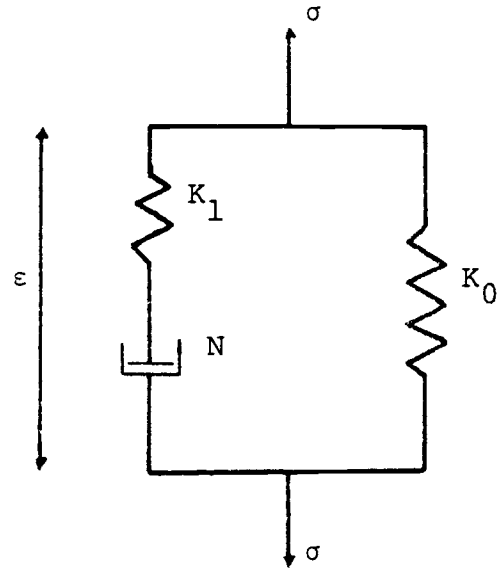

Figure 2.2.b-1. Three-parameter standard linear solid model.

The incremental form of the constitutive equation may be obtained from Equation (2.2.b.2) by approximating the quantities $\frac{d\varepsilon(t)}{dt}$ and $\frac{d\sigma(t)}{dt}$ with $\frac{\Delta\varepsilon}{\Delta t}$ and $\frac{\Delta\sigma}{\Delta t}$, respectively; i.e.,

$$\Delta\sigma = [K_o\varepsilon(t) - \sigma(t)]\frac{\Delta t}{\tau} + (K_o + K_1)\Delta\varepsilon \qquad (2.2.b.3)$$

in which $\varepsilon(t)$ = the known current strain; $\sigma(t)$ = the known current stress; and the incremental strain, $\Delta\varepsilon$, may be expressed in terms of the incremental displacement by

$$\Delta\varepsilon = \frac{1}{2}\frac{(d^S s)^2 - (d^C s)^2}{(d^I s)^2} \qquad (2.2.b.4)$$

or

$$\Delta\varepsilon = \left(\frac{d^C s}{d^I s}\right)^2 \left[\frac{d^C x_i}{d^C s}\frac{d\Delta u_i}{d^C s} + \frac{1}{2}\frac{d\Delta u_i}{d^C s}\frac{d\Delta u_i}{d^C s}\right] \qquad (2.2.b.5)$$

Substituting Equations (2.1.b.4), (2.1.b.5), and (2.2.a.3) into Equation (2.2.b.5) and neglecting the product of the incremental quantities gives the linearized approximation of the incremental strain equation,

$$\Delta\varepsilon = \lambda_C^2 \phi^\gamma(\xi)\phi^\eta(\xi)\ {}^C X_i^\gamma\ \Delta U_i^\eta \qquad (2.2.b.6)$$

Substitution of Equation (2.2.b.6) into Equation (2.2.b.3) yields

$$\Delta\sigma = (K_0 {}^{C}_{I}\varepsilon - {}^{C}_{\bar{\sigma}})\frac{\Delta t}{\tau} + (K_0+K_1)\lambda_C^2 \Phi(\xi)\Phi^{\eta}(\xi)\, {}^{C}X_i^{\gamma}\, \Delta U_i^{\eta} \quad (2.2.b.7)$$

The accuracy of Equation (2.2.b.7) increases when quantities $\frac{\Delta t}{\tau}$ and Δu are small. A typical commercial viscoelastic material has the characteristic time, τ = 5 seconds. Therefore, for $\Delta t << 5$ seconds and for small incremental displacement, Equation (2.2.b.7) approximates the exact stress-strain relationship given by Equation (2.2.b.2).

By similar procedure to the derivation of the equilibrium equation of the pseudo-Hookean material, we may

$$\int_{C_D} {}^{I}A\, {}^{C}_{\bar{\sigma}}\, \Phi^{\alpha}(\xi)\Phi^{\beta}(\xi)\, \Delta U_i^{\alpha}\, d^{C}s \; +$$

$$\int_{C_D} {}^{I}A\, [{}^{C}_{\bar{\sigma}} + \lambda_C^2\, (K_o+K_1)]\, \Phi^{\alpha}(\xi)\, \Phi^{\beta}(\xi)\, \Phi^{\gamma}(\xi)\, \Phi^{\eta}(\xi) \cdot$$

$$\cdot\, {}^{C}X_i^{\alpha}\, {}^{C}X_j^{\gamma}\, \Delta U_j^{\eta}\, d^{C}s \;=\; {}^{S}_{C}\bar{R} -$$

$$\int_{C_D} {}^{I}A({}^{C}_{I}K_o\varepsilon - {}^{C}_{\bar{\sigma}})\, \frac{\Delta t}{\tau}\, \Phi^{\alpha}(\xi)\, \Phi^{\beta}(\xi)\, {}^{C}X_i^{\alpha}\, d^{C}s -$$

$$\int_{C_D} {}^{I}A\, {}^{C}_{\sigma}\, \Phi^{\alpha}(\xi)\, \Phi^{\beta}(\xi)\, {}^{C}X_i^{\alpha}\, d^{C}s \quad (2.2.b.8)$$

write the universal equation of equilibrium (applicable both to TLD and ULD) of the viscoelastic material as

in which the external force $\overset{S}{C}\bar{R}$ is given by Equation (2.2.a.12). The second term of the right hand side of the Equation (2.2.b.8) represents a delay in the response of the cable.

3.0 FINITE ELEMENT MODEL

The fundamental concept of the finite element method is that the physical behavior within and around a typical element is characterized by the behaviors of its end points, called nodes. The displacement of the cable at any point and time is approximated sectionally by a piecewise continuous function which has an exact value at a nodal point. In this study, isoparametric finite elements are employed to model any quantities such as displacements, positions, hydrodynamic forces, etc., in the cable continuum. Because of its simplicity, the two-noded straight element is used to investigate the cable response to the hydrodynamic forces (deterministic and nondeterministic). The introduction of a higher-order element can be easily implemented. For more details on finite element modeling, one may refer to references (Zienkiewicz, 1979), (Cook, 1973), and (Desai, 1972).

3.1 Two-noded Straight Cable Element

Consider a straight element PQ (see Figure 3.1.1) with element length L . It has two nodes (node 1 and 2) located at the ends of the element. The interpolating functions which appear in Section 2.1.b may be represented

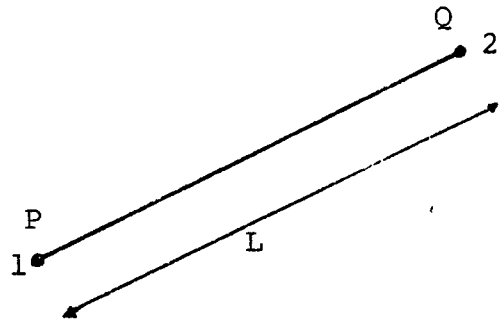

Figure 3.1-1. Straight cable element.

by

$$\psi^1(\xi) = 1 - \xi \qquad (3.1.1.a)$$

$$\psi^2(\xi) = \xi \qquad (3.1.1.b)$$

and

$$\phi^1(\xi) = -1/L \qquad (3.1.2.a)$$

$$\phi^2(\xi) = 1/L \qquad (3.1.2.b)$$

with

$$\xi = \ell/L \qquad (3.1.3)$$

in which ℓ = the location of a point in the cable measured from node 1.

Now, let the cable length in the undeformed configuration, C_I, be donoted by ^{I}L and in the deformed configuration, C_C, by ^{C}L. The derivative shape functions in C_I and C_C may be obtained from Equations (3.12.a,b); i.e.,

$$\text{in } C_I: \quad \phi^1(\xi) = -\,{}^{1}/_{I_L} \tag{3.1.4.a}$$

$$\phi^2(\xi) = {}^{1}/_{I_L} \tag{3.1.4.b}$$

$$\text{in } C_C: \quad \phi^1(\xi) = -\,{}^{1}/_{C_L} \tag{3.1.5.a}$$

$$\phi^2(\xi) = -\,{}^{1}/_{C_L} \tag{3.1.5.b}$$

The relationship between the derivative shape functions in C_I and C_C may then, in general, be expressed as

$$\phi^{\alpha}(\xi) \text{ (in } C_I) = \lambda_C \, \phi^{\alpha}(\xi) \text{ (in } C_C) \; ; \; \alpha = 1,2 \tag{3.1.6}$$

with

$$\lambda_C = {}^{C_L}/_{I_L} \tag{3.1.7}$$

as pointed out previously in Section 2.2.a.

The finite element form of the governing equations of motion may be obtained by substituting the shape functions

given by Equations (3.1.1.a,b) and (3.1.2.a,b) into either TLD or ULD form of the equations of equilibrium, which for the pseudo-Hookean material are given by Equations (2.2.a.8, 9) and (2.2.a.11,12)

$$\left({}^{I_A}C_{\bar{\sigma}}\,[K_L] + {}^{I_A}C_{\bar{\sigma}} + {}^{C}E\lambda_C)[K_{NL}]\right)\{\Delta U\} =$$

$$-\frac{I_A I_\rho}{\lambda_C}[M]\{\ddot{U}\} + \{F\} - {}^{I_A}C_{\bar{\sigma}}[K_L]\{X\} \qquad (3.1.8.a)$$

and for the viscoelastic material are given by Equation (2.2.b.8),

$$\left({}^{I_A}C_{\bar{\sigma}}[K_L] + ({}^{I_A}C_{\bar{\sigma}} + \lambda_C^2(K_o+K_1))[K_{NL}]\right)\{\Delta U\} =$$

$$-\frac{I_A I_\rho}{\lambda_C}[M]\{\ddot{U}\} + \{F\} - {}^{I_A}\left(\frac{\Delta t}{\tau}(K_o{}^{C}\varepsilon - C_{\bar{\sigma}}) + C_{\bar{\sigma}}\right)[K_L]\{X\} \qquad (3.1.8.b)$$

in which $[K_L]$ = the linear stiffness matrix due to initial stress,

$$[K_L] = \frac{1}{C_L}\begin{bmatrix} [I]_{3x3} & -[I]_{3x3} \\ -[I]_{3x3} & [I]_{3x3} \end{bmatrix} \qquad (3.1.9)$$

$[K_{NL}]$ = the nonlinear stiffness matrix due to cable distortions

$$[K_{NL}] = \frac{1}{(C_L)^3} \begin{bmatrix} [C^{11}]_{3x3} & [C^{12}]_{3x3} \\ [C^{21}]_{3x3} & [C^{22}]_{3x3} \end{bmatrix} \qquad (3.1.10)$$

with

$$C_{ij}^{11} = C_{ij}^{22} = C_{X_i^1 C_{X_j^1}} - (C_{X_i^1 C_{X_j^2}} + C_{X_i^2 C_{X_j^1}}) + C_{X_i^2 C_{X_j^2}}$$

$$C_{ij}^{12} = C_{ij}^{21} = - C_{ij}^{11} \qquad (3.1.11)$$

[M] = the mass matrix

$$[M] = C_L \begin{bmatrix} 1/3[I]_{3x3} & 1/6[I]_{3x3} \\ 1/6[I]_{3x3} & 1/3[I]_{3x3} \end{bmatrix} \qquad (3.1.12)$$

{F} = equivalent nodal forces; and {X} = nodal positions.

Equation (3.1.8.a) and (3.1.8.b) are equilibrium equations for each individual element. The global equations which represent the governing equations for the entire cable-body system are obtained from the equations of individual element by assembly process. Rules and procedures of

the assembly process are given in references (Zienkewicz, 1979), (Bathe, 1976), and (Desai, 1972).

3.2 Hydrodynamic Forces

Hydrodynamic loadings on a cable element may be grouped into three types of forces: 1) drag forces; 2) inertial forces; and 3) lift forces. Drag forces are due to skin friction and form drag (or pressure drag). Skin friction is a drag force which is solely caused by a fluid viscosity. Form drag results from the formation of vortices or eddies and from separation of flow behind the cable element (see Hoerner, 1960). Consequently, the drag forces may be decomposed into a drag tangent to the cable element and a drag perpendicular to the cable element (in the plane formed by the cable element and the relative fluid velocity vector). The drag along the cable element is equal to the skin friction of a flat plate having the same surface area as that of the cable element. The drag perpendicular to the cable element consists of both frictional drag and form drag. For the accelerating fluid, the combination of the drag force and inertia force, both perpendicular to the cable element, is given by Morison's equation (Morison et al., 1950) in which the drag and inertial coefficients are usually taken as functions of Reynold's number. Lift forces are the oscillating transverse forces (perpendicular to the

plane formed by the cable element and the relative fluid velocity vector) which results from vortex shedding. The lock-in condition is assumed to take place as the shedding frequency approaches a cable material frequency.

3.2.a Morison's Equation

Morison's equation, first introduced by Morison et al. (1950), is a semiempirical formulation for the in-line force in an accelerating fluid and has, in particular, been extensively applied to oscillatory flows. It is based on the important assumption that the total in-line wave forces may be obtained by adding two component forces, each of which may be determined separately; that is, drag force and inertial force which may be expressed by

$$F_{Ni} = C_D \rho_f \frac{D}{2} V_N V_{Ni} + C_M \rho_f \frac{\pi D^2}{4} a_{Ni} \qquad (3.2.a.1)$$

in which F_{Ni} = ith component of hydrodynamic force perpendicular to cable element; V_N = magnitude of normal fluid velocity; V_{Ni} = ith component of normal fluid velocity; a_{Ni} = ith component of normal fluid acceleration; ρ_f = fluid mass density; D = structure diameter; C_D = normal drag coefficient; and C_M = inertial force coefficient.

Equation (3.2.a.1) was originally derived for a stationary structure. When the structure is nonstationary Equation (3.2.a.1) may be modified to include the interaction between fluid and structure; i.e.,

$$F_{Ni} = C_D \rho_f \frac{D}{2} V_{NR} V_{NRi} + \rho_f \frac{\pi D^2}{4} [C_M a_{Ni} - (C_M - 1) \ddot{U}_{Ni}] \qquad (3.2.a.2)$$

in which V_{NR} = magnitude of normal relative fluid velocity; V_{NRi} = ith component of normal relative fluid velocity defined by

$$V_{NRi} = V_{Ni} - U_{Ni} \qquad (3.2.a.3)$$

where $\dot{U}_{Ni}$, $\ddot{U}_{Ni}$ = ith component of the normal structural velocity and acceleration.

Skin drag along the cable length is defined by

$$F_{Ti} = C_T \rho_f \pi \frac{D}{2} V_{TR} V_{TRi} \qquad (3.2.a.4)$$

in which F_{Ti} = ith component of hydrodynamic force tangent to cable element; C_T = tangential drag coefficient; V_{TR} = magnitude of the relative tangential fluid velocity; and V_{TRi} = ith component of the relative tangential fluid velocity which is defined by

$$V_{TRi} = V_{Ti} - \dot{U}_{Ti} \tag{3.2.a.5}$$

where V_{Ti} , $\dot{U}_T$ = fluid velocity and cable velocity in the tangent direction respectively. The quadratic term and the dependence of F_{Ni} and F_{Ti} on the position and orientation of the cable element contribute to nonlinearities in the cable equations of motion. The expression for these hydrodynamic forces at nodal point and at time $t + \Delta t$ may be obtained by Taylor expansion; i.e.,

$$F_i\Big|_{t+\Delta t} = F_{Ni}\Big|_{t+\Delta t} + F_{Ti}\Big|_{t+\Delta t} =$$

$$F_{DNi}\Big|_t + F_{Ti}\Big|_t + \{\frac{B_D}{V_{NR}} V_{NRi}\, V_{NRj} + B_D V_{NR}\, \delta_{ij}$$

$$+ (2\, B_T V_{TR} - B_D V_{NR})\theta_i\theta_j\} \cdot (\Delta V_j - \Delta\dot{U}_j)$$

$$+ B_I C_M(\delta_{ij} - \theta_i\theta_j)\, a_j - B_I(C_M - 1)(\delta_{ij} - \theta_i\theta_j)\, \ddot{U}_j$$

$$+ S_{ij}\, \Delta U_j \tag{3.2.a.6}$$

in which

$$B_D = \frac{1}{2}\, \rho_f\, C_D\, \frac{D}{2}$$

$$B_T = \frac{1}{2}\, \rho_f\, C_T\, \pi D$$

$$B_I = \rho_f\, \frac{\pi D^2}{4} \tag{3.2.a.7}$$

F_{DNi} = ith component of drag force perpendicular to cable element; θ_i = ith direction cosine of the cable at node α ; S_{ij} = the incremental stiffness due to the change of position and orientation and which may be considered negligible compared to the other; and δ_{ij} is defined by

$$\delta_{ij} = 1 \text{ for } i = j$$

$$= 0 \qquad i \neq j \qquad (3.2.a.8)$$

The hydrodynamic force anywhere along the cable element may be expressed in terms of the force at nodes on the element. However, when consistent forces (consistent with the constraint on the virtual displacement imposed on nodal points and along the cable element) is employed, the drag damping and the added mass matrix will become non-symmetric. To avoid this problem, one may integrate the force distribution along the cable and lump it at the corresponding nodal points. For example, assume that the hydrodynamic force is linearly distributed along the cable; i.e.,

$$F_{Ni}(\xi) = \psi^{\alpha}(\xi)\ F^{\alpha}_{Ni} \ ; \ \alpha = 1,2 \qquad (3.2.a.9)$$

in which $\psi^{\alpha}(\xi)$ = the straight element shape function given

by Equations (3.1.1.a,b). The lumped force may be expressed as

$$F_i^1 = L \int_0^{1/2} \psi^\alpha(\xi) F_{Ni}^\alpha \, d\xi \qquad (3.2.a.10.a)$$

$$F_i^2 = L \int_{1/2}^{1} \psi^\alpha(\xi) \, F_{Ni}^\alpha \, d\xi \qquad (3.2.a.10.b)$$

in which F_i^1 , F_i^2 = ith component of lumped hydrodynamic forces at node 1 and 2, respectively.

3.2.b Lift Force

Lift forces are the periodic transverse forces on the cable generated by vortices as they alternately shed from each side of the cable. For a simple case when the fluid flow is steady and the structure is stationary, the frequency of the oscillation of these forces is proportional to the fluid velocity and is equivalent to the shedding frequency. For unsteady flow such as for ocean waves, this frequency is assumed to take a form similar to that of steady flow with variable velocity (Vaicaitis, 1976). For a nonstationary structure the oscillating frequency is no longer equal to the shedding frequency: resonance will take place which in turn alters the response frequency. This resonance (lock-in or synchronization) phenomena

was pointed out by Bishop and Hassan (1964) in their experiment with a rigid cylinder oscillating vertically in steady, uniform horizontal flow. Later, Hartlen and Currie (1970) and Griffin et al. (1975) developed a wake-oscillator model for predicting the lift coefficient as a function of time. Iwan and Blevin (1974) derived the lift force on a cylinder by use of the momentum equation with a so-called "hidden parameter" introduced into the equation: the result is very much similar to the wake-oscillator model.

In this study the first model is employed and the resonance is assumed to occur such that the dominant structural response frequency is the structural natural frequency having a value closest to the shedding frequency, which is assumed to be constant for steady flow and variable for unsteady flow. Because the strumming (the motion due to lift forces) frequency is much higher than the response frequency due to the fluid drag and inertial force and because the transverse displacement is much smaller than the inline motions, the transverse motion may be treated independently. The transverse motion is assumed to fluctuate about the inline motion. Due to this transverse fluctuation, the wake behind the cable will magnify which may cause the form drag to increase (Skop and Griffin, 1977). Consequently, the strumming may

be evaluated by using the mode-superposition technique in which the mode shapes and natural frequencies of the structure, are recomputed every time step or every several steps of incremental response (Morris, 1977).

The computational steps which will be employed here may be summarized as follows:

(1) set the time increment, δt, which is used in the strumming analysis, note that Δt is the time increment used in the inline motion analysis;

(2) determine relative fluid velocities and shedding frequencies;

(3) form mass and stiffness matrix;

(4) compute natural frequencies and mode shapes;

(5) compute lift force coefficients by wake-oscillator model;

(6) compute lift forces;

(7) compute modal equations;

(8) compute the transverse displacements and velocities by mode-superposition technique;

(9) increment the time $t = t_1 + \delta t$ in which t_1 is the time that the mass, stiffness, shedding frequency and other quantities are evaluated;

(10) repeat steps (5) through (9) when $t < t_2$ (in which $t_2 = t_1 + \Delta t$), otherwise proceed to the

next step; and

(11) assign t_1 to t_2 and repeat steps (2) through (10).

The lift force per unit length acting on the nodal point may be expressed as

$$F_{Li} = \frac{1}{2} \rho_f D C_L \varepsilon_{ik\ell} \theta_k V_{NR} V_{NR\ell} \qquad (3.2.b.1)$$

in which F_{Li} = ith component of lift force; C_L = periodic lift force coefficient; V_{NRi} = ith component of the normal relative fluid velocity given by Equation (3.2.a.3); and the permutation symbol $\varepsilon_{ik\ell}$ is defined by

$$\begin{aligned} \varepsilon_{ik\ell} &= 0 \ ; \text{ for two indices equal} \\ &= 1 \ ; \text{ for even permutation} \\ &= -1 \ ; \text{ for odd permutation} \end{aligned} \qquad (3.2.b.2)$$

The periodic lift coefficient is assumed to be represented by a wake oscillation model and may be expressed by (Griffin et al., 1975)

$$\ddot{C}_L + \omega_s^2 C_L - [C_{L0} - C_L^2 - (\dot{C}_L/\omega_s)^2] \cdot$$

$$\cdot (\omega_s \bar{G} \dot{C}_L - \omega_s^2 \bar{H} C_L) = \omega_s \bar{F} \dot{U}_{TL}/D \qquad (3.2.b.3)$$

in which dots denotes partial derivatives with respect to time; ω_s = the Strouhal (shedding) frequency defined by

$$\omega_s = 2\pi S_T V_{NR}/D \qquad (3.2.b.4)$$

where S_T = Strouhal number; C_{L0} = constant lift force coefficient amplitude for fixed structure; $\dot{U}_{TL}$ = the transverse cable velocity magnitude; and $\bar{G}$, $\bar{H}$, and $\bar{F}$ = empirical parameters defined by

$$\log_{10} \bar{G} = 0.25 - 0.21\, S_G$$

$$\bar{H} = \xi h$$

$$\log_{10}(hS_G^2) = -0.24 + 0.66 S_G$$

$$\bar{F} = 4\bar{G}\, S_G/h$$

where

$$S_G = 2\pi S_T^2\, k_s$$

$$k_s = \frac{4\pi m\xi}{\rho_f D^2} = 45\, (\nu/\omega_s)^{1/2}/D \qquad (3.2.b.6)$$

in which m = structural mass + added mass per unit length; ν = fluid viscosity; h = dummy variable; and ξ =

damping ratio. For cables the added mass is independent of the transverse displacement amplitude (up to vibration amplitude of a full cable diameter), mode shape and wave length but slightly dependent on the Reynolds number (Ramberg, 1975).

The uncoupled equation of motion of mode n may be written as (Clough and Penzien, 1975)

$$\ddot{Z}_n + 2\xi_n \omega_n \dot{Z}_n + \omega_n^2 Z_n = f_n(t) \qquad (3.2.b.7)$$

in which ω_n = natural frequency of the structure; ξ_n = damping ratio which is defined by

$$\xi_n = \frac{12\rho_f D}{\pi m}(\nu/\omega_n)^{1/2} \qquad (3.2.b.8)$$

and the forcing function $f_n(t)$ is defined by

$$f_n(t) = \frac{\phi_{ni} F_i}{\phi_{\underline{n}i} M_{ij} \phi_{\underline{n}j}} \qquad \begin{array}{l} ; n = 1,2,3,\ldots \text{NMOD} \\ ; i,j = 1,2,3, \quad \text{NDOF} \end{array} \qquad (3.2.b.9)$$

where the underlined indices indicate that the summation rule is not applied; $F_i(t)$ = ith component force in the global equation; ϕ_{ni} = nth mode shape of the ith component in the global equation; and M_{ij} = the element of mass matrix in the global equation. The transverse displacement

and velocity may then by obtained by the following relationship

$$\bar{U}_{Ti} = \phi_{ni} Z_n \qquad (3.2.b.10.a)$$

$$\dot{\bar{U}}_{Ti} = \phi_{ni} \dot{Z}_n \qquad (3.2.b.10.b)$$

in which $\bar{U}_{Ti}$ = ith component of transverse displacement in the global equation. By assigning the value of the global transverse velocities, $\dot{\bar{U}}_{Ti}$'s, to the corresponding nodal points, the nodal velocity of the strumming becomes determined which can be used to compute the value of lift force coefficient by Equation (3.2.b.3). The new lift force coefficient is then used to calculate the new strumming kinematics. For a relatively small in-plane motion (plane formed by relative fluid velocity and the cable) the mode shape, ϕ_{ni}, and natural frequency, ω_n, may be evaluated only once.

3.2.c Wave Forces on Large Bodies

The Morison's equation presented in Section 3.2.a is valid when the motion of the fluid particle is not significantly affected by the presence of the structure. This may be assumed to be the case if the equivalent diameter of the structure is small compared to the incident wave

length (e.g., D/L = 0.02). For large objects, the scattering of the waves by the structure should be included in force calculations and a diffraction wave theory should be used. Furthermore, when the body moves, waves are produced and energy is radiated in the wave system. Consequently, for a free floating body, the flow field consists of incident waves (incoming waves), scattered waves due to the presence of the structure, and radiated waves due to structural motions. The velocity potential, for linear wave theory, may then be written in the form (Newman, 1977)

$$\psi(\bar{y},t) = \{\psi_I(\bar{y}) + \psi_s(\bar{y}) + \xi_j\psi_j(\bar{y})\}e^{i\omega t}$$

$$j = 1,2,3,4,5,6 \qquad (3.2.c.1)$$

in which ψ_I = spatial velocity potential of the incident wave; ψ_s = spatial velocity potential of the scattered wave; ξ_j = jth component of the body-displacement amplitude; ψ_j = velocity potential of the radiated wave with unit amplitude; j = subscript which represents the translation motion (surge, heave, sway) when $j = 1,2,3$, and rotation motion (roll, yaw, pitch) when $j = 4,5,6$; ω = angular incident wave frequency; and $\bar{y}$ = position vector in y coordinate system. The coordinate system for this problem is shown in Figure 3.2.c-1.

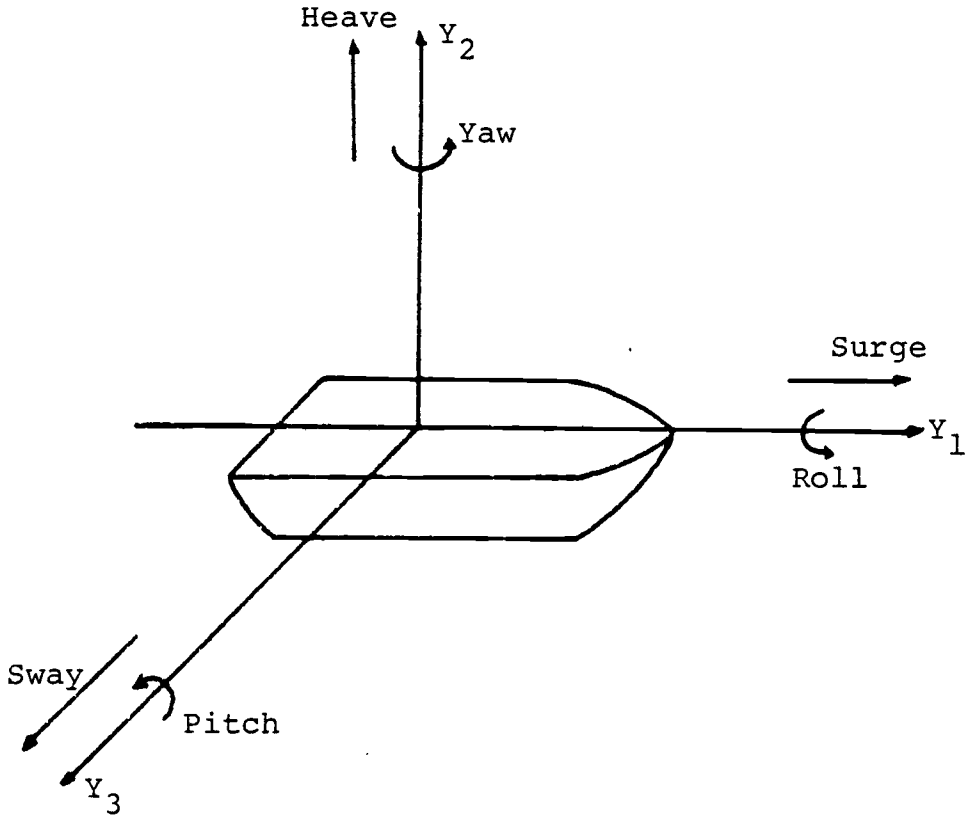

Figure 3.2.c-1. Definition sketch of body motions in six degrees-of-freedom.

Velocity potentials ψ_I, ψ_s, and ψ_j, individually, satisfy the Laplace Equation

$$\nabla^2 \psi_\ell = 0 \; ; \quad \ell = I, s, 1, 2, 3, 4, 5, 6 \qquad (3.2.c.2)$$

with free surface and radiation conditions,

$$\frac{\partial \psi_\ell}{\partial y_2} - \frac{\omega^2}{g} \psi_\ell = 0 \quad \text{at } y_2 = 0 \qquad (3.2.c.3)$$

$$\frac{\partial \psi_\ell}{\partial y_2} = 0 \qquad \text{at } y_2 = -d \qquad (3.2.c.4)$$

$$\lim_{R \to \infty} R^{1/2} \left(\frac{\partial \psi_\ell}{\partial R} - ik \, \psi_\ell \right) = 0 \qquad (3.2.c.5)$$

where g = gravitational acceleration; $R = \sqrt{y_1^2 + y_3^2}$; d = water depth; and k = wave number. The body surface condition is given by

$$\frac{\partial \psi_S}{\partial n} = - \frac{\partial \psi_I}{\partial n} \qquad (3.2.c.6)$$

$$\xi_{\underline{j}} \frac{\partial \psi_j}{\partial n} = v_{\underline{j}} n_{\underline{j}} \qquad j = 1,2,3,4,5,6 \qquad (3.2.c.7)$$

in which underlined indices denote that the summation convention is not applied; v_j = jth component of the body-

velocity amplitude; and n_j = jth component ($j \leq 3$) of unit normal vector, positive outward. For $j > 3$

$$n_4 = y_2 n_3 - y_3 n_2$$

$$n_5 = y_3 n_1 - y_2 n_3 \qquad (3.2.c.8)$$

$$n_6 = y_3 n_2 - y_2 n_1$$

The problem defined by Equation (3.2.c.6) is generally known as the wave diffraction problem while the problem defined by Equation (3.2.c.7) is known as the wave radiation problem. The diffraction problem is to define the scattering potential, ψ_s, which is identical to finding the flow field equation around the fixed structure. However, it will be seen later that ψ_s is often not needed explicitly since it is possible to express the wave forces directly in terms of ψ_j.

For small amplitude waves (small wave slope), the body displacement is sinusoidal in time with the same frequency as the incident waves,

$$\bar{\xi}_j(t) = \xi_j e^{i\omega t} \qquad j = 1,2,3,4,5,6 \qquad (3.2.c.9)$$

The velocity of the body may then be written as

$$\bar{v}_j(t) = v_j e^{i\omega t} = i\omega \xi_j e^{i\omega t} \qquad (3.2.c.10)$$

in which $i = \sqrt{-1}$. Substituting Equation (3.2.c.10) into Equation (3.2.c.7), one obtains

$$\frac{\partial \psi_j}{\partial n} = i\omega n_j \qquad (3.2.c.11)$$

The oscillatory force and moment acting on the body can be obtained by substituting Equation (3.2.c.1) into the linearized Bernoulli equation in which the fluid pressure on the body surface is given by

$$p = -\rho_f \left(\frac{\partial \phi}{\partial t} + g y_2\right)$$

$$p = -\rho_f (\psi_I + \psi_S + \xi_j \psi_j) i\omega e^{i\omega t} - \rho_f g y_2 \qquad (3.2.c.12)$$

The force and moment can then be determined by integrating the fluid pressure over the wetted surface, S_w (Newman, 1977); i.e.,

$$F_\ell = -\rho_f \left[\int_{S_w} n_\ell (\psi_I + \psi_S)\, dS\right] i\omega e^{i\omega t}$$

$$- \rho_f \left[\int_{S_w} n_\ell \xi_j \psi_j dS\right] i\omega e^{i\omega t}$$

$$- \rho_f g \int_{S_w} n_\ell y_2\, dS \qquad \ell, j = 1,2,3,4,5,6 \qquad (3.2.c.13)$$

in which F_ℓ = force for $\ell = 1,2,3,$ and moment for $\ell = 4, 5, 6$. The first term in Equation (3.2.c.13) represents the wave forces on the fixed body, the second term is the wave forces caused by the motion of the body, and the last term is the restoring force resulting from the hydrostatic pressure on the body. Applying these forces onto the body, we may write the equation of motion of the body as

$$m_{B\ell j}\,\ddot{\bar{\xi}}_j + K_{C\ell j}\,\bar{\xi}_j = -\rho_f\left[\int_{S_w} n_\ell\,(\psi_I+\psi_S)\,dS\right]i\omega e^{i\omega t}$$

$$-\rho_f\left[\int_{S_w} n_\ell\xi_j\psi_j\,dS\right]i\omega e^{i\omega t} - \rho_f g\int_{S_w} n_\ell y_2\,dS + \bar{F}$$

$$\ell,j = 1,2,3,4,5,6 \qquad (3.2.14)$$

in which m_{Bj} = body mass for $\ell,j = 1,2,3,$; the second moment for $\ell,j = 4,5,6,$ and zero otherwise; $K_{C\ell j}$ = stiffness due to cable; and $\bar{F}$ = external forces other than hydrodynamic forces.

Substituting Equation (3.2.c.11) for n_ℓ in Equation (3.2.14), one obtains

$$m_{B\ell j}\,\ddot{\bar{\xi}}_j + f_{\ell j}\bar{\xi}_j + (K_{C\ell j}+K_{R\ell j})\,\bar{\xi}_j = C_\ell\,e^{i\omega t} + \bar{F} \qquad (3.2.c.15)$$

in which $K_{R\ell j}$ = hydrostatic stiffness coefficient; $f_{\ell j}$ is defined by

$$f_{\ell j} = \rho_f \int_{S_w} \frac{\partial \psi_\ell}{\partial n} \phi_j \, dS \qquad (3.2.c.16)$$

and C_ℓ = exciting force coefficient defined by

$$C_\ell = - i\omega\rho_f \int_{S_w} \frac{\partial \phi_\ell}{\partial n} (\phi_I + \phi_S) \, dS \qquad (3.2.c.17)$$

which, by Green's theorem and Equation (3.2.c.11), can be expressed as

$$C_\ell - i\omega\rho_f \int_{S_w} (\phi_I \frac{\partial \phi_\ell}{\partial n} - \phi_\ell \frac{\partial \phi_I}{\partial n}) \, dS \qquad (3.2.c.18)$$

The coefficients, $f_{\ell j}$, are complex as a result of the free surface where energy is consumed to accelerate the fluid as well as to generate waves. The real part of $f_{\ell j}$ is proportional to the body acceleration while the imaginary part is proportional to the body velocity,

$$f_{\ell j} = -\omega^2 m_{a\ell j} + i\omega c_{\ell j} \qquad (3.2.c.19)$$

where $m_{a\ell j}$ = added mass coefficient proportional to the body acceleration; and $c_{\ell j}$ = radiating damping-coefficient proportional to the body velocity and associated with a net outward flux of energy in the radiated wave. Substituting Equation (3.2.c.19) into Equation (3.2.c.15) yields

$$(m_{B\ell j} + m_{a\ell j})\ddot{\bar{\xi}}_j + c_{\ell j}\dot{\bar{\xi}}_j + (K_{C\ell j} + K_{R\ell j})\,\bar{\xi}_j =$$

$$C_\ell\, e^{i\omega t} + \bar{F} \qquad (3.2.c.20)$$

Expressions for $m_{B\ell j}$ and $K_{R\ell j}$ are given by Wehausen (1971) and Newman (1977). Added mass coefficient $m_{a\ell j}$, and radiation damping coefficient, $c_{\ell j}$, for the two-dimensional problem have been computed by W. D. Kim (1965) for elliptical sections, C. H. Kim (1965) for various ship-like sections, and by Hudspeth (1979) for a floating circular disc. The exciting force coefficient, C_ℓ, for a cylindrical shape structure was presented by Black (1969) and for an axisymmetric body by Garrison (1977) and by Hudspeth (1979). For bodies of arbitrary geometry, $m_{a\ell j}$, $c_{\ell j}$, and C_ℓ may be evaluated by means of the wave source distribution method in which the source potential per unit strength is represented by a Green's function. The expression for the Green's function which satisfies the boundary value problem defined by Equations (3.2.c.2-4) is given by Wehausen and Laitone (1960). The source strength is determined from the requirement that the normal velocity of the fluid-particle on the body surface be equal to the normal body velocity which is stated in Equations (3.2.c.6,7).

Another method which has found increasing use in treating many wave diffraction problems is the finite element method. The application of this method may be found in references (Bettes and Zienkiewicz, 1978) (Bai, 1977). In this thesis, no attempt is made to evaluate the quantities $m_{a\ell j}$, $c_{\ell j}$, and C_{ℓ} . The body is assumed to be an element unit to which cables are attached. Therefore, the Equation (3.2.c.20) may be assembled with the cable element equation of the motion to obtain the global equation of motion.

3.3 Modified Form of the Equation of Motion Due to the Existence of Large Bodies

For a mooring problem, a system of mooring lines is attached to one or several bodies at arbitrary locations on the body surfaces. Each rigid body is considered as a separate element having six degrees of freedom. Transformation is required for the equations of the cable elements adjacent to the rigid body. For example, let a rigid body 1, in Figure (3.3-1) be connected with a cable element 2-3 at point 2. The six degree-of-freedom equation of motion of the body is given by Equation (3.2.c.20) and may be written in matrix form as

$$[M_B]\{\ddot{\xi}\} + [C_B]\{\dot{\xi}\} + [K_B]\{\xi\} = \{F_B\} \qquad (3.3.1)$$

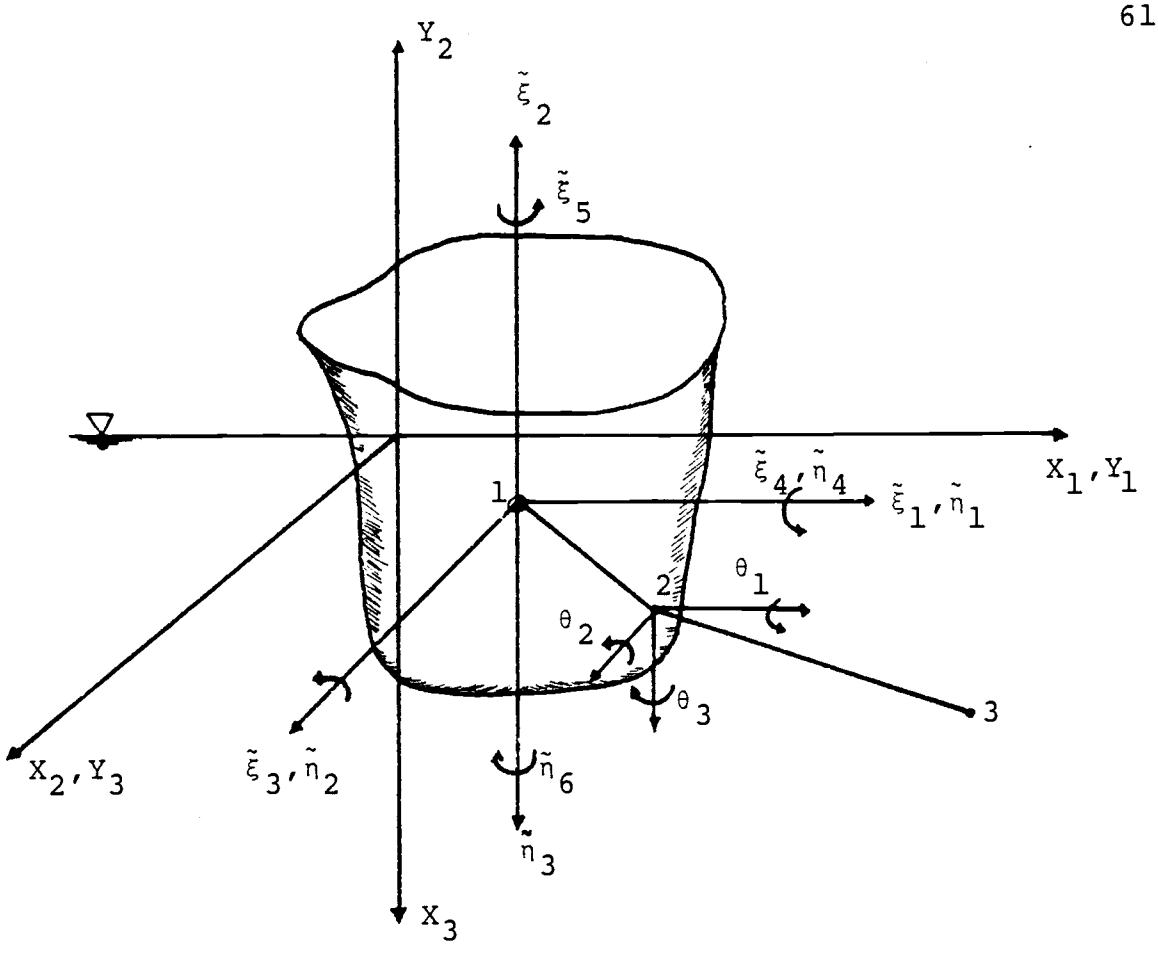

Figure 3.3-1. Definition sketch.

in which $[M_B]$ = body mass + added mass matrix; $[C_B]$ = radiation damping matrix; $[K_B]$ = cable stiffness + restoring force coefficient matrix; and F_B = hydrodynamic force vector calculated by a diffraction method + other external forces. The cable equation of motion given by Equation (3.1.8.a) or Equation (3.1.8.b) may be expressed in matrix form by

$$[M_c]\{\ddot{U}\}_{t+\Delta t} + [C_c]_t\{\Delta\dot{U}\} + [K_c]_t\{\Delta U\} = \{\Delta F_c\} \qquad (3.3.2)$$

in which $[M_c]$ = structural mass + added mass of the cable $[C_c]$ = incremental drag damping matrix; $[K_c]$ = incremental cable stiffness matrix; and F_c = hydrodynamic forces and external forces.

Before proceeding to the assembly procedure for these two elements (rigid body and cable element), it is necessary to transform Equation (3.3.1) from the Y coordinate system used in the rigid body equation to the X coordinate system used in the cable equation; i.e.,

$$[\bar{M}_B]\{\ddot{\bar{\eta}}\} + [\bar{C}_B]\{\dot{\bar{\eta}}\} + [\bar{K}_B]\{\eta\} = \{\bar{F}_B\} \qquad (3.3.3.a)$$

or in incremental form

$$[\bar{M}_B]\{\ddot{\bar{\eta}}\}_{t+\Delta t} + [\bar{C}_B]\{\Delta\dot{\bar{\eta}}\} + [\bar{K}_B]\{\Delta\bar{\eta}\} = \{\Delta\bar{F}_B\} \qquad (3.3.3.b)$$

in which

$$[\bar{M}_B] = [T]^T[M_B][T] \qquad (3.3.4.a)$$

$$[\bar{C}_B] = [T]^T[C_B][T] \qquad (3.3.4.b)$$

$$[\bar{K}_B] = [T]^T[K_B][T] \qquad (3.3.4.c)$$

$$\{\bar{F}_B\} = [T]^T\{F_B\} \qquad (3.3.4.d)$$

$$\{\Delta\bar{F}_B\} = \{\bar{F}_B\} - [\bar{C}_B]\{\dot{\bar{\eta}}\}_t - [\bar{K}_B]\{\bar{\eta}\}_t \qquad (3.3.4.e)$$

where [T] = coordinate transformation matrix given by

$$[T] = \begin{bmatrix} \begin{bmatrix} 1 & 0 & 0 \\ 0 & 0 & -1 \\ 0 & 1 & 0 \end{bmatrix} & [0] \\ [0] & \begin{bmatrix} 1 & 0 & 0 \\ 0 & 0 & -1 \\ 0 & 1 & 0 \end{bmatrix} \end{bmatrix} \qquad (3.3.5)$$

and $\bar{\eta}$ = body displacement in the X system.

The attachment point 2 shown in Figure (3.3.1) has six degrees of freedom which are dependent on the motion of the nodal point 1. The motion at node 2 (slave to node 1) may be related to the motion at node 1 by the following equation.

$$\begin{Bmatrix} U_{21} \\ U_{22} \\ U_{23} \\ \Theta_1 \\ \Theta_2 \\ \Theta_3 \end{Bmatrix}_{\text{node 2}} = [\Lambda_1] \begin{Bmatrix} \bar{\eta}_1 \\ \bar{\eta}_2 \\ \bar{\eta}_3 \\ \bar{\eta}_4 \\ \bar{\eta}_5 \\ \bar{\eta}_6 \end{Bmatrix}_{\text{node 1}} \qquad (3.3.6)$$

in which the first subscript of U_{ij} denotes the node and the second subscript denotes component; $[\Lambda_1]$ = transformation given by

$$[\Lambda_1] = \begin{bmatrix} [I]_{3x3} & [R]_{3x3} \\ [0]_{3x3} & [I]_{3x3} \end{bmatrix} \qquad (3.3.7.a)$$

with

$$[R] = \begin{bmatrix} 0 & X_{13}-X_{23} & X_{22}-X_{12} \\ X_{23}-X_{13} & 0 & X_{11}-X_{21} \\ X_{12}-X_{22} & X_{21}-X_{11} & 0 \end{bmatrix} \qquad (3.3.7.b)$$

If we substitute the translation expression of node 2 in terms of displacements $\bar{\eta}$ of node 1 into Equation (3.3.2), we find the following relationship

$$[M_c]\{\ddot{\bar{u}}\}_{t+\Delta t} + [C_c]\{\Delta\dot{\bar{u}}\} + [K_c]\{\Delta\bar{u}\} = \{\Delta F_c\} \qquad (3.3.8)$$

in which

$$\{\Delta\bar{u}\} = [\Lambda_2] \begin{Bmatrix} \{\Delta\bar{\eta}\}_{6x1} \\ \{u_3\}_{3x1} \end{Bmatrix} \qquad (3.3.9.a)$$

where

$$[\Lambda_2] = \begin{bmatrix} [I]_{3x3} & [R]_{3x3} & [0]_{3x3} \\ [0]_{3x3} & [0]_{3x3} & [I]_{3x3} \end{bmatrix} \qquad (3.3.9.b)$$

Premultiplying Equation (3.3.8) by the transpose of the transformation matrix, $[\Lambda_2]$ gives

$$[\bar{M}_c]\{\ddot{\bar{u}}\}_{t+\Delta t} + [\bar{C}_c]\{\Delta\dot{\bar{u}}\} + [\bar{K}_c]\{\Delta\bar{u}\} = \{\Delta\bar{F}_c\} \qquad (3.3.10)$$

which can be readily assembled with the rigid body equation of motion to get the global equation of motion of the cable-large body system. If there are more than one attachment points, the same procedures can also be applied with the rigid body equation assembled with only one of any adjacent cable elements.

4.0 SOLUTION PROCEDURES

Procedures for solution of nonlinear problems in structural analysis can be classified as following: 1) iterative procedures; 2) incremental (step by step) procedures; and 3) combination of incremental and iterative procedures. Iterative procedures include the successive approximation and the Newton-Raphson method. The incremental procedures include the purely step-by-step loading method and the residual feedback method. These procedures have been reivewed and discussed by Stricklin et al. (1975) for static problems and by Webster (1974) for both static and dynamic problems. The residual feedback method with the introduction of artificial damping (viscous relaxation) has proven to be an effective method for predicting the static configuration of the geometrically nonlinear cable (Webster, 1980), and the incremental iterative technique is effective for evaluating the cable response due to dynamic loads (Lo, 1981). Therefore, those methods and their applications to the dynamic response of cable systems in the fluid domain will be considered in this chapter.

4.1 Solution Methods for the Static Equations

One of the primary interests in finding the static configuration of the cable system is to provide a stable starting configuration for a dynamic problem. The dynamic response is generally considered as a disturbance from the static configuration.

Consider a set of incremental equations given by Equation (2.2.a.11) whose global form may be written in matrix form, for the increments $\{\Delta U\}$ of displacement as

$$[K]_n \{\Delta U\} = \{\Delta F_e\} \tag{4.1.1}$$

for purely incremental equations, in which $\{\Delta F_e\}$ = increment in external applied forces; and

$$[K]_n \{\Delta U\} = \{F_e\}_{n+1} - \{F_i\}_n \tag{4.1.2}$$

for the residual feedback method, in which $\{F_e\}$ = external applied forces; $\{F_i\}$ = internal force in the cables due to previous loads; and the subscript n refers to the nth increment. The displacement at the $(n+1)$th increment is

$$\{U\}_{n+1} = \{U\}_n + \{\Delta U\} \tag{4.1.3}$$

Equation (4.1.1) is simple to apply. However, unless the load steps are very small, the solution may drift from the true response because equilibrium is not satisfied exactly at any step. The accuracy of the solution can be improved by applying the equilibrium corrections as expressed by Equation (4.1.2). Here, the incremental load is represented by the difference between the load during the (n+1)th increment and the internal load accumulated to the nth incremental load.

The computational steps involved in the use of Equations (4.1.1,2) are

1) divide load in N increments,
2) form incremental stiffness,
3) compute internal load vector $\{F_i\}$ for residual feedback method, otherwise proceed to the next step,
4) form incremental load vector $\{\Delta F_e\}$ for purely incremental method, and $\{F_e\}_{n+1} - \{F_i\}_n$ for residual feedback method,
5) compute incremental displacement vector ΔU ,
6) compute displacement vector $\{U\}$ according to Equation (4.1.3)
7) calculate new cable stress,
8) repeat steps 2) through 7) until the Nth of increment load has been applied.

The residual feedback method is equivalent to the Newton-Raphson method when the total load is applied in a single increment instead of in multiple increments. The computation ends when the residual load

$$|\{R\}_n| = |\{F_e\}_{n+1} - \{F_i\}_n| \leq \text{TOL (Tolerance)} \quad (4.1.4)$$

in which the subscript n, in this case, is the number of iterations. To reduce the amount of computational effort, the displacement-dependent stiffness matrix may be held constant for several steps depending on the degree of the nonlinearity involved.

If the initial tension of the cable is low relative to the applied load, the stiffness [K] becomes too small to sustain the load. The solution will diverge, and will lead to an incorrect response. This problem may be overcome by introducing artificial damping into the structure (Webster, 1980). This approach is known as the "viscous relaxation method." In general, the damping constants are lumped at nodal points and their values are adjusted intuitively based on the value of the diagonal stiffness and the residual force $\{R\}_n$ given by Equation (4.1.4). For example, for a suspended cable with a point load in the middle, the damping constants may be reduced as time increases. This will be shown subsequently in an example problem.

Introducing damping forces to Equation (4.1.2) and replacing subscript n by time t and (n+1) by $t+\Delta t$, one obtains

$$[C]_t \{\dot{U}\}_{t+\Delta t} + [K]_t\{\Delta U\} = \{R\}_{t+\Delta t} \qquad (4.1.5)$$

in which $[C]_t$ = artificial damping; and $\{R\}_{t+\Delta t}$ = residual force at time $t+\Delta t$. The velocity $\{\dot{U}\}_{t+\Delta t}$ may be expressed by

$$\{\dot{U}\}_{t+\Delta t} = \frac{\Delta U}{\Delta t} \qquad (4.1.6)$$

Substituting Equation (4.1.8) into Equation (4.1.7) leads to

$$[K_{eq}]_t \{\Delta U\} = \{R\}_{t+\Delta t} \qquad (4.1.7)$$

in which

$$[K_{eq}]_t = \frac{1}{\Delta t}[C]_t + [K]_t \qquad (4.1.8)$$

The structure is stiffened and the solutions, initially, do not give the correct displacement. The solutions will converge to the true static displacements as t increases; this is because the velocities decrease as t increases and the damping force is proportional to the velocity.

The computational steps are similar to that for the residual feedback method except that adjustment of the damping constant is recommended to accelerate the convergence.

4.2 Solution Methods for the Dynamic Equations

The global form of the incremental dynamic equations derived in Chapter 3 may be written in matrix form as:

$$[M]\{\ddot{U}\}_{t+\Delta t} + [K]_t\{\Delta U\} = \{F_e\}_{t+\Delta t} - \{F_i\}_t \qquad (4.2.1)$$

in which $[M]$ = structural mass; $[K]_t$ = nonlinear stiffness matrix evaluated at time t ; $\{F_e\}_{t+\Delta t}$ = external force at $t+\Delta t$; and $\{F_i\}_t$ = internal force evaluated at time t . The external force $\{F_e\}$ may be decomposed into conservative and nonconservative terms; i.e.;

$$\{F_e\} = \{F_{ec}\} + \{F_{enc}\} \qquad (4.2.2)$$

The nonconservative force, in this case, is the hydrodynamic force whose magnitude and direction are dependent on the cable kinematics and orientations. The expression for this force is given in Section (3.2.a) by Equation (3.2.a.6) and its global form may be written as

$$\{F_{enc}\}_{t+\Delta t} = [M_a]\{\ddot{U}\}_{t+\Delta t} + [C]_t\{\Delta\dot{U}\}$$

$$+ [C]_t\{\dot{U}\}_t + \{F_{eH}\}_{t+\Delta t} \qquad (4.2.3)$$

in which $[M_a]$ = added mass matrix; $[C]_t$ = incremental drag damping evaluated at time t ; and $\{F_{eH}\}_{t+\Delta t}$ is the known force defined as

$$\{F_{eH}\}_{t+\Delta t} = [M_I]\{a\}_{t+\Delta t} + [C]_t\{V\}_{t+\Delta t} \qquad (4.2.4)$$

where $[M_I]$ = inertial force matrix; a = fluid particle acceleration; and V = fluid particle velocity. Substituting Equations (4.2.3,4) into Equation (4.2.1) and rearranging slightly yields

$$[M_T]\{\ddot{U}\}_{t+\Delta t} + [C]_t\{\Delta\dot{U}\} + [K]_t\{\Delta U\} =$$

$$\{F_{eH}\}_{t+\Delta t} + \{F_{ec}\}_{t+\Delta t} - \{F_{iH}\}_t \qquad (4.2.5)$$

in which

$$[M_T] = [M] + [M_a] \qquad (4.2.6.a)$$

$$\{F_{iH}\}_t = \{F_i\} + [C]_t\{\dot{U}\}_t \qquad (4.2.6.b)$$

Various explicit and implicit, single and multistep integration operators have been used to solve equations of motion for linear equations, and the stability and accuracy of these operators, have been investigated (Newmark, 1950; Webster, 1974). For example, Newmark's β-γ-δ operator and Wilson's θ operator (Bathe, 1976) are used extensively in linear dynamic analysis. In nonlinear analysis, the stability limits of these operators may no longer be valid. The accuracy of the response in nonlinear analysis will depend on the type of the nonlinearity, the solution scheme, the nature of the iterative process, etc. However, for cable structures, numerical experiments reported by several investigators (Webster, 1974, and Lo, 1981) have shown that the single step-implicit Newmark's β-γ-δ method with $\beta = 1/4$, $\gamma = 1/2$, and $\delta = 0$ has given satisfactory results. Therefore, this method will be employed in this thesis.

The velocity and the acceleration at time $t+\Delta t$ are related to the incremental displacement, velocity, and acceleration at time t,

$$\{\dot{U}\}_{t+\Delta t} = \frac{2}{\Delta t}\{\Delta U\} - \{\dot{U}\}_t \qquad (4.2.7.a)$$

$$\{\ddot{U}\}_{t+\Delta t} = \frac{4}{(\Delta t)^2}\{\Delta U\} - \frac{4}{\Delta t}\{\dot{U}\}_t - \{\ddot{U}\}_t \qquad (4.2.7.b)$$

These equations are equivalent to assuming a constant average acceleration and have been shown to be an unconditionally stable method for linear analysis.

Substitution of Equations (4.2.7.a,b) into Equation (4.2.5) with slight rearrangement yields the static-equivalent equation

$$[K_{eff}]_t \{\Delta U\} = \{F_{eff}\}_{t+\Delta t} \tag{4.2.8}$$

in which the effective stiffness, $[K_{eff}]$, is defined by

$$[K_{eff}]_t = \frac{4}{(\Delta t)^2} [M_T] + \frac{2}{\Delta t} [C]_t + [K]_t \tag{4.2.9.a}$$

and the effective force, $\{F_{eff}\}$ by

$$\{F_{eff}\}_{t+\Delta t} = \{F_{eH}\}_{t+\Delta t} + \{F_{ec}\}_{t+\Delta t} - \{F_{iH}\}_t + \left(\frac{4}{\Delta t} [M_T] + 2[C]_t\right) \{\dot{U}\}_t + [M_T]\{\ddot{U}\}_t \tag{4.2.9.b}$$

The computational steps involved in the use of Equation (4.2.5) may be ordered as follows:

1) Compute the stable static equilibrium configuration by methods given in Section 4.1;
2) Specify time step, Δt and convergence tolerance, TOL ;

3) Form element stiffness, $[K]_t$ and structural mass, [M] ;

4) Form element added mass, $[M_a]$ and incremental drag damping, $[C]_t$;

5) Form total mass $[M_T]$;

6) Calculate the internal force, $\{F_{iH}\}_t$, conservative force, $\{F_{ec}\}_{t+\Delta t}$, and hydrodynamic force, $\{F_{eH}\}_{t+\Delta t}$;

7) Assemble the element stiffness, mass, and damping matrices into the global form;

8) The same as 7) for force;

9) Compute effective shiftness, $[K_{eff}]$ according to Equation (4.2.9.a);

10) Compute effective force, $\{F_{eff}\}$ according to Equation (4.2.9.b);

11) Solve for ΔU from Equation (4.2.8);

12) Compute the state of motion at time $t+\Delta t$ by Equations (4.1.3), (4.2.7.a) and (4.2.7.b). If no iterations in this time step, repeat steps 3 through 11 for the next time step, otherwise proceed as follows;

13) Compute the effective residual force

$$\{R_{eff}\}^{n+1} = \{F_{eff}\}^{n+1}_{t+\Delta t} - [M_T]\ \{\ddot{U}\}^{n}_{t+\Delta t} \qquad (4.2.10)$$

in which n denotes the iteration step and

$\{F_{eff}\}^{n+1}_{t+\Delta t}$ is given by Equation (4.2.9.b) with new hydrodynamic force, $\{F_{eH}\}$ and internal force, $\{F_{iH}\}$.

14) Solve δU as

$$\{\delta U\}^{n+1} = [K_{eff}]_t \{R_{eff}\}^{n+1} \qquad (4.2.11)$$

15) Compute new incremental displacement as

$$\{\Delta U\}^{n+1} = \{\Delta U\}^{n} + \{\delta U\}^{n+1}$$

16) Compute new incremental velocity and acceleration by Equations (4.2.7.a, b).

17) Check the convergence

if $\left|\{R_{eff}\}^{n+1}\right| < TOL$ iteration ends,

if not, repeat steps 13 through 16.

These computational steps were incorporated in a computational algorithm in the computer implementation.

5.0 DYNAMIC RESPONSE OF A CABLE-LARGE BODY SYSTEM DUE TO RANDOM WAVE LOADINGS

The assumptions made in the stochastic analysis of a cable-large body system subjected to random wave loadings are that displacements of the system from the static equilibrium configuration are small enough such that the cable stiffness is not affected significantly by changes in cable positions, and that the nonlinear fluid drag force can be linearized. It is further assumed that the waves are small amplitude waves whose random realization is distributed according to the Gaussian distribution. Thus, the system is linear: the superposition method may be employed to determine the cable response. Furthermore, as a consequence of the linearity and Gaussian waves assumption, the cable response may also be assumed to be a Gaussian process (Lin, 1965).

The approach taken in this study is first to determine the static configuration where all of the nonlinear effects are included, and then to determine the dynamic response by mode-superposition techniques in the frequency domain. The nonlinear fluid drag is linearized by a method of statistical linearization (Borgman, 1972). The coupled modal fluid damping is decoupled by a method presented by Foss (1958). The time series of the cable response is then

computed by taking the inverse Fourier transform of the cable frequency response.

The general global incremental equation of motion of a cable system is expressed by

$$[M_G]\{\ddot{U}\} + [C_G]\{\dot{U}\} + [K_G]\{U\} = \{F_{DG}\} + \{F_{DI}\} \qquad (5.1)$$

in which $[M_G]$ = structural + added mass coefficient matrix; $[C_G]$ = linearized fluid drag coefficient matrix; $[K_G]$ = incremental stiffness coefficient matrix; $\{U\}$ = displacement measured relative to the static equilibrium position; $\{F_{DG}\}$ = linearized drag force; and $\{F_{IG}\}$ = inertial force. All of the coefficients and forces in Equation (5.1) depend on the positions and tensions in the state reached under static loadings. These coefficients are obtained by methods discussed in the previous chapters. The external forces are linearly dependent on the wave kinematics; that is, on the fluid particle velocities and accelerations. Therefore, before any attempt is made to model the stochastic wave forces, it is necessary to consider simulation models and techniques for generating a random wave realization.

5.1 Ocean Waves Model and Simulations

A mathematical model for ocean wave simulation was first introduced by Borgman (1969) and was later extended

to weakly nonlinear and slightly nonGaussian second-order waves utilizing a Fast Fourier Transform (FFT) algorithm by Hudspeth (1974) and Sharma (1979). Since there is a similarity in the statistical properties of the representation of the noise current (Rice, 1944, pp.328-330) to that of random waves, it is appropriate to express linear random sea waves at a fixed location in discrete form by

$$\eta(n\Delta t) = \sum_{m=0}^{N-1} A_m \cos\left[(m\Delta\omega)(n\Delta t) - \theta_m\right] \qquad (5.1.1)$$

in which n and m are positive integers such that

$$\Delta t = n\Delta t = \frac{nT_L}{2N} \qquad (5.1.2.a)$$

$$\omega_m = m\Delta\omega = \frac{2\pi m}{T_L} \qquad (5.1.2.b)$$

where T_L = the period of $\eta(t)$, which in this case is the record length; $2N$ = number of discrete points; and θ_m = random phase angle which is uniformly distributed over the range $(-\pi, +\pi)$. Wave amplitude A_m is either deterministic or nondeterministic. Deterministic A_m can be computed by

$$A_m = \left[0.5\, S_{\eta\eta}(\omega_m)\Delta\omega\right]^{1/2} \qquad (5.1.3.a)$$

and nondeterministic A_m by

$$A_m = [0.25\, S_{\eta\eta}(\omega_m)\,\Delta\omega]^{1/2}\,(\alpha_m^2 + \beta_m^2)^{1/2} \qquad (5.1.3.b)$$

in which $S_{\eta\eta}(\omega_m)$ = wave power spectral density evaluated at frequency ω_m ; and α_m , β_m = independent random variables which are normally distributed with zero mean and unit variance. When Equation (5.1.3.a) is used in Equation (5.1.1), the model is called deterministic spectral amplitude (DSA), whereas if Equation (5.1.3.b) is used, then the model is called nondeterministic spectral amplitude (NSA). Tuah and Hudspeth (1981) have used these two models to simulate both linear and slightly nonlinear second-order random wave realizations by utilizing the FFT algorithm. The complex representation of Equation (5.1.1) may be written as

$$\eta(n\Delta t) = \sum_{m=-N}^{N} A_m \exp\,[i(m\Delta\omega)(n\Delta t)] \qquad (5.1.4)$$

in which

$$A_m = A_m \exp - i\theta_m \qquad (5.1.5)$$

The simulation procedures of the wave realization are as follows:

1) Generate the real amplitude A_m by either Equation (5.1.3.a) or Equation (5.1.3.b),
2) Generate a sequence of uniformly distributed random phase $\theta_1, \theta_2, \ldots, \theta_N$,

3) Compute the complex amplitude A_m according to Equation (5.1.5),

4) Compute random waves realization by taking the inverse FFT of A_m's .

5.2 Wave Force Model and Simulation

The wave forces on the cable line are modeled by Morison's equation for the normal components and by the flat plate friction formula for the tangential component. The combination of these components evaluated at nodal point α may be written as follows

$$\begin{aligned} F_{Hj}^{(\alpha)} = & - [B_{DL}\delta_{j\ell} - (B_{DL}-B_{DT})\theta_j^{(\alpha)}\theta_\ell^{(\alpha)}]\dot{U}_\ell \\ & + [B_{DL}\delta_{j\ell} - (B_{DL}-B_{DT})\theta_j^{(\alpha)}\theta_\ell^{(\alpha)}]V_\ell \\ & - B_I(C_M-1)[\delta_{j\ell}-\theta_{j\ell}^{(\alpha)}\theta_\ell^{(\alpha)}]\ddot{U}_\ell^{(\alpha)} \\ & + B_I C_M(\delta_{j\ell}- \theta_j^{(\alpha)}\ \theta_\ell^{(\alpha)})a_\ell^{(\alpha)} \end{aligned} \qquad (5.2.1)$$

in which

$$B_{DL} = (\frac{2}{\pi})^{1/2} C_D\ \rho_f D\ \sigma_{V_{NR}V_{NR}} \qquad (5.2.2.a)$$

$$B_{DT} = (2\pi)^{1/2} C_T\ \rho_f D\ \sigma_{V_{TR}V_{TR}} \qquad (5.2.2.b)$$

where $\sigma_{V_{NR}V_{NR}}$, $\sigma_{V_{TR}V_{TR}}$ = standard deviation of the

normal and tangential relative velocity; and other variables are given in Section 3.2. Details on the linearization procedure of the quadratic drag force are given by Borgman (1972). The fluid particle velocity was assumed to be Gaussian and coefficients B_{DL} and B_{DT} were obtained by a statistical linearization technique.

The standard deviations $\sigma_{V_{NR}V_{NR}}$ and $\sigma_{V_{TR}V_{TR}}$ can be determined by the following relationship:

$$\sigma^2_{V_{NR}V_{NR}} = E\{[V_{NR} - E(V_{NR})]^2\} = E(V^2_{NR}) - [E(V_{NR})]^2 \quad (5.2.3.a)$$

$$\sigma^2_{V_{TR}V_{TR}} = E\{[V_{TR} - E(V_{TR})]^2\} = E(V^2_{TR}) - [E(V_{TR})]^2 \quad (5.2.3.b)$$

in which the operator $E(\cdot)$ denotes the statistical expectation and is defined by

$$E(\cdot) = \int_{-\infty}^{\infty} (\cdot) p(\cdot) d(\cdot) \quad (5.2.4)$$

with $p(\cdot)$ = probability density function of $(\cdot)$. Means $E(V_{NR})$ and $E(V_{TR})$ are both zero when the sea waves are a zero mean Gaussian process which is the case in this study. Therefore, substitution of the expression for V_{NR} and V_{TR} in terms of fluid and cable kinematics yields

$$\sigma^2_{V_{NR}V_{NR}} = E(V_j V_j) + E(\dot{U}_j \dot{U}_j) - 2E(V_j \dot{U}_j) - \sigma^2_{V_{TR}V_{TR}} \quad (5.2.5.a)$$

$$\sigma^{2}_{V_{TR}V_{TR}} = \Theta_j\Theta_\ell\{E(V_jV_\ell) + E(\dot{U}_j\dot{U}_\ell) - 2\,E(V_j\dot{U}_\ell)\} \quad (5.2.5.b)$$

The direction cosines, Θ_j's, are assumed to be constant and equal to the values at the static equilibrium positions, the cable velocities U_j's are unknown. An iteration process is required in order to obtain values of standard deviations $\sigma_{V_{NR}V_{NR}}$, $\sigma_{V_{TR}V_{TR}}$ which are required to linearize the drag term which in turn will be used to determine displacements, U_j's and velocities, $\dot{U}_j$'s. The iteration is continued until a desired degree of accuracy is achieved.

Substitution of Equation (5.2.1) into the element equations of motion and separation of the structural and hydrodynamic kinematics results in

$$[M_T]\{\ddot{U}\} + [C]\{\dot{U}\} + [K]\{U\} = [B_D]\{V\} + [B_I]\{a\} \quad (5.2.6)$$

in which $[B_D]$ = linearized drag coefficient matrix and $[B_I]$ = inertial coefficient matrix. The global form of this equation is given by Equation (5.1) with

$$\{F_{DG}\} = [B_{DG}]\{V\} \quad (5.2.7.a)$$

$$\{F_{IG}\} = [B_{IG}]\{a\} \quad (5.2.7.b)$$

where $[B_{DG}]$ = global linearized drag coefficient matrix and $[B_{IG}]$ = global inertial coefficient matrix. The

expression for the random fluid particle velocities are given by (Wheeler, 1969)

$$V_j(n\Delta t) = \sum_{m=-N}^{N} H_{V_j}(m)\ A_m \exp[i(m\Delta\omega)(n\Delta t)]$$

$$j = 1,\ 2,\ 3 \qquad (5.2.8)$$

and for the fluid particle accelerations by

$$a_j(n\Delta t) = \sum_{m=-N}^{N} H_{a_j}(m)\ A_m \exp[i(m\Delta\omega)(n\Delta t)]$$

$$j = 1,\ 2,\ 3 \qquad (5.2.9)$$

in which A_m is the complex wave amplitude given by Equation (5.1.4) and the complex transfer functions H_{V_j} and H_{a_j} are determined from

$$H_{V_1}(m) = \frac{gk_{m1}}{(m\Delta\omega)} \frac{\cosh[k_m(h-x_3)]}{\cosh\ k_m h} \exp\ \ i(k_{m1}x_1+k_{m2}x_2) \qquad (5.2.10.a)$$

$$H_{V_2}(m) = \frac{gk_{m2}}{(m\Delta\omega)} \frac{\cosh[k_m(h-x_3)]}{\cosh\ k_m h} \exp\ \ i(k_{m1}x_1+k_{m2}x_2) \qquad (5.2.10.b)$$

$$H_{V_3}(m) = -\,i\ \frac{gk_m}{(m\Delta\omega)} \frac{\sinh[km(h-x_3)]}{\cosh\ k_m h} \exp\ \ i(k_{m1}x_1+k_m\ x_2) \qquad (5.2.10.c)$$

$$H_{a_j}(m) = -\,i\ (m\Delta\omega)\ H_{V_j}(m) \qquad j=1,2,3 \qquad (5.2.10.d)$$

where the wave number k_m satisfies the dispersion equation

$$(m\Delta\omega)^2 = gk_m \tanh k_m h$$

and

$$\begin{aligned} k_{m1} &= k_m \cos \gamma \\ k_{m2} &= k_m \sin \gamma \\ k_{-m} &= -k_m \end{aligned} \qquad (5.2.11)$$

with h = water depth and γ = incident wave direction. The randomness of these wave kinematics is represented by the complex amplitude, A_m, which is associated with a discrete frequency $m\Delta\omega$. Consequently, the simulation of the random wave forces on the cable line is equivalent to generating the random amplitude A_m which has been discussed in Section 5.1. The complex amplitudes of the wave kinematics may then be obtained by multiplying A_m by transfer functions given by Equations (5.2.10.a-d). Force spectra on large bodies in a mooring system may be included in Equation (5.2.6) by the procedure presented in Section 3.3. Added mass and radiation damping are assumed to be constant over the whole range of frequencies. The constant added mass and radiation damping may be determined according to formulas given by Pierson (1956).

5.3 Mode-Superposition Solution Technique

This technique has been discussed in Section 3.2, and its application in the stochastic response analysis of a cable system is to transform a set of coupled linear equations of motion into a set of uncoupled equations from which modal frequency response can be calculated. The cable displacement is expressed as a sum of the modal components over all the natural frequencies; i.e.,

$$\{U\} = [\phi]\{Z\} \tag{5.3.1}$$

in which $[\phi]$ = modal shape matrix and $\{Z\}$ = modal response vector.

Substitution of Equation (5.3.2) and Equations (5.2.7. a,b) into Equation (5.1) leads to

$$[M_G][\phi]\{\ddot{Z}\} + [C_G][\phi]\{\dot{Z}\} + [K_G][\phi]\{Z\} =$$

$$[B_{DG}]\{V\} + [B_{IG}]\{a\} \tag{5.3.2}$$

Premultiply Equation (5.3.2) by $[\phi]^T$ to get

$$[\hat{M}]\{\ddot{Z}\} + [C_u]\{\dot{Z}\} + [\hat{K}]\{Z\} =$$

$$[\hat{B}_{DG}]\{V\} + [\hat{B}_{IG}]\{a\} \tag{5.3.3}$$

in which

$[\hat{M}] = [\phi]^T[M_G][\phi]$ = diagonal generalized mass matrix (NEQ X NMOD)

$[C_u] = [\phi]^T[C_G][\phi]$ = full damping matrix (NEQ X NMOD)

$[\hat{K}] = [\phi]^T[K_G][\phi]$ = diagonal generalized stiffness matrix (NEQ X NMOD)

$[\hat{B}_{DG}] = [\phi]^T[B_{DG}]$ matrix size (NMOD X NEQ)

$[\hat{B}_{IG}] = [\phi]^T[B_{IG}]$ matrix size (NMOD X NEQ)

where NEQ = number of equations and NMOD = number of modes.

The damping matrix $[\hat{C}_u]$ is coupled between natural modes. An uncoupled damping matrix may be obtained by a method introduced by Foss (1958).

Equation (5.3.3) may be written as

$$[C_q]\{\dot{q}\} + [K_q]\{q\} = Q \tag{5.3.4}$$

in which

$$[C_q] = \begin{bmatrix} [0] & [\hat{M}] \\ [\hat{M}] & [C_u] \end{bmatrix} \tag{5.3.5}$$

$$[K_q] = \begin{bmatrix} -[\hat{M}] & [0] \\ [0] & [\hat{K}] \end{bmatrix} \tag{5.3.6}$$

$$\{q\} = \begin{Bmatrix} \{\dot{Z}\} \\ \{\dot{Z}\} \end{Bmatrix} \tag{5.3.7}$$

$$\{Q\} = \begin{Bmatrix} \{0\} \\ \{\hat{F}\} \end{Bmatrix} \tag{5.3.8.a}$$

with

$$\{\hat{F}\} = [\hat{B}_{DG}]\{V\} + [\hat{B}_{IG}]\{a\} \tag{5.3.8.b}$$

The homogeneous solution of Equation (5.3.4) may be obtained by assuming

$$\{q\} = \{\theta\}e^{\Omega t} \tag{5.3.9}$$

This gives

$$\Omega[C_q]\{\theta\} + [K_q]\{\theta\} = \{0\} \tag{5.3.10}$$

The nontrivial solution exists when

$$\Omega[C_q] + [K_q] = \{0\} \tag{5.3.11}$$

which is an eigenvalue problem. The eigenvector $\{\theta\}_j$ associated with eigenvalue Ω_j is orthogonal with respect to $[C_q]$ and $[K_q]$; i.e.,

$$\{\theta\}_j^T[C_q]\{\theta\}_\ell = c_{qj}\delta_{j\ell} \tag{5.3.12}$$

and

$$\{\theta\}_j^T[K_q]\{\theta\}_\ell = k_{qj}\delta_{j\ell} \tag{5.3.13}$$

To obtain the uncoupled equation let

$$\{q\} = \sum_{n=1}^{2NMOD} \{\theta\}_n r_n(t) \tag{5.3.14}$$

Substitute Equation (5.3.14) into Equation (5.3.4) and premultiply by $\{\theta\}_j^T$ to get

$$c_{qj}\,\dot{r}_j + k_{qj}\,r_j = R_j(t) \tag{5.3.15}$$

in which c_{qj} and k_{qj} are given by Equations (5.3.12,13) and

$$R_j(t) = \{\Theta\}_j^T\{Q\} \tag{5.3.16}$$

Considering Equations (5.3.7) and (5.3.9), we may write the eigenvector $\{\Theta\}_j$ as

$$\{\Theta\}_j = \begin{Bmatrix} \Omega_j \{\chi\}_j \\ \{\chi\}_j \end{Bmatrix} \qquad j= 1,2,\ldots,2NMOD \tag{5.3.17}$$

The expressions for c_{qj}, k_{qj}, and $R_j(t)$ may be reduced by substituting Equations (5.3.5), (5.3.6), (5.3.8.a), and (5.3.17) into Equations (5.3.12), (5.3.13), and (5.3.16); i.e.,

$$C_{qj} = 2\Omega_j\{\chi\}_j^T[\hat{M}]\{\chi\}_j + \{\chi\}_j^T[C_u]\{\chi\}_j \tag{5.3.18}$$

$$k_{qj} = -\Omega_j^2\{\chi\}_j^T[\hat{M}]\{\chi\}_j + \{\chi\}_j^T[R]\{\chi\}_j \tag{5.3.19}$$

$$R_j(t) = \{\chi\}_j^T\{\hat{F}\} \tag{5.3.20}$$

Substitute Equation (5.3.8.b) into Equation (5.3.20) to get

$$R_j(t) = B_{DRj\ell}V_\ell + B_{IRj\ell}a_\ell \tag{5.3.21}$$

$$j=1,2,\ldots,NMOD$$

$$\ell=1,2,\ldots,NEQ$$

in which $B_{DRj\ell}$ is the ℓth element of the matrix

$$\{B_{DR}\}_j^T = \{\chi\}_j^T[\hat{B}_{DG}] \tag{5.3.21}$$

and $B_{IRj\ell}$ is the ℓth element of the matrix

$$\{B_{IR}\}_j^T = \{\chi\}_j^T[\hat{B}_{IG}] \tag{5.3.23}$$

Substituting expressions for V_ℓ and a_ℓ given by Equations (5.2.8.a-c) and (5.2.9.a-c) into Equation (5.3.21) gives the Fourier series representation for force $R_j(t)$; i.e.,

$$R_j(t) = \sum_{m=-N}^{N} H_{R_j}(m)\ A_m \exp(i\omega_m t) \tag{5.3.24}$$

in which the force transfer function is given by

$$H_{Rj}(m) = B_{DRj\ell}H_{V\ell}(m) + B_{IRj\ell}H_{a\ell}(m) \tag{5.3.25}$$

and angular frequency ω_m by

$$\omega_m = m\Delta\omega \tag{5.3.26}$$

The solution of Equation (5.3.15) with forcing function given by Equation (5.3.24) may be expressed as

$$r_j(t) = \sum_{m=-N}^{N} H_{rj}(m) A_m \, m \exp(i\omega_m t) \tag{5.3.27}$$

in which the response transfer function is given by

$$H_{rj}(m) = \frac{H_{Rj}(m)}{(k_{qj} + i\omega_m c_{qj})} \tag{5.3.28}$$

where $i = \sqrt{-1}$

The cable displacement may be computed according to

$$U_\ell(t) = \theta_{\ell n} \chi_{nj} r_j(t) \tag{5.3.29}$$

$$n=1,2,\ldots,NMOD$$

$$j=1,2,\ldots,2NMOD$$

in which χ_{nj} is the nth element of eigenvector $\{\chi\}_j$. The Fast Fourier Transform (FFT) algorithm may be utilized to get the discrete time series of cable displacement U_j.

The computational steps for the stochastic response analysis may be summarized as follows:

(1) Form mass and stiffness matrix.

(2) Compute natural frequencies and mode shapes.

(3) Generate random complex wave amplitude as indicated in Section 5.1.

(4) Compute the fluid particle velocity and acceleration complex amplitude as indicated in Section 5.2.

(5) Compute the initial standard deviations $\sigma_{V_{NR}V_{NR}}$ and $\sigma_{V_{TR}V_{TR}}$ according to Equations (5.2.5.a,b) by assuming the cable velocities equal to zero.

(6) Compute fluid drag damping, drag forces, and inertial forces according to Equation (5.2.1).

(7) Form matrices $[C_q]$ and $[K_q]$ according to Equations (5.3.5,6).

(8) Compute eigenvalues Ω_n's and eigenvectors $\{\theta\}_n$'s.

(9) Compute C_{qj} by K_{qj}, and $R_j(t)$ by Equations (5.3.18), (5.3.19), and (5.3.20), respectively.

(10) Compute the complex amplitude of $r_j(t)$.

(11) Transform the complex amplitudes obtained in step (10) to the nodal response amplitudes by Equation (5.3.13).

(12) Compute the new standard deviations $\sigma_{V_{NR}V_{NR}}$ and $\sigma_{V_{TR}V_{TR}}$.

(13) Check whether the new values of $\sigma_{V_{NR}V_{NR}}$ and $\sigma_{V_{TR}V_{TR}}$ are unchanged relative to their previous values; if so, continue to the next step, otherwise, repeat steps (6) through (13).

(14) Take the inverse FFT of the nodal response amplitudes to get the time series of the stochastic nodal response.

6.0 PROBLEM EXAMPLE

The validation of the proposed mathematical model for both static and dynamic responses of cable and cable-large body systems in an ocean environment will be demonstrated here by seven examples. Examples 1 and 2 are to demonstrate the ability of the residual feedback and viscous relaxation models to determine the static response of a strong geometrically nonlinear cable. Example 3 is used to verify the viscoelastic material model of cable response with a time history due to a static load. Example 4 is used to test the accuracy of the time integration scheme employed. The two-dimensional dynamic response of a cable-large body system to both deterministic and non-deterministic wave loadings is investigated in Example 5. A wake-oscillator model for cable strumming in an uniform flow is tested in Example 6. The last example considered is the three-dimension dynamic response of a three-leg single mooring subjected to a deterministic wave loading in which cable strumming effects are included.

6.1 Example 1: Point Load on a Horizontal String

This problem was used by Webster (1974) to demonstrate three static solution methods: a purely linear increment

method, a residual feedback method, and a modified Newton-Raphson method. In this example, the viscous relaxation method will be employed. Results are compared to an analytic solution.

The cable is fixed at both ends (Figure 6.1.1) and a point load is applied at the middle of the cable. The cable is linearly elastic and has the following properties:

Young's modulus	,	$E = 10{,}000{,}000$ psf
Initial area	,	$A_0 = 0.1$ ft^2.
Initial stress	,	$\sigma_0 = 500$ psf

The initial configuration of the cable is unstable because it has no vertical stiffness. The parameters used in the viscous relaxation technique are:

Initial artificial damping constant	,	$C_0 = 100{,}000$
Tolerance	,	TOL = 0.001
Decrement factor	,	$\mu = 0.5$

In this example the following formula is used for determining the artificial damping at time t

$$C(t) = \mu C(t-\Delta t) \qquad (6.1.1)$$

in which Δt = time increment (1 second in this example). This parameter combination is not necessarily the optimum combination. One of the guidances to determine the initial

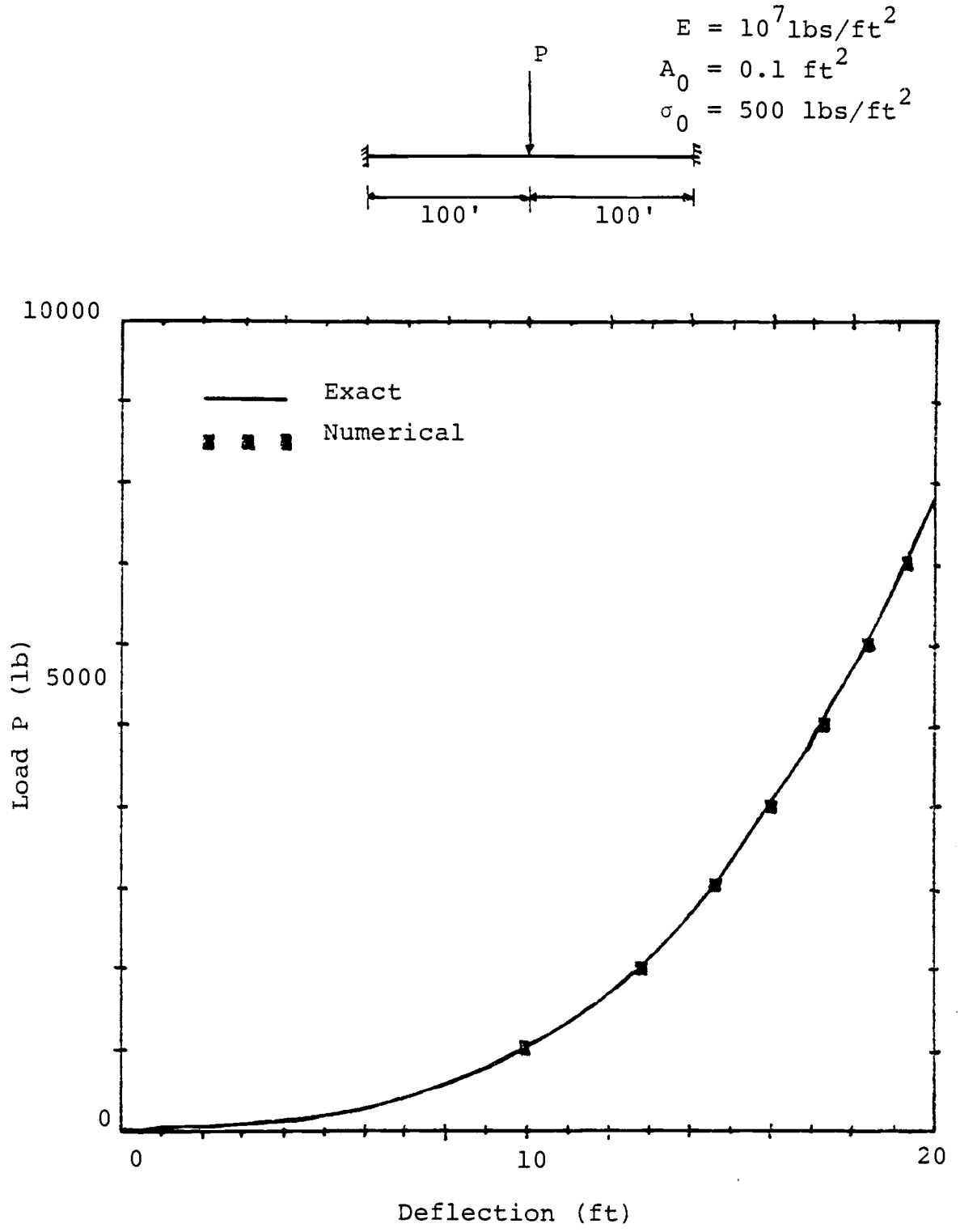

Figure 6.1.1. Midpoint deflection of a stretched string with point load.

value when the ratio of the applied load to the stiffness is large. As geometric stiffness is developed the damping constant is reduced at a rate dependent, again, on the ratio of the applied load to the cable stiffness.

Webster (1974) used 100 load steps in a purely incremental solution scheme and used 55 iterations in a modified Newton-Raphson method. In this example, 44 iterations were required (2.01 seconds CPU execution time on a Cyber 170/720). The stiffness matrix was updated every 10 steps. Results are displayed in Figure 6.1-1 where close agreement to the analytic solution is shown.

6.2 Example 2: Static Response of a Suspended Cable

The static deflection of a suspended cable which is submerged in sea water and having a large cable length and span ratio is investigated in this example. Two catenary segments of length 500 feet and 1000 feet, respectively, span between coordinate (0,0) and (1200', 500') (see Figure 6.2-1). In addition to cable weight and fluid pressure, a buoyant load of 900 pounds is attached at the junction of the two segments.

The viscous relaxation technique is used to solve the problem. The assumed initial configuration is a straight line stretched from the position (0,0) to the position (1417', 500'). The cable weight, fluid pressure and

motions of the right support to its fixed position are applied in 20 increment steps. The cable, fluid, and load data are listed below

Cable length	, L = 1500 ft
Initial cross-sectional area	, A_0 = 0.0218 ft^2
Initial stress	, σ_0 = 0.5 psf
Young's modulus	, E = 8,120,000 psf
Cable mass density	, ρ = 3.35 $slugs/ft^3$
Fluid mass density	, ρ_f = 2.0 $slugs/ft^3$
Concentrated load	, P = 900 lbs.
Tolerance	, TOL = 0.001
Number of elements	, NOE = 6

The combination of parameters used for viscous relaxation computation is the same as for Example 1. When the cable elements become slack (due to potential compression states), the modulus E for the slack element is set to a very small value in the neighborhood of zero and stiffness matrix is recomputed. Otherwise, the stiffness matrix is updated for every 10 steps. The solution converged after 100 iterations and required 40 seconds CPU execution time on Cyber 170/720. The results are compared in Figure 6.2-1 with the exact solution computed from the catenary equation in which the cable is assumed inextensible

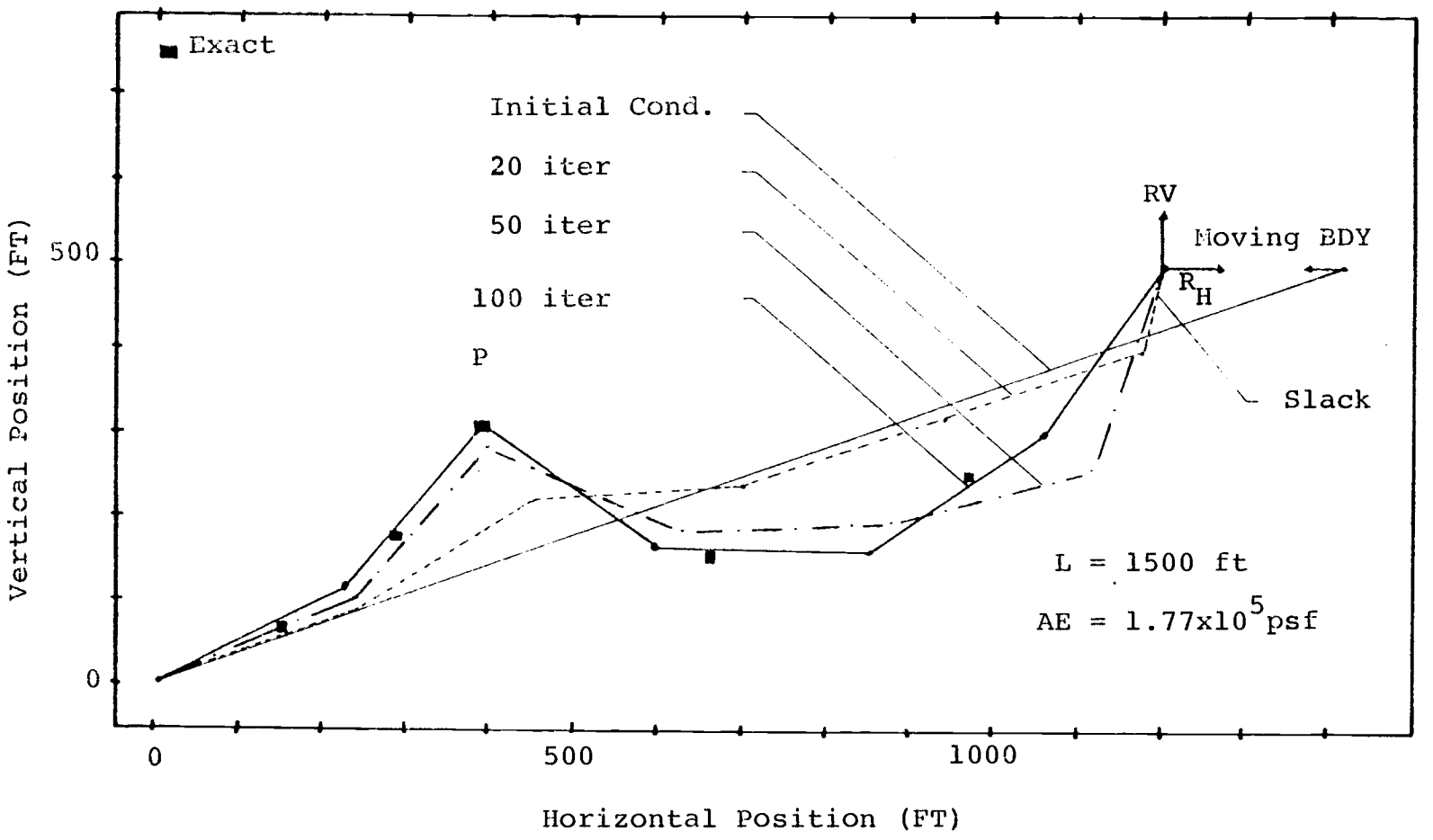

Figure 6.2_1. Static deflection of a suspended cable.

6.3 Example 3: Point Load at the Lower End of Hanging Cable

This example is used to show the history of the response of a viscoelastic cable subjected to a static load. The numerical results computed by the residual feedback method and the purely incremental method were compared to the exact solution. The material properties and the initial geometry along with the loading history is illustrated in Figure 6.3-1. The exact and numerical results for the strain are tabulated in Table 6.3-1. The exact solution is obtained by solving the viscoelastic constitutive equation given in Section 2.2.b by Equation (2.2.b.2) in which the stress function is assumed a given quantity. The cable continues to stretch after the load remains constant. The final strain is equal to the elastic strain with modulus K_0 and, theoretically, it is reached at time approaching infinity. It can be seen from Table 6.3-1 that the solution obtained by the purely incremental method is drifting from the exact solution as time increases. The residual method, which is shown in the third column, corrects this drifting tendency and improved the solution.

TABLE 6.3-1

STRAIN COMPARISON OF NUMERICAL SOLUTIONS
WITH THE EXACT SOLUTION

Time (sec) (1)	Strain $\varepsilon(t)$		
	Exact (2)	Residual Feedback (3)	Purely Increment (4)
0.0	0.0	0.0	0.0
0.2	0.0194	0.0188	0.0198
0.4	0.0386	0.0377	0.0390
0.6	0.0584	0.0572	0.0585
0.8	0.0788	0.0774	0.0783
1.0	0.0999	0.0982	0.0985
1.2	0.1022	0.1019	0.1014
1.4	0.1053	0.1051	0.1044
1.6	0.1084	0.1083	0.1073
1.8	0.1115	0.1114	0.1102
2.0	0.1148	0.1145	0.1130
2.5	0.1229	0.1228	0.1201
3.0	0.1306	0.1305	0.1270
60.	0.6066	--	--
∞	0.7692	--	--

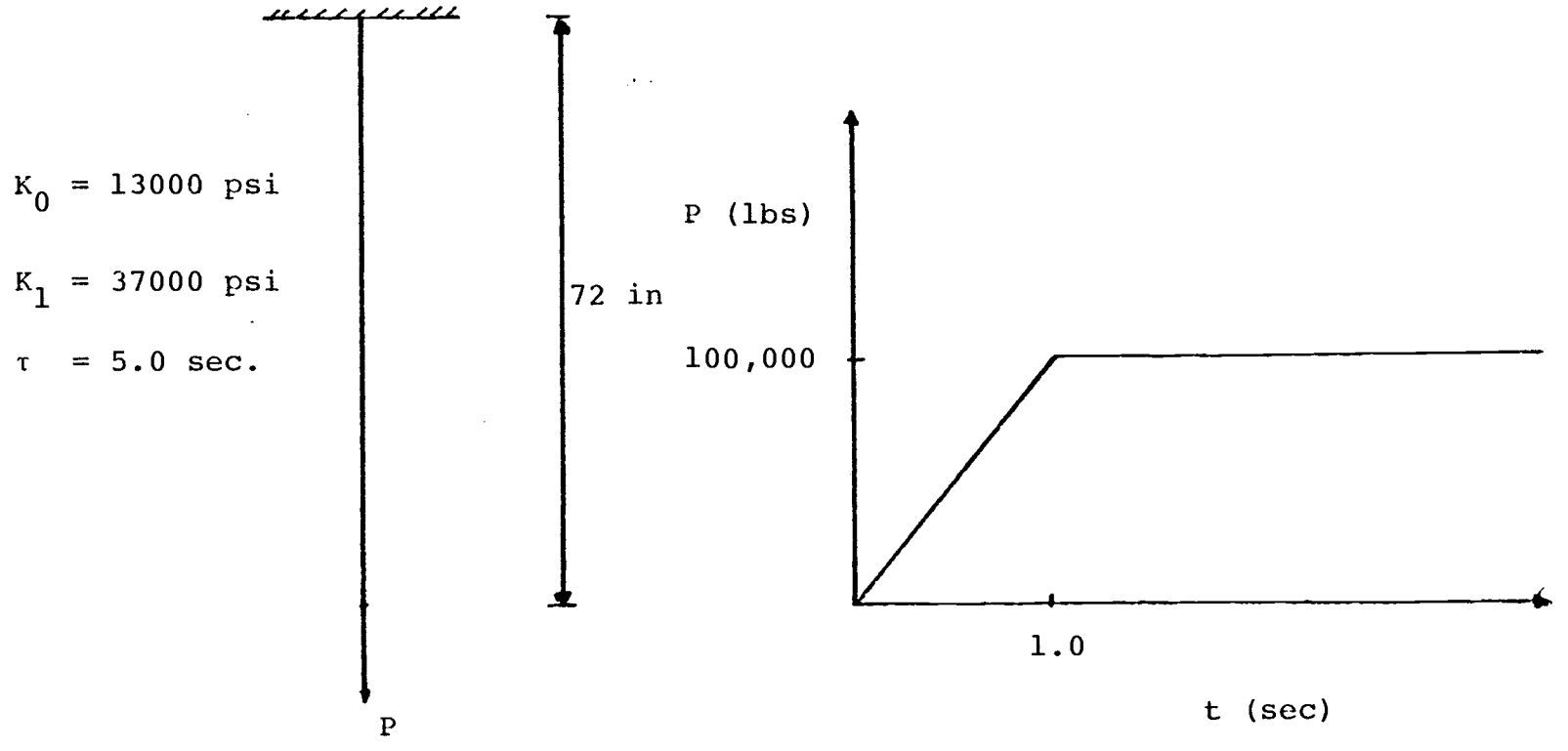

Figure 6.3-1. Quasi-static problem for a linear viscoelastic material.

6.4 Example 4: Point Mass on a Horizontal String

This example is used to compare the dynamic responses for cables comprised of elastic and linear viscoelastic materials. A lumped mass of 5 slugs/ft^3 is placed at midspand of a 20-foot string which is fixed at both ends. The mass is initially displaced two feet and suddenly released. The material properties of the cable are given in Example 1 for the elastic material and in Example 3 for the viscoelastic material. The residual feedback method is employed in the numerical calculation. The time increment is 0.001 sec. and the stiffness is updated at every 10 steps.

The typical dynamic response and stress variation of the model using two elements and lumped mass are shown in Figure 6.4-1 and Figure 6.4-2, respectively. The exact response for the elastic material, obtained by integrating the exact equation derived from the geometry of the system, coincides with the numerical results. The period of response for the elastic material is 0.65 seconds while for the viscoelastic material the period increases as the amplitude dampens. The phase lag between the elastic response and the viscoelastic response becomes more pronounced and the stress in viscoelastic cable decreases as time increases. A slack condition occurs in the viscoelastic model after a few cycles and its duration increases as the number of cycles

increases. These phenomena arise due to the inherent nature of the viscoelastic material, wherein the energy is dissipated and the modulus is reduced to its quasi-static modulus, K_0 (see Bitting, 1978).

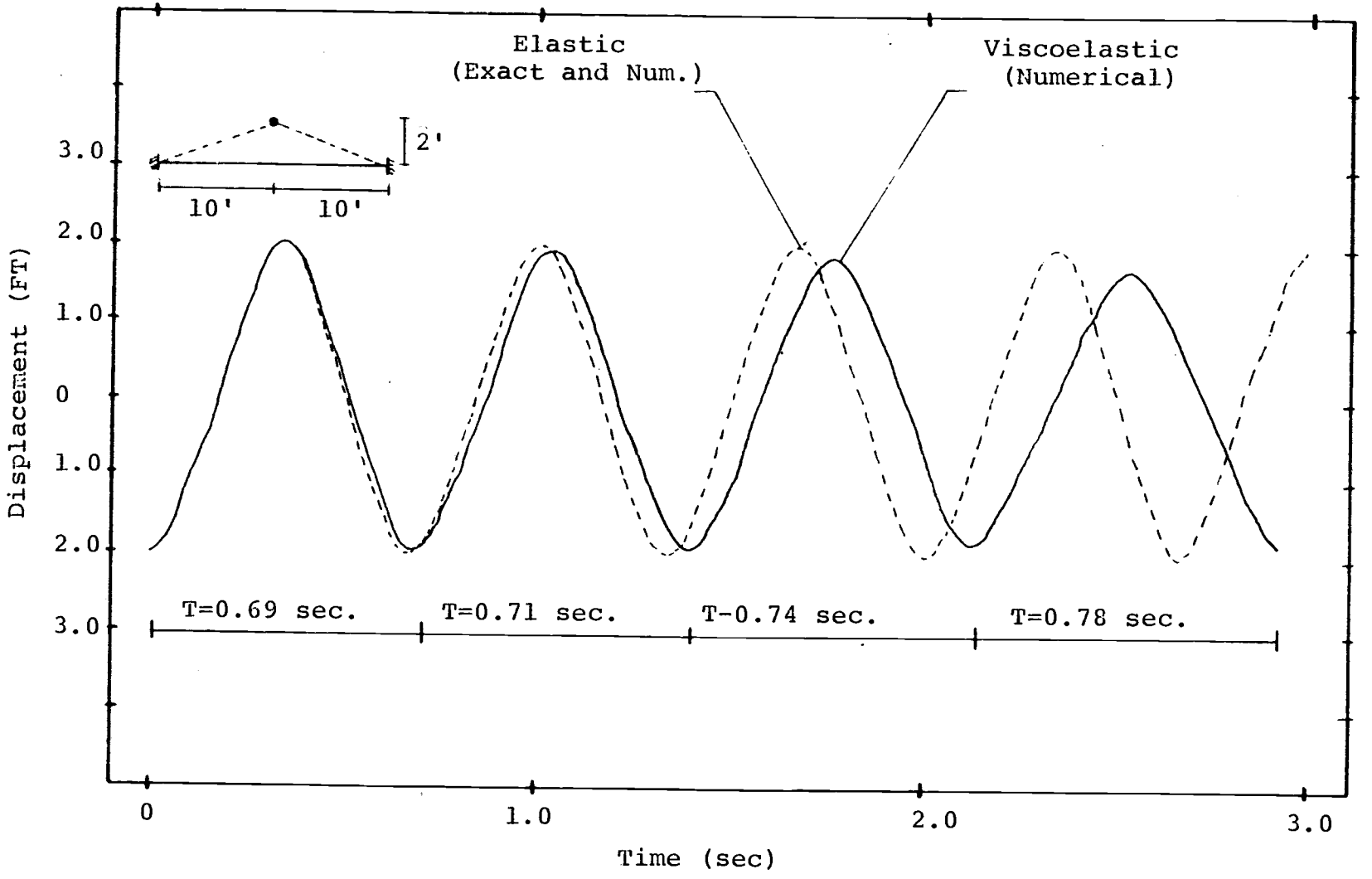

Figure 6.4.1. The displacement of the midpoint.

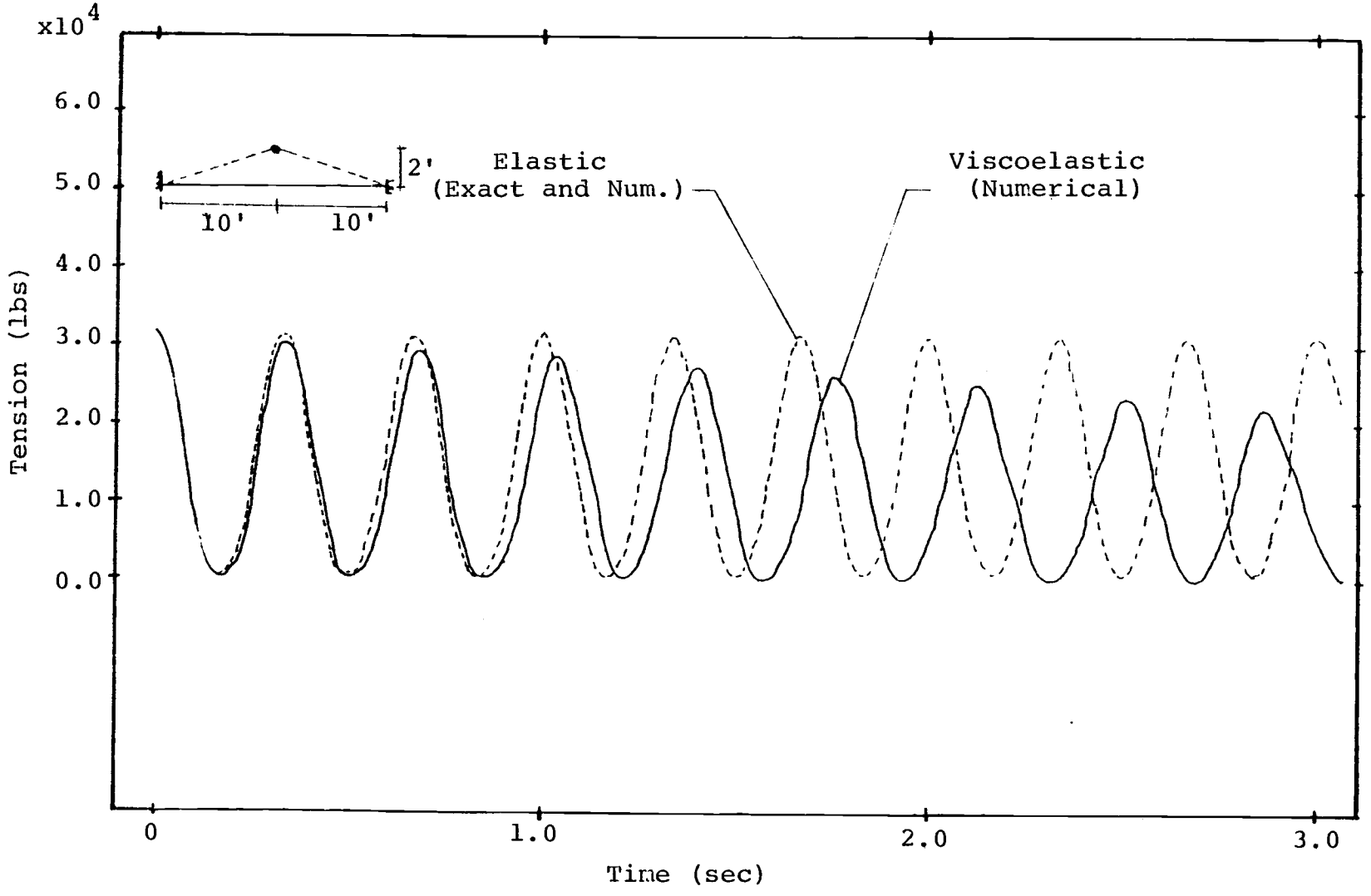

Figure 6.4-2. Tension variation in the string.

6.5 Example 5: Two-Dimensional One-Leg Single Point Mooring

This example is used to demonstrate both the deterministic and nondeterministic dynamic analysis procedure for a hydrodynamically loaded cable body system. The example involves a single linearly elastic cable attached to a floating disc at the water surface. The static loads on the system are a wind load of 100 pounds, the buoyant force, and the cable weight. The cable is initially stretched from the bottom of the ocean to the position (300, 2.5) as shown in Figure 6.5-1. The static deflection is determined by the viscous relaxation method with a parameter combination similar to that given in Example 2. The cable and fluid properties and the problem definition sketch are given in Figure 6.5-1.

Deterministic response. A ten-foot wave with three-second period is applied to the system. The forces and hydrodynamic coefficients on the disc in this problem are those which are computed by Hudspeth (1980). The surge motion for the buoy is given in Figure 6.5-2 for the three-element cable and Figure 6.5-3 for the eight-element cable. To avoid the high frequency initial fluctuation of the system responses, the wave amplitude is assumed to be zero initially and approaches five feet as time increases. This amplitude may be represented by 5exp(-0.005/t). The

solid line is the displacement computed by the incremental/ iterative method with 0.02 second time increment and the dashed line is the displacement computed by the residual feedback method with 0.005 second time increment. The stiffness matrix is recomputed at every five steps. The residual feedback method gives false results and the solution is diverging. This is because of the small resistance to horizontal motion of the cable so that the incremental displacement is no longer small. The incremental/ iterative method gives better results because the solution is obtained by iteration until equilibrium during each increment is achieved. The computational execution time with the convergence tolerance 0.01 for both methods is almost the same (400 second CPU execution time on the Cyber 170/ 720).

The response period is slightly longer than the wave period. The surge for the eight-element model of the cable is slightly larger than for the three-element model. This larger value occurs because the wave forces are lumped at nodal points. The fluid particle velocity and acceleration decay exponentially with depth. Therefore the wave force on the top element is much higher than on the lower element. The top element for the eight-element model of the cable is shorter than the three-element model. Consequently, the

force on the eight-element model is concentrated nearer to the disc than on the three-element model.

The high frequency fluctuation in the heave motion occurs because of the sudden release of the disc when the cable slackens.

Nondeterministic response. The Pierson-Moskowitz spectrum shown in Figure 6.5-6 is employed to simulate the wave realization from which wave forces are calculated by Morison's equation (Morison et al., 1950) for cable segments and by diffraction theory for the disc buoy. The values for the energy content, m_0, which is equivalent to the area under the spectral curve, and the spectral peak, ω_p, are the values obtained from the Hurricane Carla wave record (Hudspeth, 1974); that is, $m_0 = 28\ ft^2$ and $\omega_p = 0.5$ rad/sec. The solid line in Figure 6.5.6 represents the expected spectrum which can be obtained by the Deterministic Spectral Amplitude (DSA) simulation method while the broken line represents the sample spectrum which can be obtained by the Nondeterministic Spectral Amplitude (NSA) simulation method (refer to Section 5.1). In this example, the DSA method is employed. The spectrum is discretized by 200 discrete frequencies with an 0.0245 rad/sec. increment. The simulation time length is 256 seconds with a 0.25 second increment, equivalent to 1024 discretized time points.

The frequency-dependent coefficients of the wave forces acting on the disc which were computed by Hudspeth (1980) are interpolated to obtain the force spectrum on the disc. The cable is divided into three elements and the mass and stiffness matrix of the system are computed at the static configuration state. Six natural frequencies and six mode shapes are calculated by the subspace iteration method (Bathe, 1976). These mode shape vectors are used to transform the global equation of motion which includes the fluid drag damping to modal equations which then decoupled by a method introduced by Foss (1958). The linearized drag force coefficients are obtained after eight iterations with 0.01 convergence tolerance and after 193 second CPU execution time on the Cyber 170/720.

The typical spectral responses of the disc are shown in Figures 6.5-7,8,9. Several peaks in the spectral curve for surge indicate resonance at the natural frequencies. The spectral shape for the heave is almost identical with the wave surface spectral shape. This indicates that the disc is responding to the wave exciting forces with motion similar to that of the wave surface. An interesting behavior of the pitch motion can be seen in Figure 6.5-9 where the spectral response peaks at a frequency ω = 4.6 rad/sec. equal to the natural frequency where the modal shape is predominantly pitch. Even if resonance is anticipated to

occur, the magnitude of the response is predicted as larger than would be expected in that the amplitude at that frequency is insignificant. The explanation for this abnormality may be that the linearized drag coefficient, which is a function of the wave amplitude, is very small so that the motion is practically undamped and therefore contributes significantly to the response magnification.

The random time responses of the disc are shown in Figure 6.5-10 for surge, Figure 6.5-11 for heave, and Figure 6.5-12 for pitch. The erratic motion of the pitch is caused by the unexpectedly large significance of the high frequency pitch response predicted, as previously indicated.

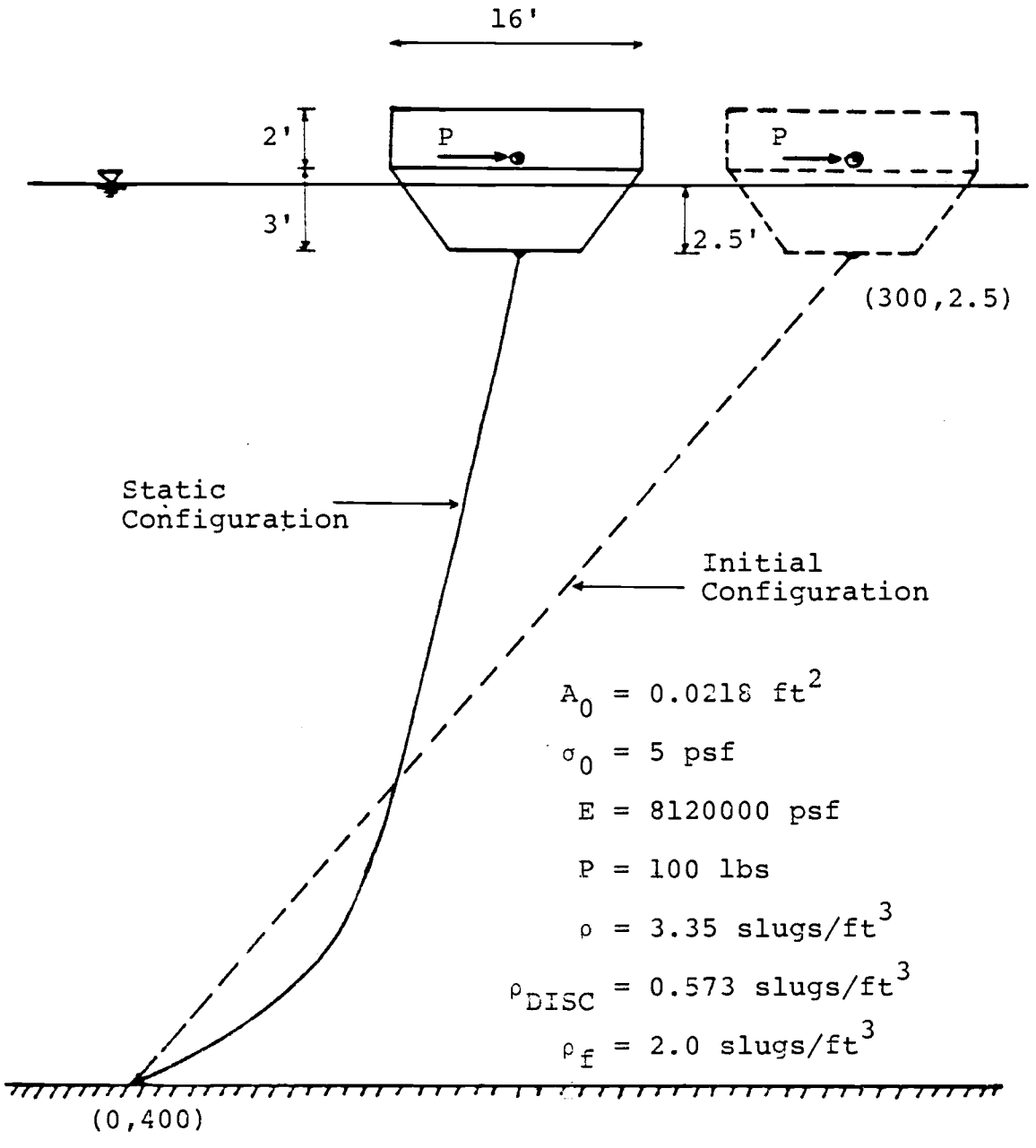

Figure 6.5-1. Static configuration of a one-leg single-point mooring.

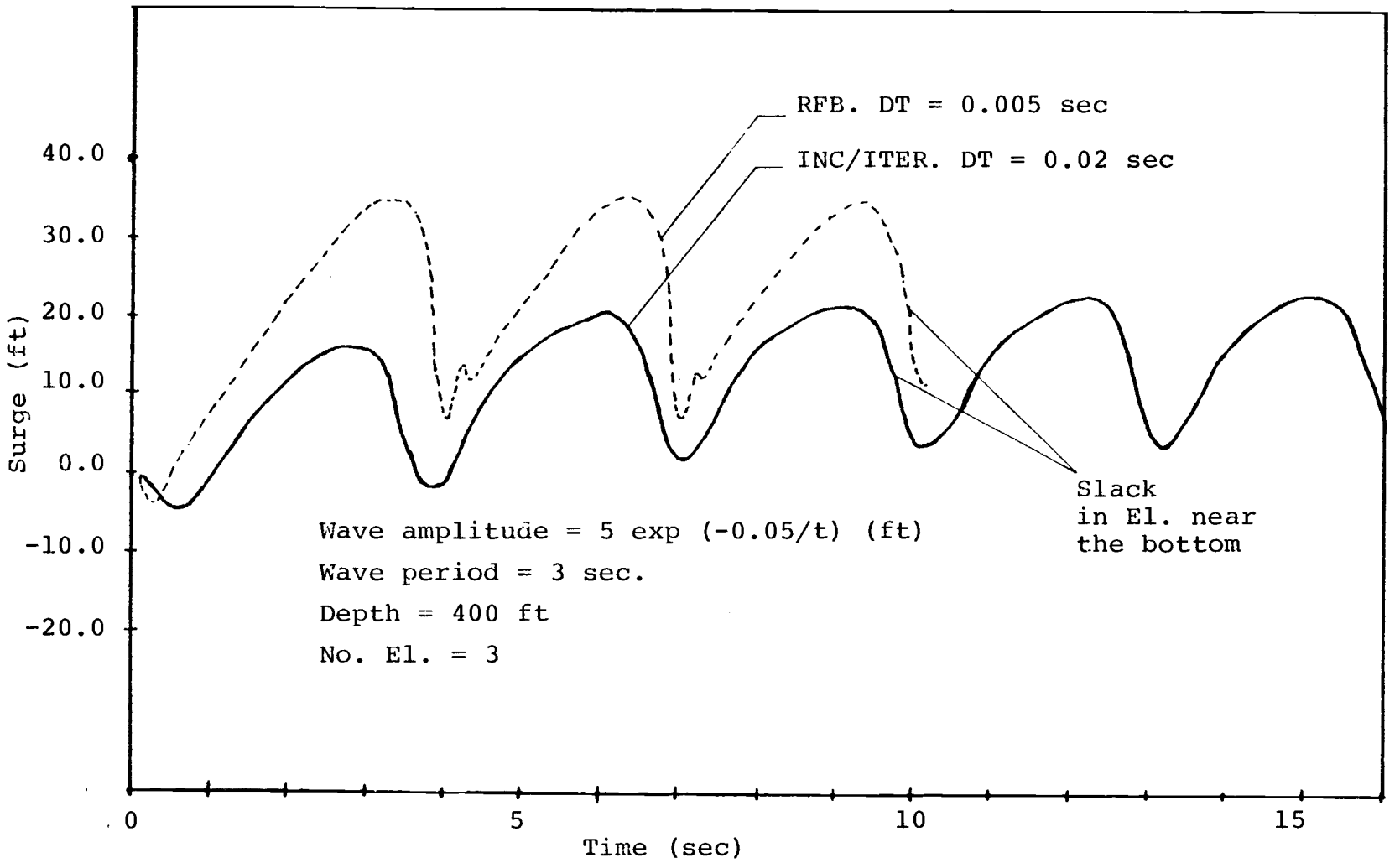

Figure 6.5-2. Surge vs. time, cable with three elements.

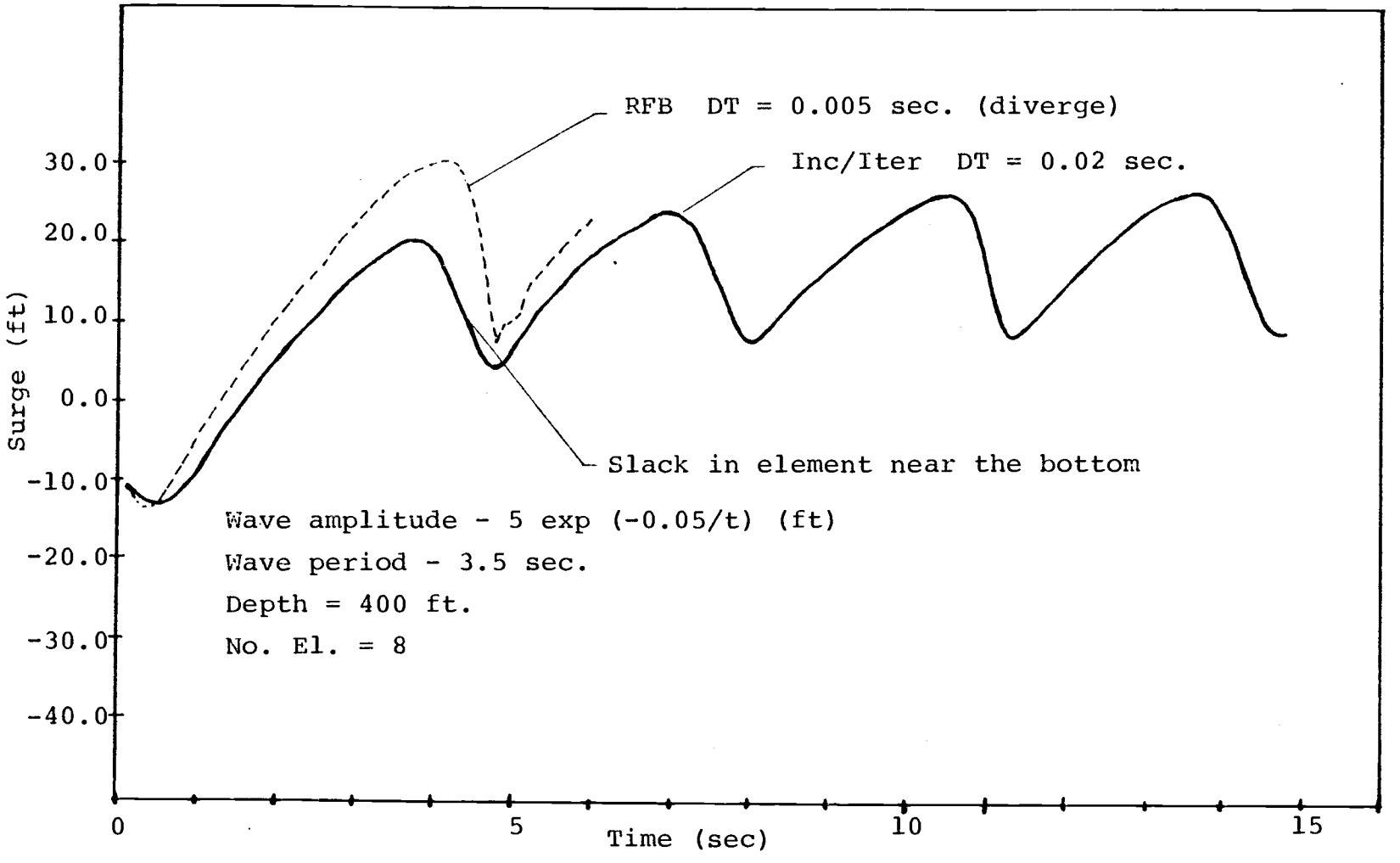

Figure 6.5-3. Surge vs. time, cable with eight elements.

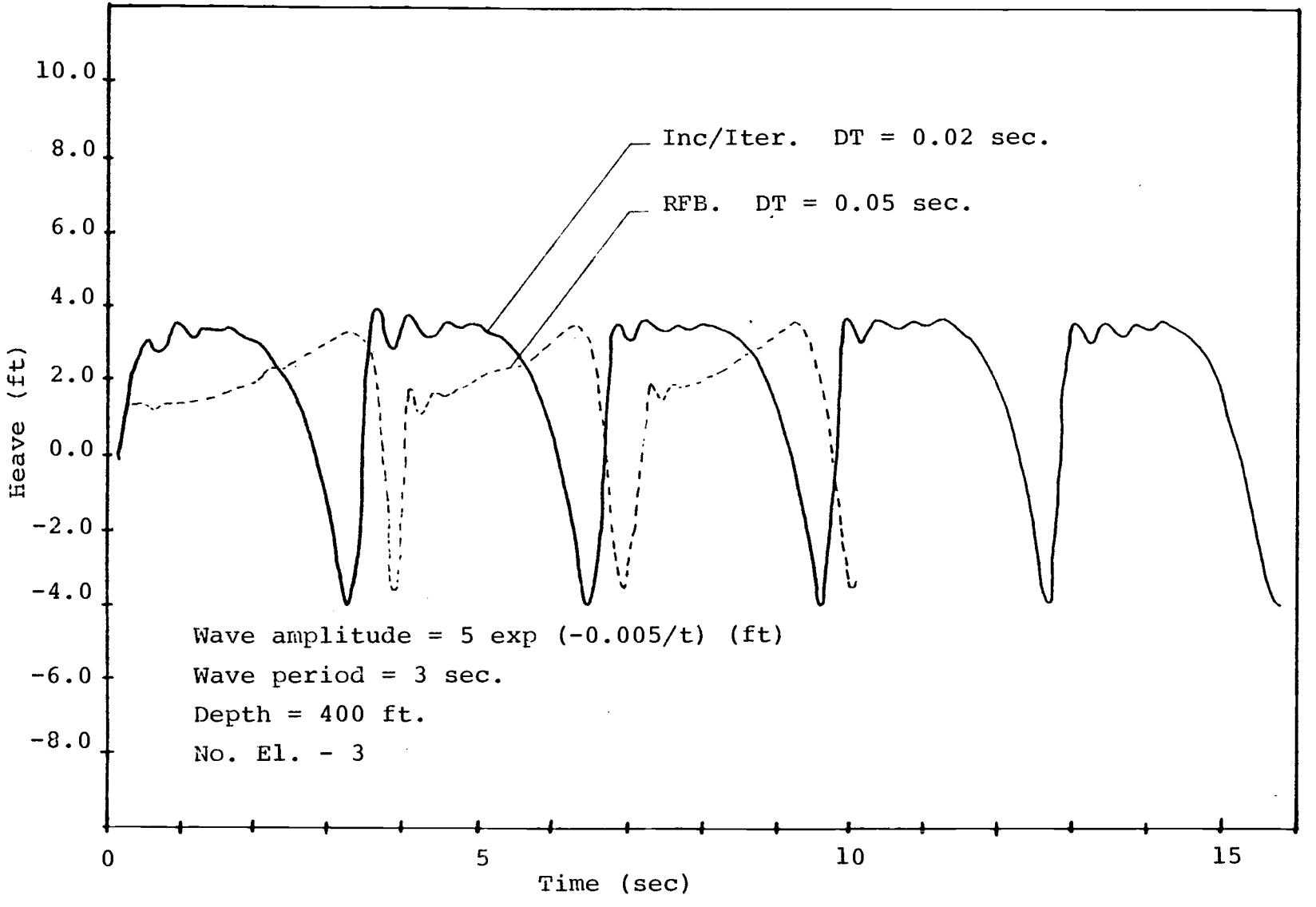

Figure 6.5-4. Heave vs. time, cable with three elements.

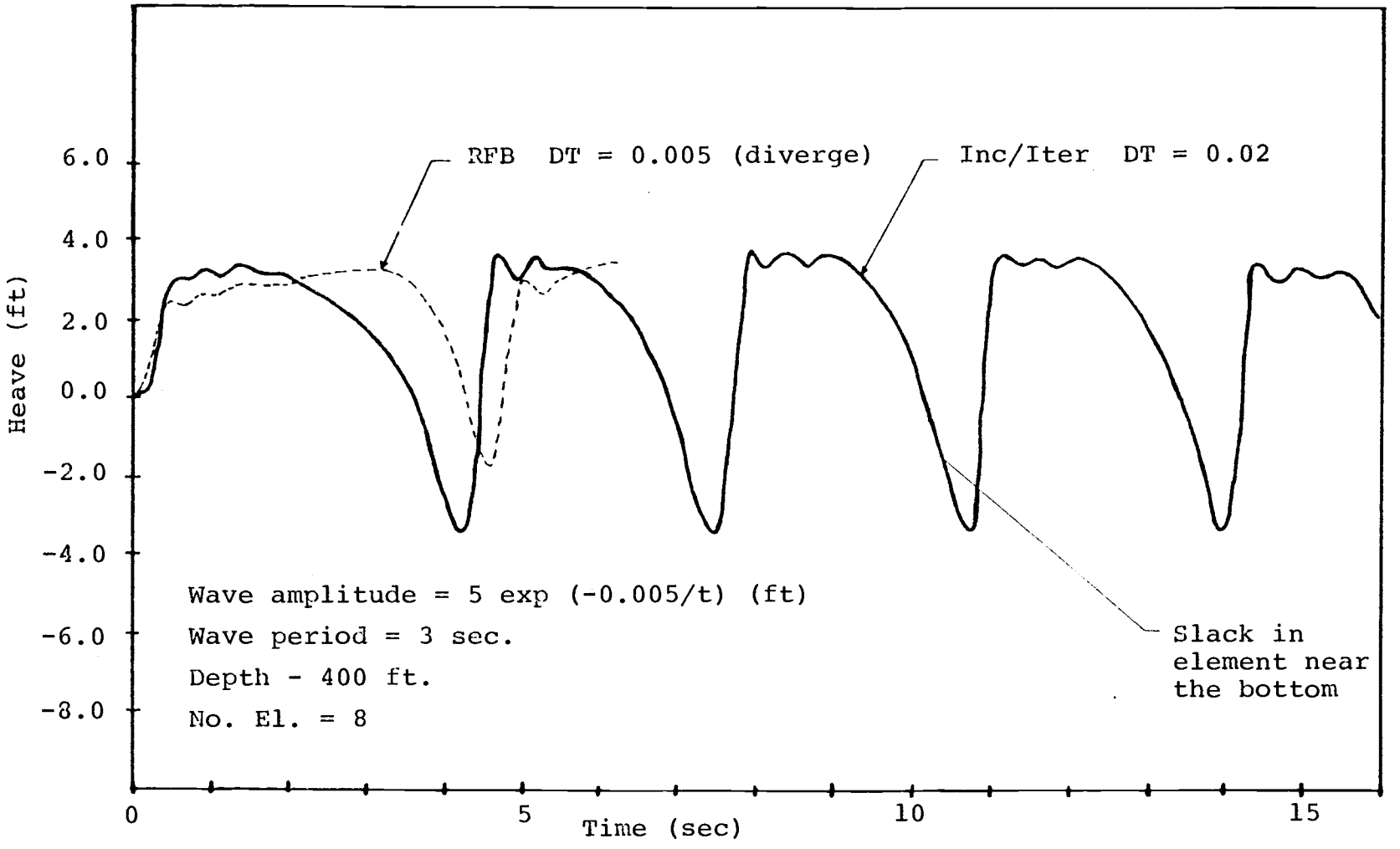

Figure 6.5-5. Heave vs. time, cable with eight elements.

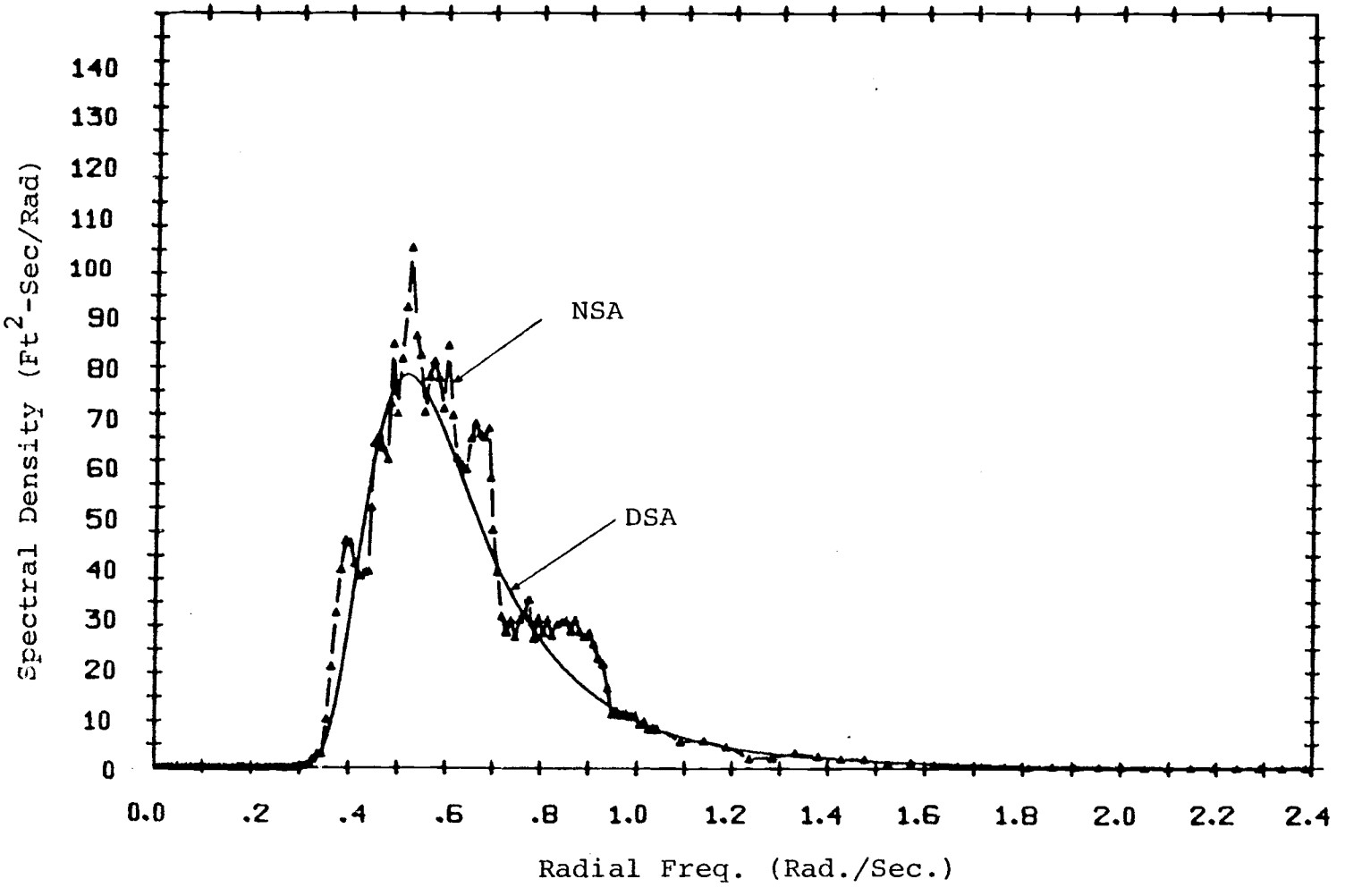

Figure 6.5-6. Pierson-Moskowitz spectrum with energy content m_0 = 28.00 ft^2, peak frequency ω_p = 0.5 rad/sec.

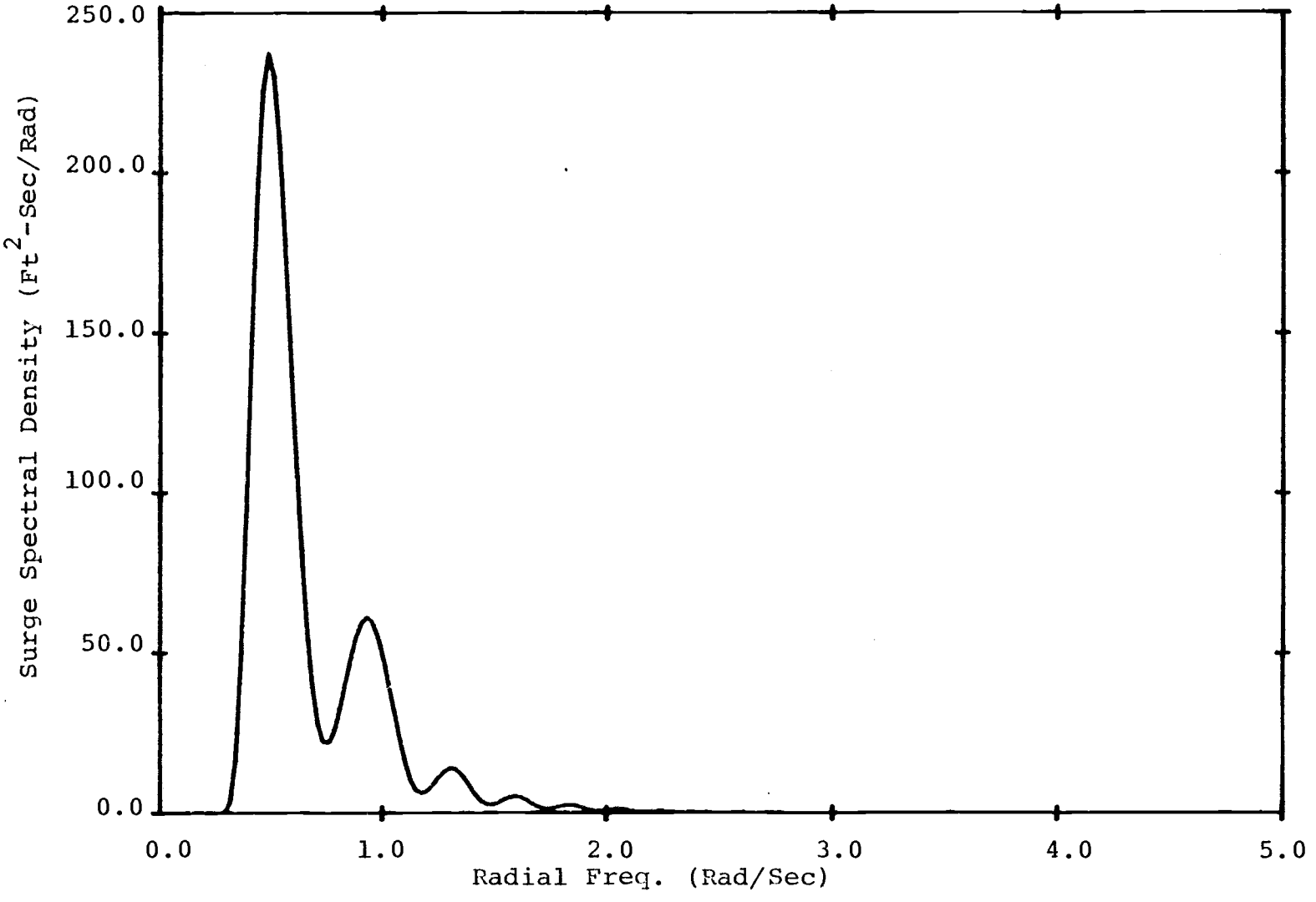

Figure 6.5-7. Energy spectral density for surge simulated by Pierson-Moskowitz spectrum.

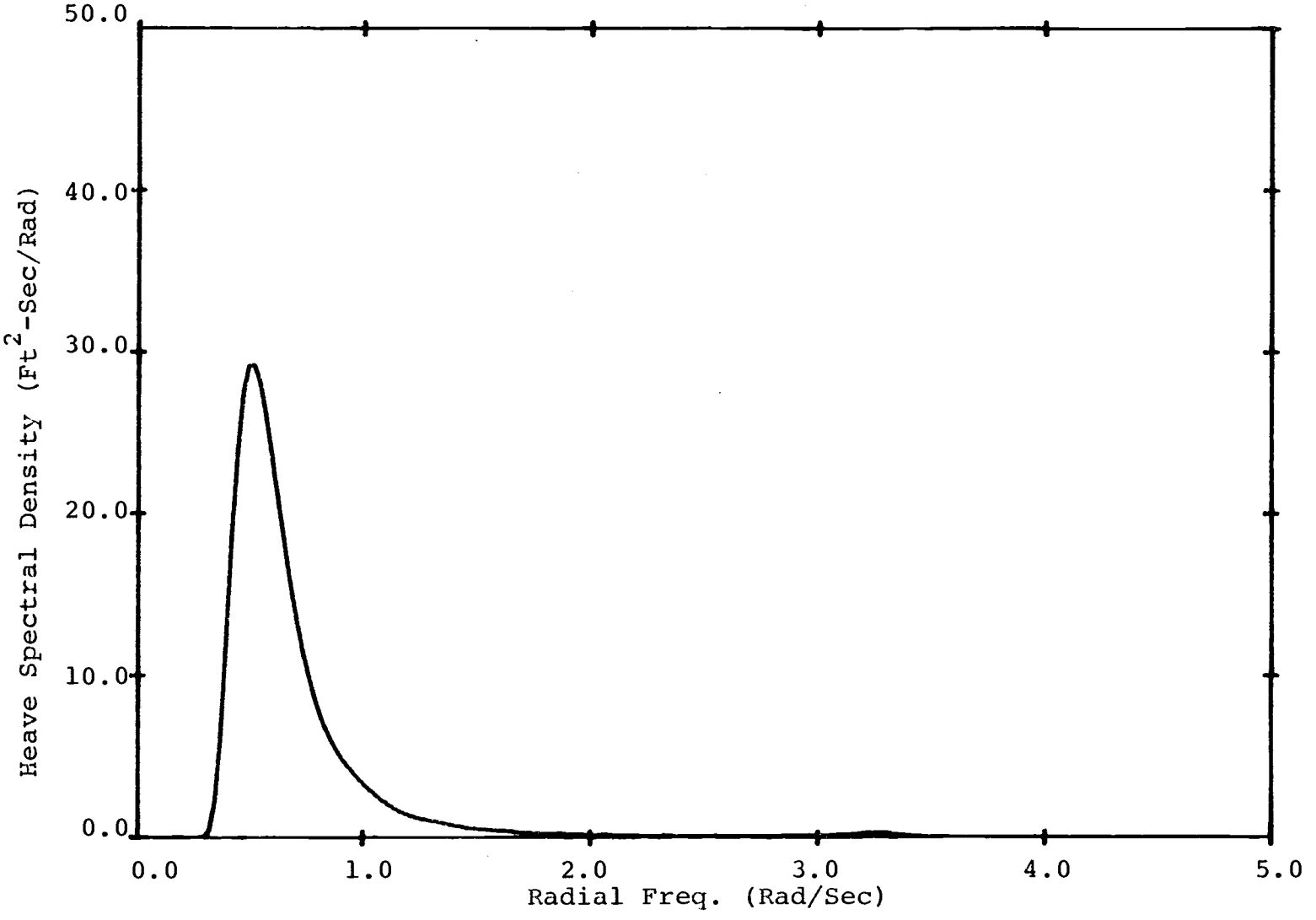

Figure 6.5-8. Energy spectral density for heave simulated by Pierson-Moskowitz spectrum.

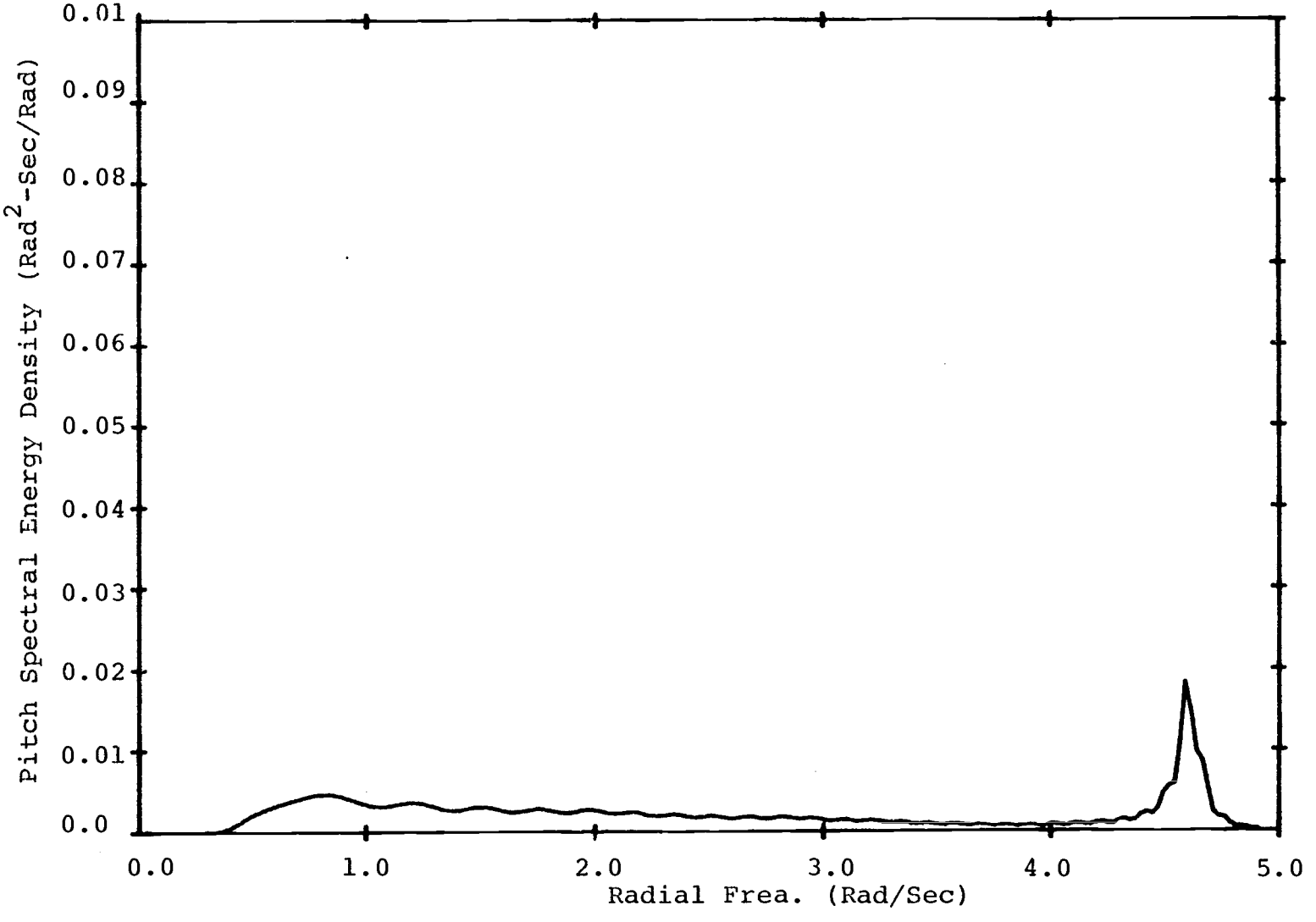

Figure 6.5-9. Energy spectral density for pitch simulated by Pierson-Moskowitz spectrum.

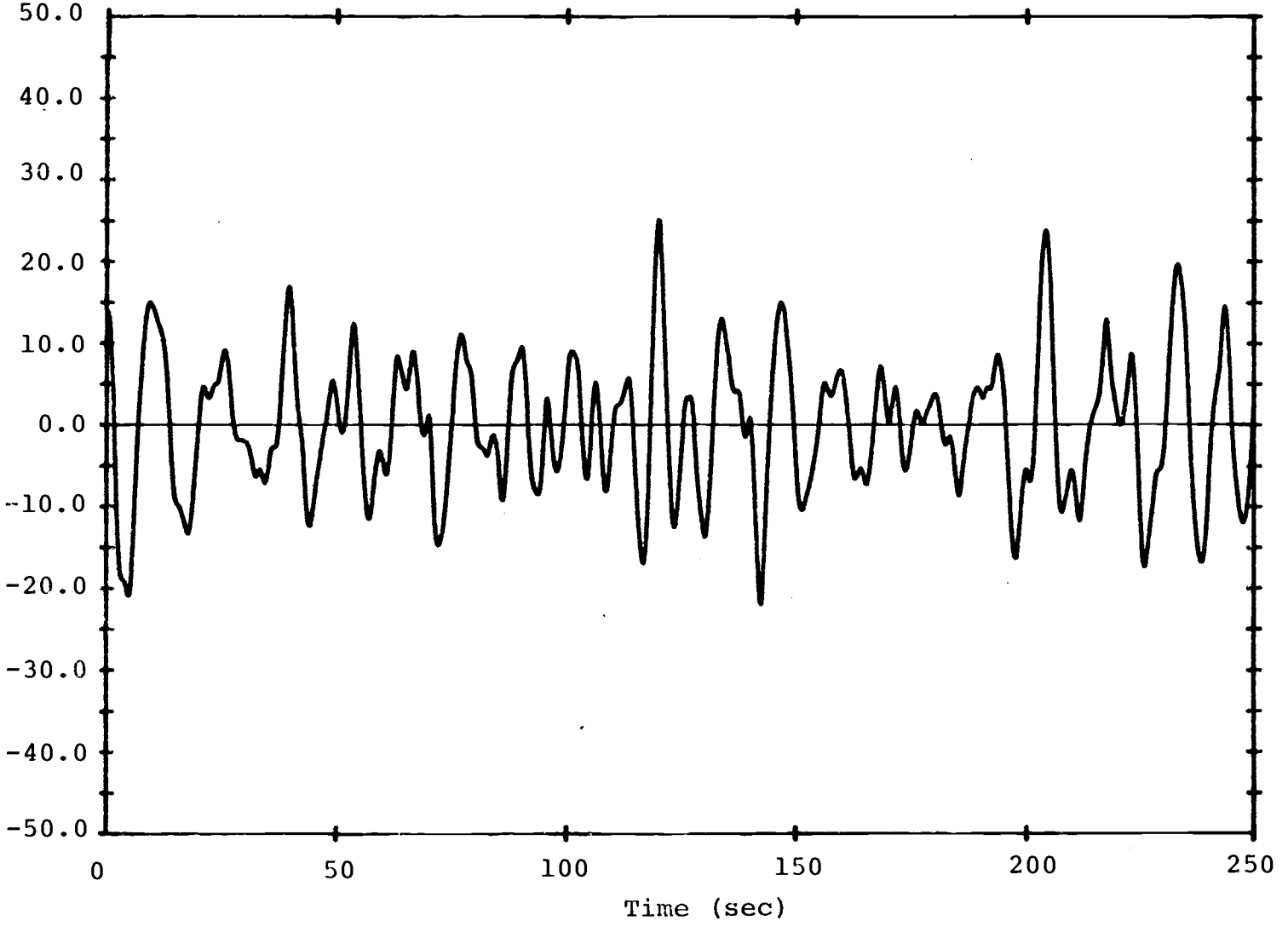

Figure 6.5-10. Surge vs. time.

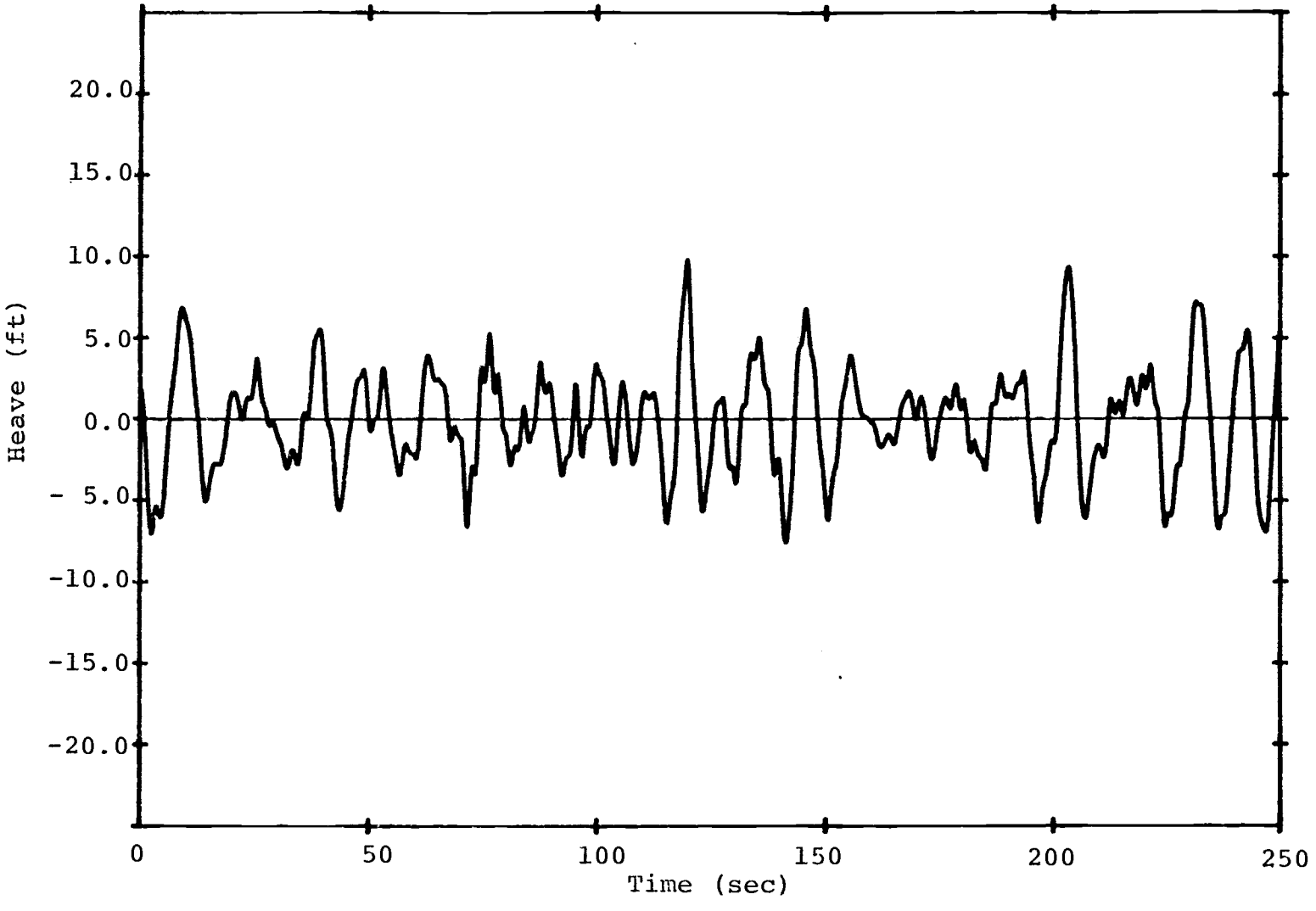

Figure 6.5_11. Heave vs. time.

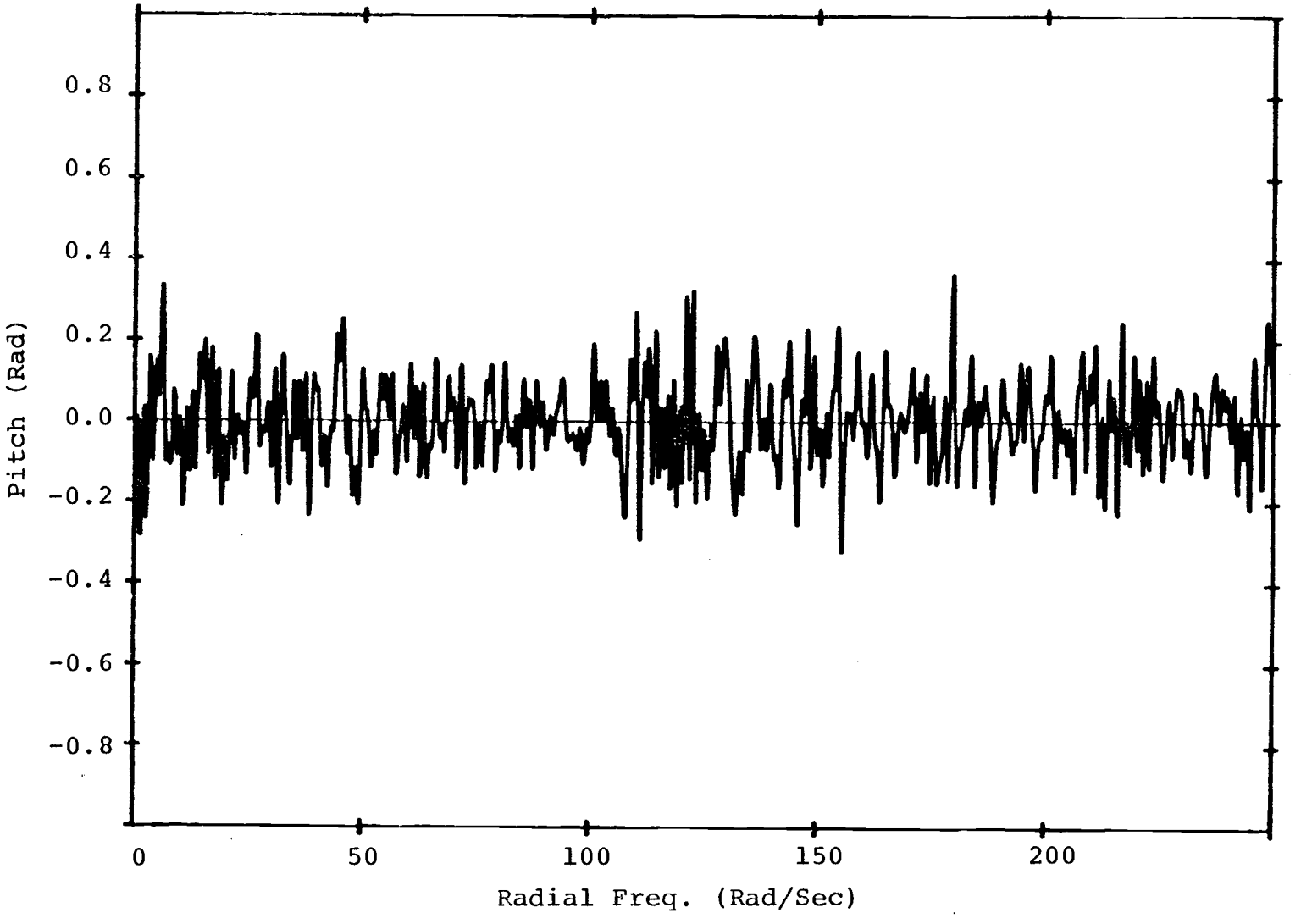

Figure 6.5_12. Pitch vs. time.

6.6 Example 6: Transversal Displacement of a Horizontal String in a Steady Uniform Flow

This example is used to validate the model for cable strumming prediction. Experiments for this kind of problem were conducted by Ramberg, et al. (1980). The cable and fluid properties are given as follows:

Cable diameter	,	$D = 0.05$ feet
Cable length	,	$L = 14.37$ feet
Number of elements	,	$NOE = 4$
Time increment	,	$\Delta t = 0.001$ seconds
Initial stress	,	$\sigma_0 = 33100$ psf
Cable mass density	,	$\rho = 7.78$ slugs/ft^3
Young's modulus	,	$E = 8{,}113{,}100$ psf
Fluid velocity	,	$V = 0.695$ fps
Fluid mass density	,	$\rho_f = 2.0$ slugs/ft^3
Kinematic viscosity	,	$\nu = 0.0000113$ ft^2/sec.
Stationary lift coefficient	,	$C_{L0} = 0.2$

The cable is divided into four elements. The static displacement of the cable due to the cable weight and fluid drag force is determined by the viscous relaxation method. The transverse vibration is then computed by the mode superposition technique. The Strouhal frequency and the

fundamental structural frequency are 15.73 rad/sec and 14.6 rad/sec, respectively.

The lift coefficient, C_L, computed by the wake-oscillator model, is shown in Figure 6.6-1. The value of C_L is larger than the value of the stationary lift coefficient, C_{L0}, and is maximum at t = 2.0 seconds, the same time at which the transverse displacement is also maximum. The beat seen in the transverse displacement shown in Figure 6.6-2 occurs because of the lock-in assumption: the structural response frequency is the natural frequency whose value is near the lift force frequency.

The maximum displacement obtained in this example is 0.016 feet which is equal to the experimental value reported by Ramberg, et al. (1980).

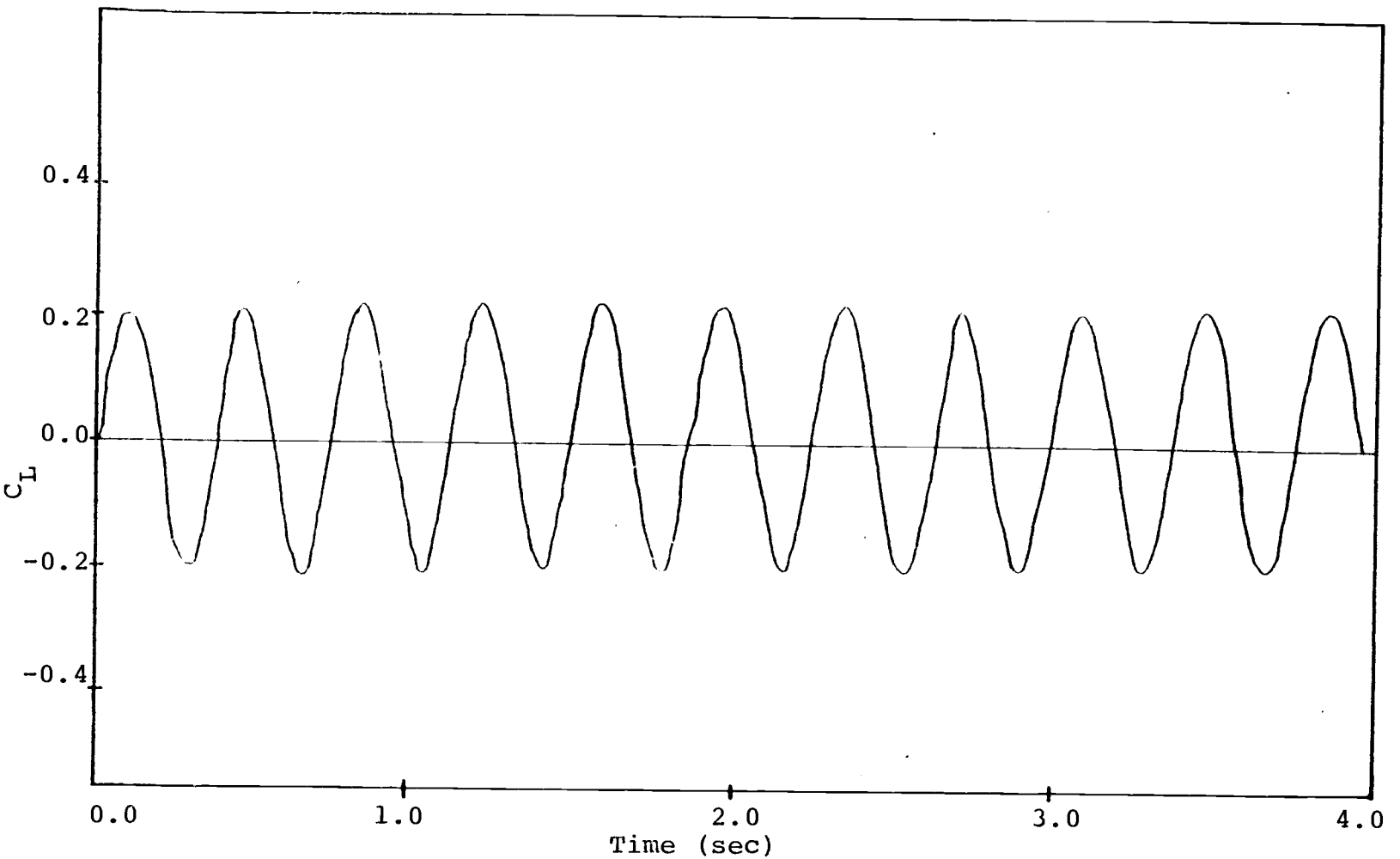

Figure 6.6-1. Lift force coefficient.

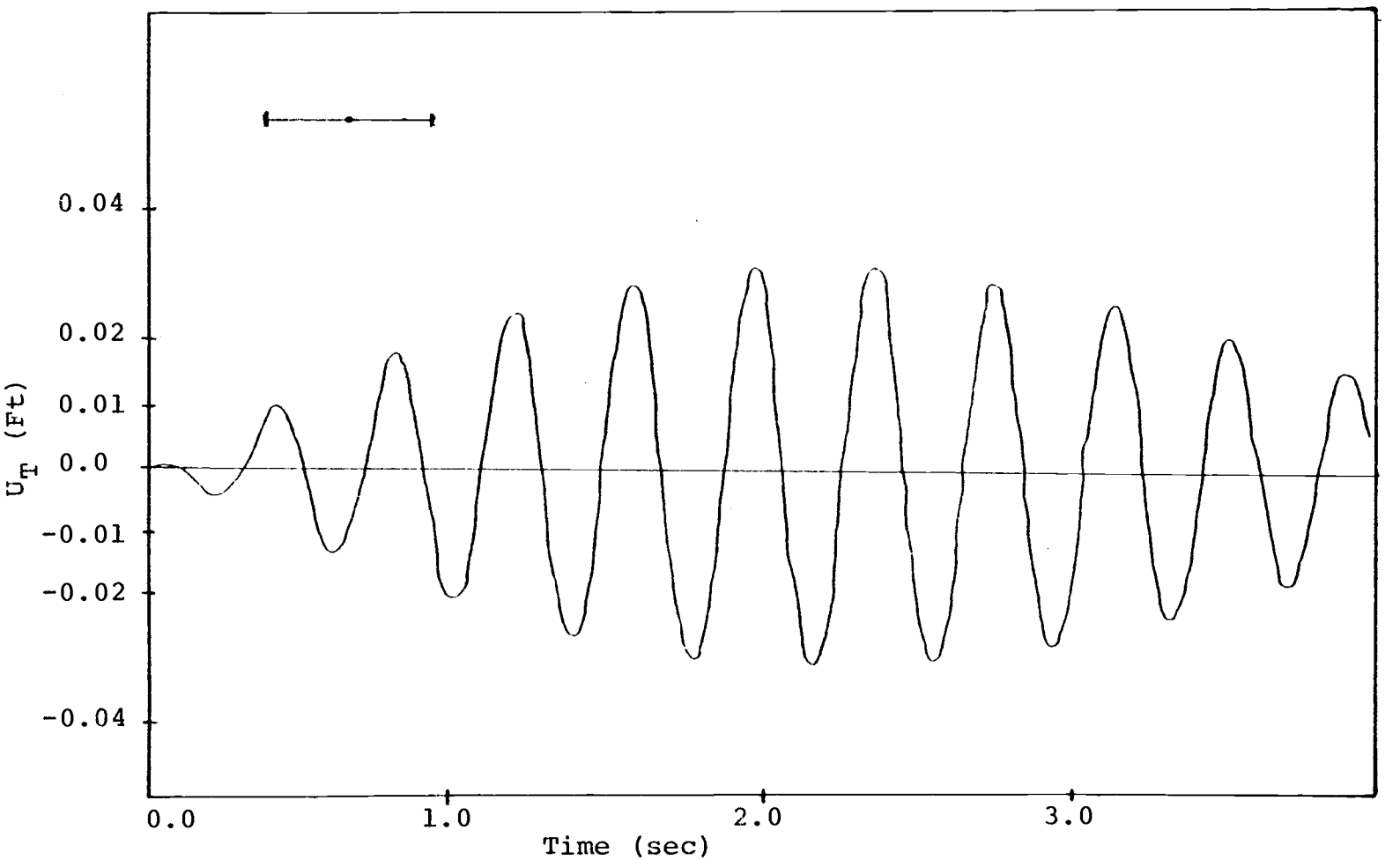

Figure 6.6-2. Transverse displacement of the cable midpoint.

6.7 Example 7: Three-Dimensional Responses of a Three-Leg Single Point Mooring

In this example, three-dimensional responses of a three-leg single point mooring to both inline and transverse wave forces are investigated. The descriptions of the problem are given in Figures 6.7-1,2. Each leg is modeled with three straight elements. The initial configuration for the determiniation of the static configuration is an unstretched straight line as shown by dashed line in Figure 6.7-1. The cable, fluid, and wave data are the same as for Example 5. The incremental/iterative method with a time increment of 0.005 seconds is employed to compute the response due to inline force and the mode-superposition and Runge-Kutta integration methods with a time increment of 0.001 seconds were employed to treat the transverse force. This example requires 20 minutes of CPU time on the Cyber 170/720 for prediction of six minutes of real time response.

The time history of responses of the disc are shown in Figure 6.7-3 for surge and in Figure 6.7-4 for heave. The disc moves slowly in the wave direction until the internal force in the cable balances the external force. At that time the disc remains still and then reverses direction when the wave force reduces. Because the stiffness in the opposite direction to the wave propagation is very

small, as can be seen from the time variation of the stress shown in Figure 6.7-5 where the stress in element 7 reduces drastically, the disc moves as a free body. The heave motion behaves similarly to the surge motion in which a suddent reversal of motions occurs at the same time as the cable slackens.

Figure 6.7-6 shows the time variations of the unsteady lift coefficient: the solid line represents the lift coefficient for a nonstationary structure omputed by a wake-oscillator model (Ramberg et al., 1975) and the dashed line represents the lift coefficient for a stationary structure. The period of oscillation of the stationary lift force is smaller than the nonstationary lift force. This is because the tendency of the nonstationary lift frequency to remain constant when the Strouhal frequency is in the vicinity of a structural natural frequency.

The disc response due to the transverse force is predominantly sway motion and is shown in Figure 6.7.7. Since the strumming frequency is much higher than the wave frequency, the response shows a long period (slowly varying) motion which can be identified with the wave frequency and a short period motion which is shown by a high frequency fluctuation about the long period motion. Again, the low frequency sway motion changes its direction suddenly as the cable slackens.

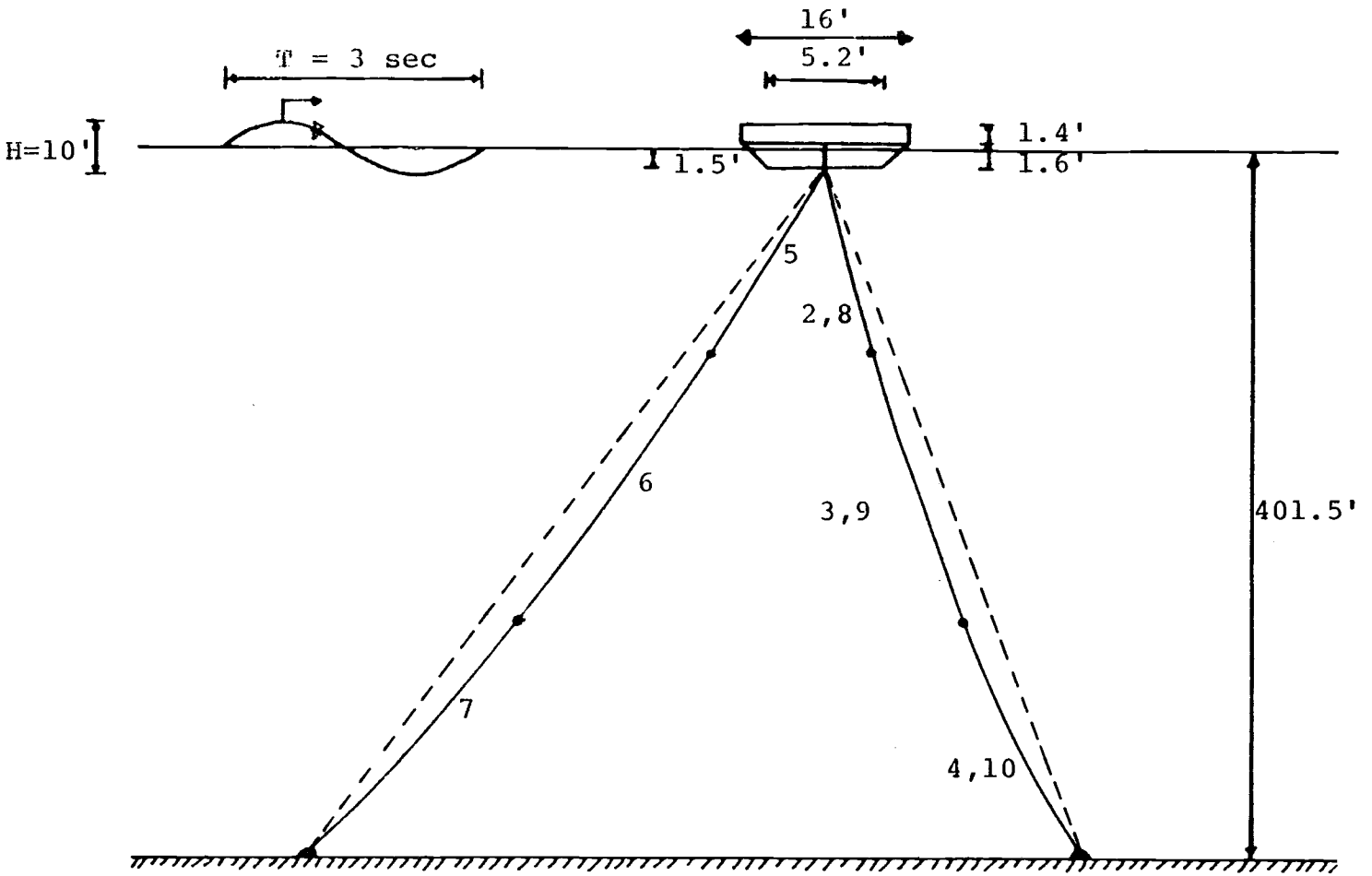

Figure 6.7-1. Disc buoy supported by three mooring lines (vertical view).

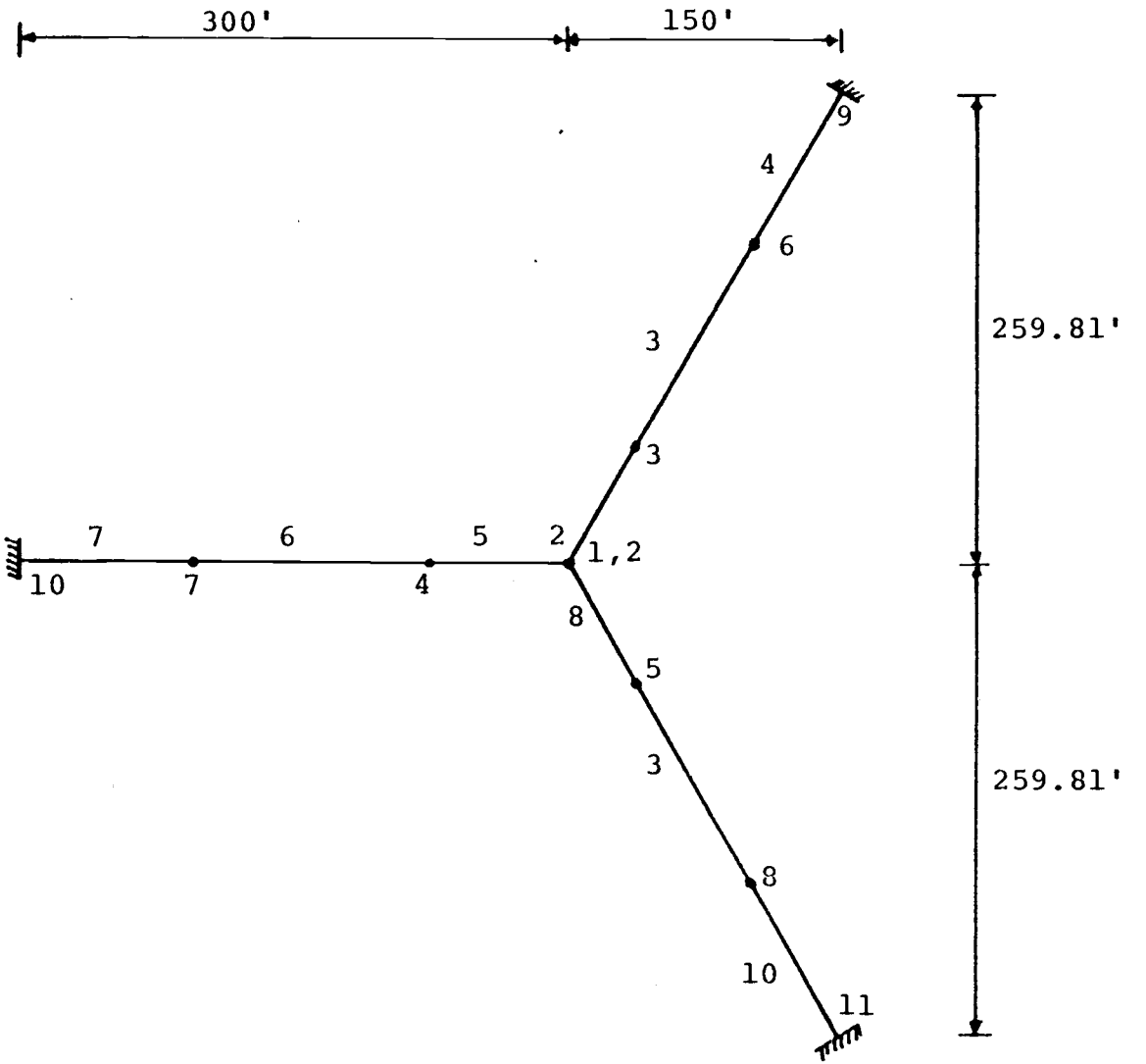

Figure 6.7-2. Disc buoy supported by three mooring lines (plan view).

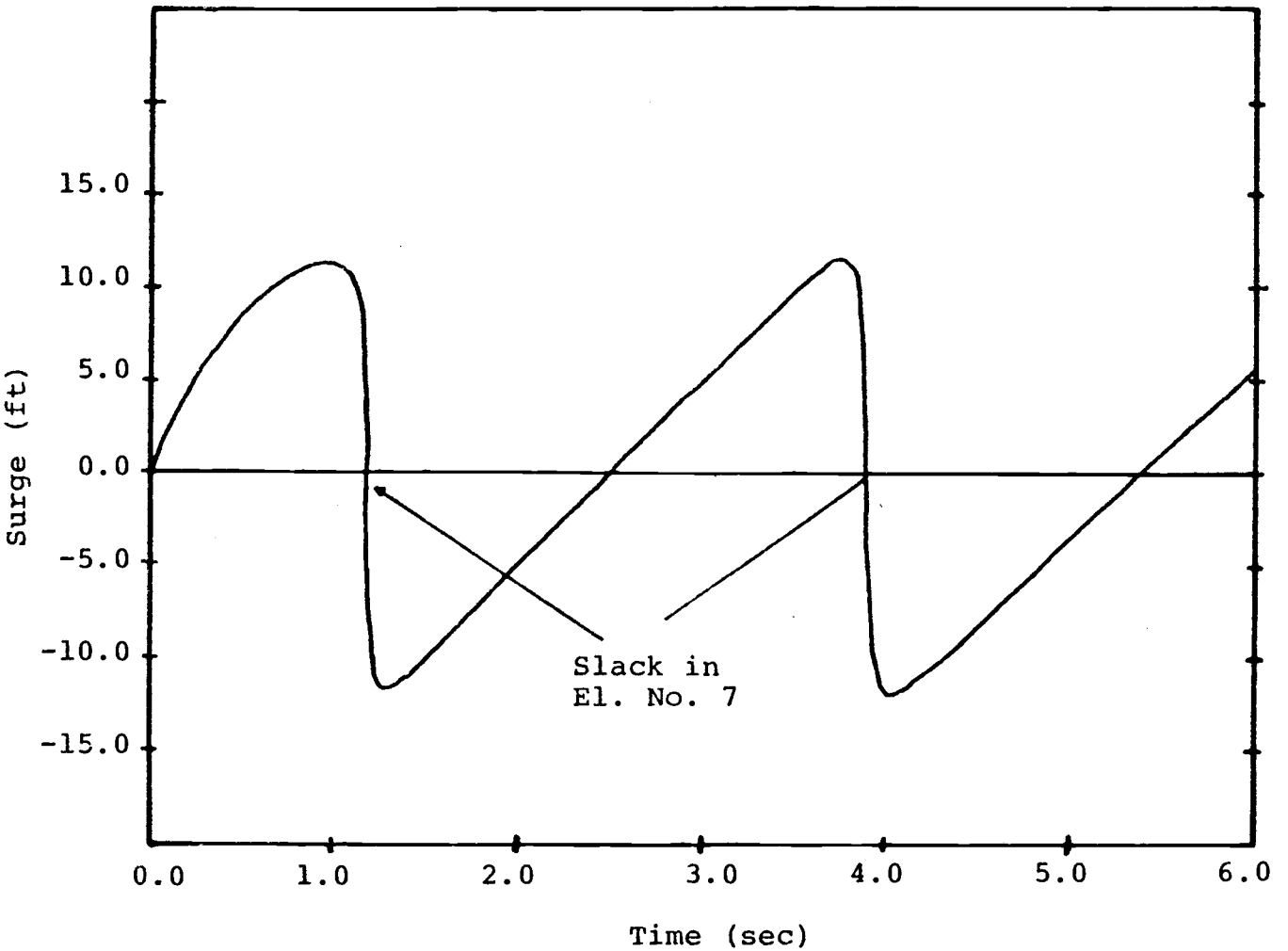

Figure 6.7-3. Surge vs. time of the disc supported by three mooring lines.

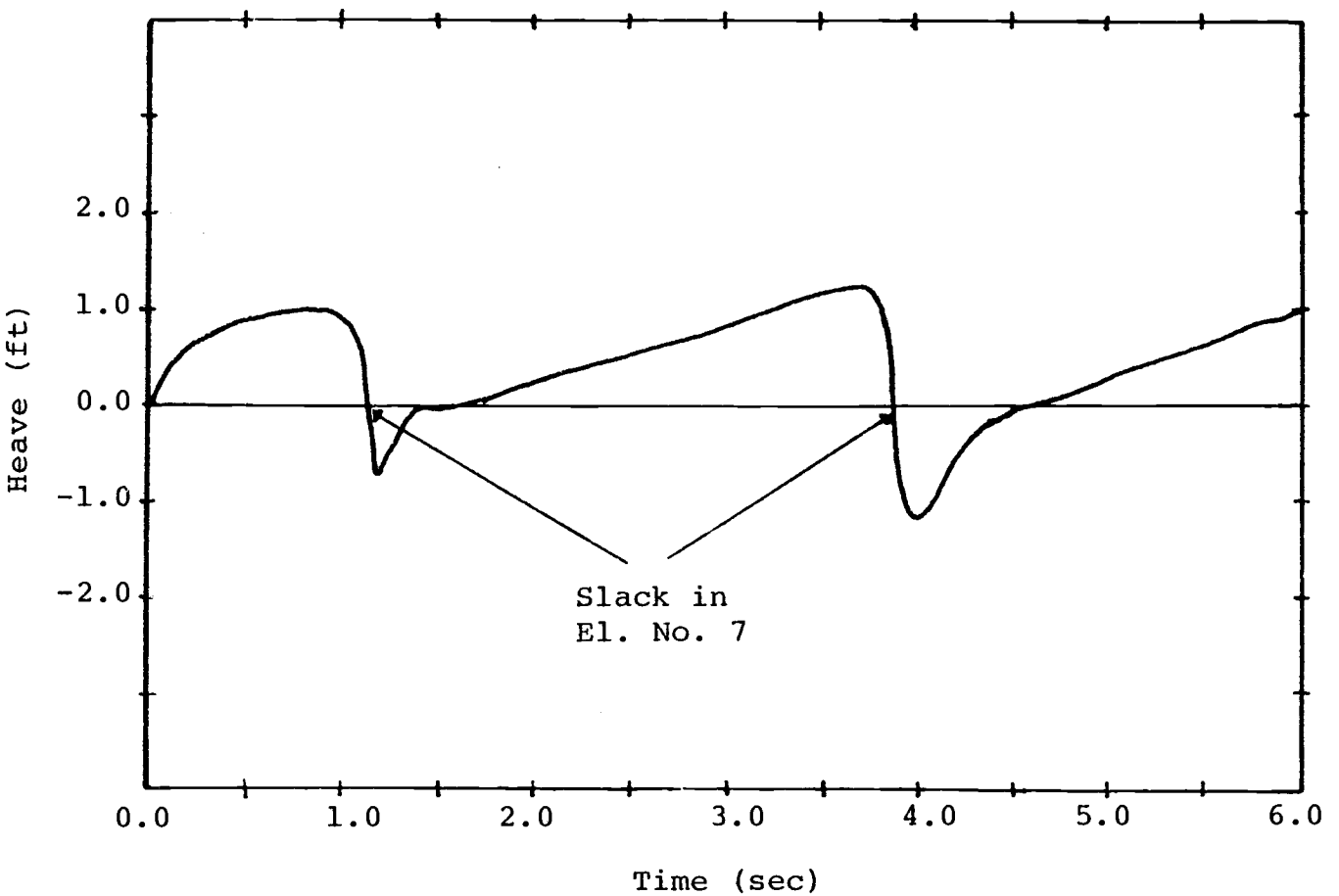

Figure 6.7-4. Heave vs. time of the disc supported by three mooring lines.

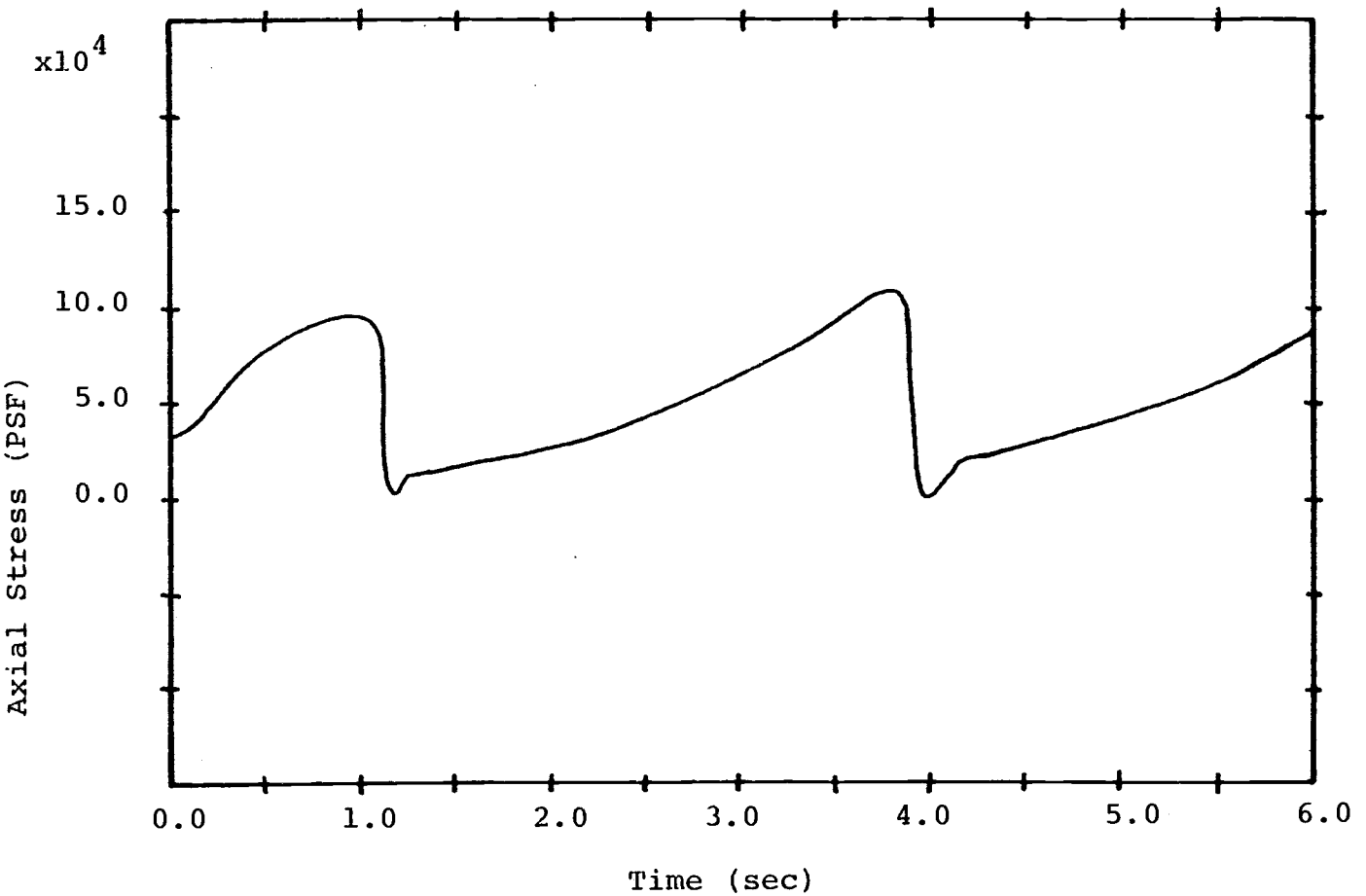

Figure 6.7-5. Stress variation in Cable Element No. 7.

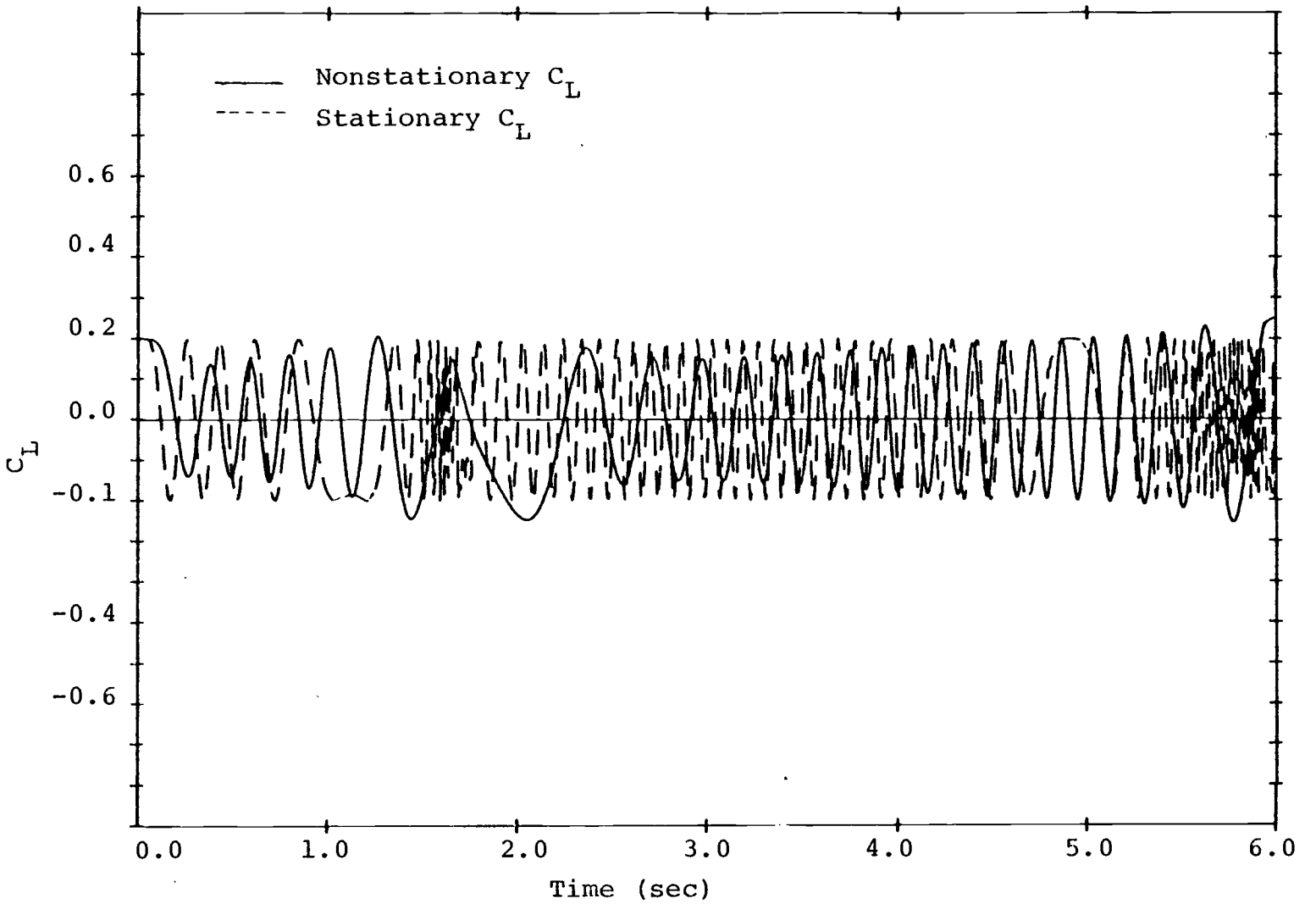

Figure 6.7-6. Time variation for lift force coefficient.

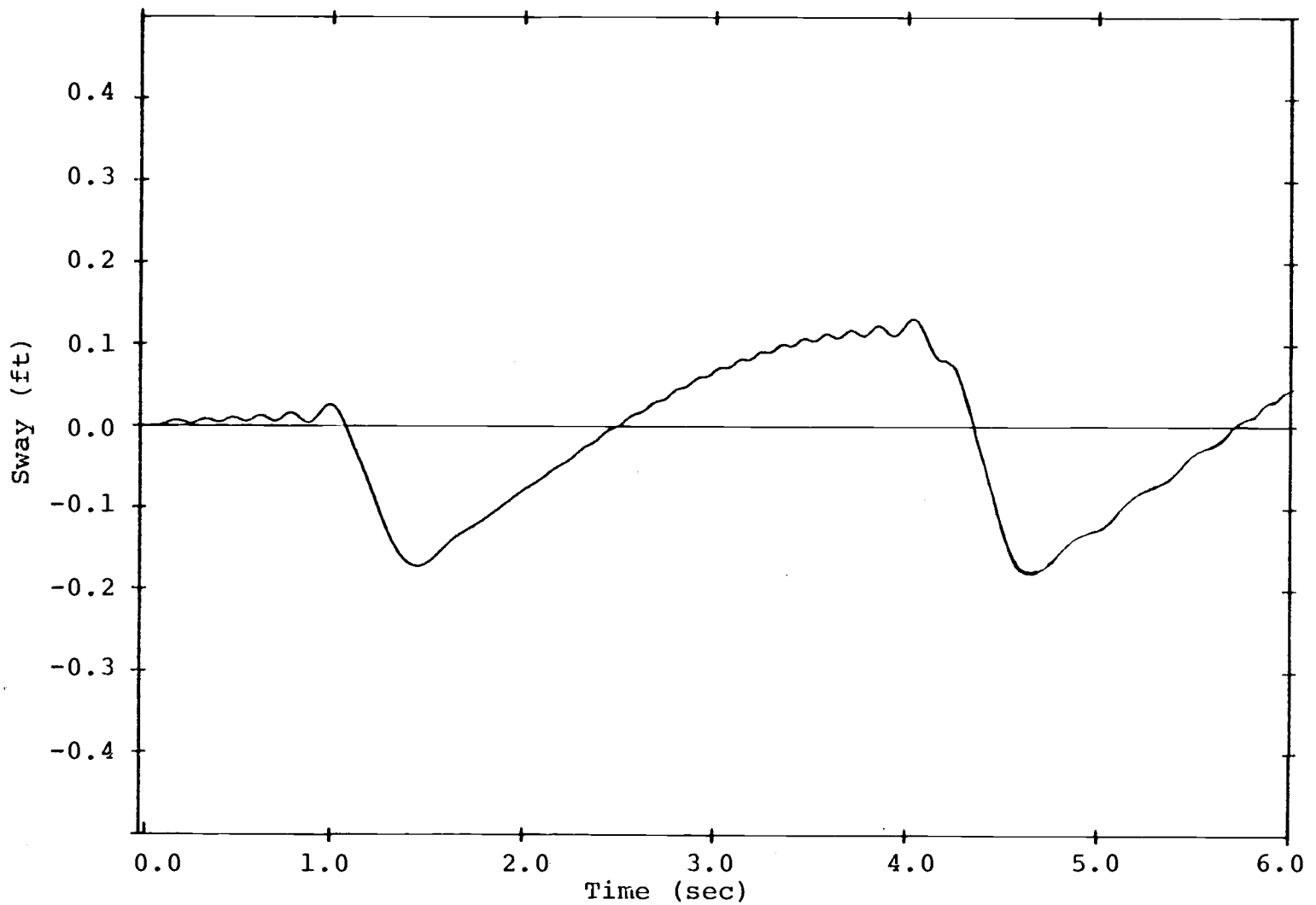

Figure 6.7-7. Sway motion of the disc supported by three mooring lines due to lift force.

7.0 CONCLUSIONS

In this study a numerical simulation method for the predicition of nonlinear response of cable systems and cable-large body systems is presented. Two types of material, piecewise linear elastic and linear viscoelastic material, are investigated. The finite element technique is used to model the cable line and the six-degrees-of-freedom rigid motions of large bodies. Cable strumming is modeled by a wake-oscillator model and the lock-in condition is assumed to occur in the transverse vibration. The residual feedback method and the incrementally iterative technique are used to solve the equation of motions. The viscous relaxation method is employed to obtain the static configuration of the highly geometrically nonlinear cable structure. Newmark's integration method is utilized to compute dynamic responses.

The deterministic response of cable-large body systems due to monochromatic waves is simulated numerically by solving the linearized incremental equation. The residual feedback method has been compared with the incremental/iterative method. For the single point mooring, it was found that the incremental/iterative solution procedure provides a better result than the residual feedback method. The

residual feedback method requires a very small time increment in order for the solution to converge to the true results.

The nondeterministic response of cable-large body systems due to random waves is simulated in the frequency domain: the system is assumed to vibrate about its static configuration.

The decoupling technique proposed by Foss (1958) is found to be a very effective tool in the computation of the stochastic response due to the random waves. This is particularly true when the wave energies are concentrated in the low frequencies.

The cable strumming response in which the lift coefficient is obtained by the wake-oscillator model is calculated numerically by the mode-superposition technique. For a horizontal cable immersed in a steady uniform flow, the results obtained agree with reported experimental results.

The validity of the fluid force model and the capability of the computer program developed in this study to handle three-dimensional problems has been demonstrated. A smaller time increment than is necessary for the two-dimensional problem is needed for obtaining a stable solution of a three-dimensional problem. Again the incremental/iterative method has proved itself to be an

effective technique for solving nonlinear dynamic equations with nonconservative fluid forces. The small motion assumption for the strumming motion was verified. Subharmonic response (high frequency motion about the low frequency motion) was observed with a subharmonic frequency equal to the lift coefficient frequency. A slowly varying response with frequency equal to the wave frequency is noticeable in the results. It was beyond the scope of this work to include the effect of strumming displacement on the inline fluid drag force, as indicated by Skop et al. (1977). This type of problem is left for future study.

REFERENCES

1. Bai, K. J., "The Added Mass of Two Dimensional Cylinders Heaving in Water of Finite Depth," Journal of Fluid Mechanics, Vol. 81, part 1, 1977, pp.85-105.

2. Bathe, K. J., Ramm, E., and Wilson, E. L., "Finite Element Formulation for Large Deformation Dynamic Analysis," International Journal of Numerical Method in Engineering, Vol. 9, 1975, pp.353-386.

3. Bathe, K. J. and Wilson, E. L., Numerical Methods in Finite Element Analysis, Prentice-Hall, Inc., Englewood Cliffs, New Jersey, 1976.

4. Bettes, P. and Zienkiewicz, O. C., "Diffraction and Refraction of Waves Using Finite and Infinite Elements," International Journal of Numerical Methods in Engineering, Vol. 11, 1977, pp.1271-1290.

5. Bishop, R. E. D. and Hassan, A. Y., "The Lift and Drag Forces on a Circular Cylinder Oscillating in a Flowing Fluid," Proceedings Royal Society, Series A, London, England, Vol. 277, 1964.

6. Bitting, K. R. and Lincoln, W. B., "Mooring Configuration Analysis," Third Interim Report 782702.4.2, Unpublished report, April 1978.

7. Black, J. L. and Mei, C. C., "Scattering and Radiation of Water Waves," Report. No. 121, MIT, April 1970.

8. Borgman, L. E., "Ocean Wave Simulation for Engineering Design," Journal of Waterways and Harbors Div., Proc. ASCE, Vol. 95, WW4, November 1969, pp.557-583.

9. Borgman, L. E., "Statistical Models for Ocean Wave Forces," Advances in Hydrosciences, edited by V. T. Chow, Academic Press, New York, New York, 1972, pp.139-181.

10. Cannon, T. C. and Genin, J., "3-D Dynamical Behavior of a Flexible Towed Cable," Aeronautical Quarterly, Vol. 23, 1970, pp.201-210.

11. Cescotto, S., Frey, F., and Fonder, G., "Total and Updated Lagrangian Descriptions in Nonlinear Structural Analysis: A Unified Approach," Energy Methods in Finite Element Analysis, edited by Glowinski, R., Rodin, E. Y., and Zienkiewicz, O. C., 1979, pp.281-296.

12. Clough, R. W. and Penzien, J., Dynamics of Structures, McGraw-Hill Book Co., New York, New York, 1975.

13. Cook, R. D., Concepts and Applications of Finite Element Analysis, 2nd edition, John Wiley & Sons, 1981.

14. Coons, S. A., "Surfaces for Computer Aided Design for Space Forms," Project MAC-TR-41 Report, MIT June 1967.

15. Desai, C. S. and Abel, J. F., Introduction to the Finite Element Method for Engineering Analysis, Van Nostrand Co., New York, New York, 1972.

16. Dominguez, R. F. and Smith, C. E., "Dynamic Analysis of Cable Systems," ASCE Journal of Structural Division, Vol. 98, ST 8, Paper 9127, August 1972, pp.1817-1834.

17. Foss, K. A., "Coordinates Which Uncouple the Equations of Motion of Damped Linear Dynamic Systems,' Journal of Applied Mechanics, ASME, Paper No. 57-A-86, September, 1958, pp.361-364.

18. Fung, Y. C., Foundation of Solid Mechanics, Prentice-Hall, Inc., Englewood Cliffs, New Jersey, 1965.

19. Garrison, G. J., "Hydrodynamic Loading of Large Offshore Structures: Three-Dimensional Source Distribution Methods," Numerical Methods in Offshore Engineering, edited by Zienkiewicz, O. C., Lewis, P., and Stagg, K. G., John Wiley, Chichester, England, pp.87-139, 1977.

20. Griffin, O. M., Skop, R. A., and Ramberg, S. E., "The Resonant, Vortex-Excited Vibrations of Structures and Cable Systems," Paper OTC 2319, presented at the Seventh Annual Offshore Technology Conference, Houston, Texas, May 1975.

21. Griffin, O. M., Pattison, J. H., Skop, R. A., Ramberg, S. E., and Meggitt, D. J., "Vortex-Excited Vibrations of Marine Cables," Journal of the Waterway Port Coastal and Ocean Division, ASCE, May 1980, pp.143-203.

22. Hartlen, R. T. and Currie, G. I., "Lift-Oscillator Model of Vortex-Induced Vibration," Journal of Engineering Mechanics Division, ASCE, October 1970, pp.577-590.

23. Hoener, S. F., Fluid Dynamic Drag, Published by the Author, Midland Park, New Jersey, 1965.

24. Hudspeth, R. T., "Prediction of Wave Forces from Nonlinear Random Sea Simulations," thesis presented to the University of Florida at Gainesville, Fla., in 1974, in partial fulfillment of the requirements for the degree of Doctor of Philosophy.

25. Hudspeth, R. T., Nakamura, T., and Leonard, J. W., "Floating Vessel Simulator by an Axisymmetric Green's Function," Final Report submitted to Marathon Oil Company, June 1980.

26. Irvine, H. M. and Caughey, T. K., "The Linear Theory of Free Vibrations of a Suspended Cable," Proceedings of the Royal Society of London, Series A, Vol. 341, 1974, pp.299-315.

27. Iwan, W. D. and Blevins, R. D., "A Model for Vortex-Induced Oscillation of Structures," Journal of Applied Mechanics, Vol. 96, Sec. 3, 1974, pp. 581-586.

28. Jayaraman, H. B. and Knudson, W. C., "A Curved Element for the Analysis of Cable Structures," Computers and Structures, Vol. 14, No. 3-4, 1981, pp.325-333.

29. Kim, C. H., "Hydrodynamic Forces and Moments for Heaving, Swing, and Rolling Cylinders on Water of Finite Depth," Journal of Ship Research, Vol. 13, 1969, pp.137-154.

30. Leonard, J. W., "Curved Finite Element Approximation to Nonlinear Cables," Paper OTC 1533, presented at the Fourth Annual Offshore Technology Conference, Houston, Texas, May 1972.

31. Leonard, J. W., "Newton-Raphson Iterative Method Applied to Circularly Towed Cable-Body System," Engineering Structure, 1979, pp.73-79.

32. Lin, Y. K., Probabilistic Theory of Structural Dynamics, McGraw-Hill Book Co., New York, New York, 1967.

33. Lo, A. and Leonard, J. W., "Dynamic Analysis of Underwater Cables," in review.

34. Lo, A. "Nonlinear Dynamic Analysis of Cable and Membrane Structures," a thesis submitted to Oregon State University in partial fulfillment of the requirements for the degree of Doctor of Philosophy, June 1982.

35. Ma, D. C., "Finite Element Analysis of Nonlinear Elasto-Plastic Slack Cable Networks," Doctoral Thesis submitted to the School of Civil Engineering, Illinois Institute of Technology, Chicago, Illinois, December 1976.

36. Morison, J. R., O'Brien, M. P., Johnson, J. W., and Schaaf, S. A., "The Force Exerted by Surface Waves on Piles," Petroleum Transactions, AIME, Vol. 189, Technical Report 2846, May 1950, pp.149-154.

37. Morris, N. F., "The Use of Modal Superposition in Nonlinear Dynamics," Computers and Structures, Vol. 7, 1977, pp.65-72.

38. Newman, J. N., Marine Hydrodynamics, MIT Press, Cambridge, Massachusetts, 1977.

39. Nath, J. H., "Dynamics of Single Point Ocean Moorings of a Buoy--A Numerical Model for Solution by Computer," Oregon State University, Corvallis, Oregon, Report 69-10, July 1969.

40. Nath, J. H. and Tresher, R. W., "Anchor-Last Deployment Procedure for Mooring," OTC 2364, presented at Seventh Annual Offshore Technology Conference, Houston, Texas, May 1975.

41. Newmark, N. M., "A Method of Computation for Structural Dynamics," Journal of the Engineering Mechanics Division, ASCE, EM3, July 1959, pp.67-94.

42. O'Brien, W. T. and Francis, A. J., "Cable Movements Under Two Dimensional Loads," Journal of Structural Division, ASCE, Vol. 90, ST3, 1964, pp.89-123.

43. O'Brien, W. T., "General Solution of Suspended Cable Problems," Journal of Structural Division, ASCE, Vol. 93, 1967, pp.1-26.

44. Patel, J. S., "Static and Dynamic Analysis of MABS-II Horizontal Array Installation," Naval Underwater Systems Center, Newport, Rhode Island, TM No. EM-20-74, April 1974.

45. Peyrot, A. H. and Goulois, A. M., "Analysis of Flexible Transmission Lines," Journal of Structural Division, ASCE, Vol. 104, No. ST5, 1978, pp. 763-779.

46. Peyrot, A. H. and Goulois, A. M., "Analysis of Cable Structures," Computers and Structures, Vol. 10, 1979, pp.805-813.

47. Peyrot, A. H., "Marine Cable Structures," Journal of Structural Division, ASCE, No. ST12, December 1980, pp.2391-2405.

48. Pierson, W. J., "Motions of Ships in Confused Seas," Journal of Ship and Naval Architecture, 1956, pp. 322-332.

49. Ramberg, S. E., Griffin, O. M., and Skop, R. A., "Some Resonant Vibration Properties of Marine Cables with Application to the Prediction of Vortex-Induced Structural Vibrations," ASME Ocean Engineering Mechanics, 1975, pp.29-42.

50. Rayleigh, J. W. S., Theory of Sound, 2nd edition, Vol. I, Dover Publications, New York, New York, 1945.

51. Reid, R. O., "Dynamics of Deep-Sea Mooring Lines," Texas A&M Project 204 Ref. 68-11F, July 1968.

52. Rice, S. O., "Mathematical Analysis of Random Noise," Bell System Technical Journal, Vol. 23, 1944, pp. 282-332.

53. Sergev, S. and Iwan, W. D., "The Natural Frequencies and Mode Shapes of Cables with Attached Masses," TM No. M-44-79-3, Civil Engineering Laboratory, Naval Construction Battalion Center, Port Hueneme, California, April 1979.

54. Sharma, J. N. and Dean, R. G., "Development and Evaluation of a Procedure for Simulating a Random Directional Second Order Sea Surface and Associated Wave Forces," Ocean Engineering Report No. 20, University of Delaware, Newark, Delaware, July 1979.

55. Skop, R. A. and O'Hara, G. J., "The Method of Imaginary Reaction--A New Technique for Analyzing Structural Cable Systems," Marine Technology Society Journal, Vol. 4, No. 1, January-February 1970, pp.21-30.

56. Skop, R. A., Griffin, D. M., and Ramberg, S. E., "Strumming Predictions for the SEACON II Experimental Mooring," Paper OTC 2884, presented at the Ninth Annual Offshore Technology Conference, Houston, Texas, May 1977.

57. Tillerson, J. R., Stricklin, J. A., and Haisler, W. A., "Numerical Methods for the Solution of Nonlinear Problems in Structural Analysis," ASME, AMD, Vol. 6, 1974, pp.67-101.

58. Tuah, H., and Hudspeth, R. T., "Comparisons of Numerical Random Sea Simulations," to be published in Journal of the Waterways Port Coastal and Ocean Division.

59. Vaicaitis, R., "Cross-Flow Response of Piles Due to Ocean Waves," Journal of Engineering Mechanics Division, ASCE, Vol. 102, No. EM1, 1976, pp.121-134.

60. Webster, R. L., "An Application of the Finite Element Method for the Determination of Nonlinear Static and Dynamic Response of Underwater Cable Structures," Doctoral thesis submitted to the School of Civil Engineering, Cornell University, Ithaca, New York, 1974.

61. Webster, R. L., "On the Static Analysis of Structures with Strong Geometric Nonlinearity," Computers and Structures, 1980, pp.137-145.

62. Wehausen, J. V. and Laitone, E. V., "Surface Waves," Encyclopedia of Physics, Vol. 9, Springer-Verlag, Berlin, 1960, pp.446-778.

63. Wehausen, J. V., "The Motion of Floating Bodies," Review in Fluid Mechanics, 1971, pp.237-268.

64. Wheeler, J. D., "Method for Calculating Forces Produced by Irregular Waves," Preprints 1969 Offshore Technology Conference, Vol. I, Paper No. OTC 1007, May 18-21, 1969, pp.83-94.

65. Zienkiewicz, O. C., The Finite Element Element Method, 3rd edition, McGraw-Hill Book Co., 1977.